Università degli studi di Modena e Reggio Emilia

PhD "Enzo Ferrari" in Industrial and Environmental Engineering

XXXIV° Cycle

Coordinator: Prof. Alberto Muscio

Experimental and numerical analysis of non-conventional combustion process in internal combustion engine

Academic Discipline (SSD) ING-IND/08

Candidate: Dr. Tommaso Savioli

Supervisors:

Prof. Carlo A. Rinaldini

Prof. Enrico Mattarelli

Alla scienza, alla verità

e alla libertà del pensiero

Ringraziamenti

Questa pagina non è sicuramente di facile stesura. Ci sono da ringraziare tantissime persone che hanno contribuito direttamente ed indirettamente a questo risultato per me veramente inaspettato che mi rende personalmente molto orgoglioso. Cercherò di ringraziarle una per una. Primo fra tutti mio nonno Livio, un grande uomo prima di un fantastico nonno, che mi ha donato il coraggio di superarmi , la forza per resistere ai colpi, ma soprattutto una profonda umanità, semplicemente il mio unico modello, spero che mi guardi. Federica, il mio amore, una compagna di vita che ha saputo regalarmi una tranquillità che mancava e che non smette mai di farmi crescere; è stata e sarà sempre una straordinaria scoperta. Mio padre e Mia madre, i miei fratelli e la mia famiglia , che mi hanno cresciuto e mi hanno dato l'opportunità di essere qui oggi, molti purtroppo non ci sono più, ma ciò non significa che non condivideranno con me questo momento. Un pensiero particolare va allo zio Otto, un esempio di come non perdere mai la voglia di sorridere anche di fronte al grande dolore. Una particolare menzione va anche allo zio Luca, con cui purtroppo non ho più contatti, ma che ha avuto il grande merito avvicinarmi al fascino della scienza.

Gli amici sono e saranno sempre per me una parte importantissima, senza di loro non sarei qui, e senza i consigli , il continuo confronto , i litigi , le condivisioni, non sarei mai chi sono oggi. E quindi :

Alessio, che mi ha insegnato un po' di pazienza, a Ioannis così tanto diverso da me ,ma che tante volte mi ha ispirato, Debbio un fiume di idee con lui ho condiviso molto, Elia uno di famiglia schietto sincero provocante, Gianluca ha saputo farmi vedere avanti quando non riuscivo, Luca il mio primo vero amico, Racca un genio, Roby un altro genio, Solla la meccanica senza lui sarebbe ancora un mistero, Zotti per lo stesso motivo, Leo, semplicemente non avrei la laurea senza il suo aiuto, Nikla mi ha aiutato in momenti difficili, Matte non scorderò mai le estati passate a casa tua, e il JeJ Disco, Elisa per la dolcezza, Timo per il black humor, Miky per il cub, Riky per le belle giornate in pista, Lucrezia il primo amore, la ricorderò sempre con dolcezza, Pecio un mentore, Touch il primo compagno di studi

all’università, Vallo un altro genio, Morand un grande vulcanologo, Pinto un amico ritrovato, Lorenz un personaggio d’altri tempi.

Un ringraziamento speciale va ad Antonio Bandello, un amico , un collega e un socio, un vero professionista appassionato, dotato di grande capacità di sintesi. Lo ringrazio perché riesce a farmi osservare i miei limiti. Senza il suo aiuto parte del lavoro non sarebbe potuto essere scritto qui.

Sicuramente qualcuno mancherà come sempre, ma non per questo non è stato meno importante per arrivare sino a qua.

Indiscutibilmente ci tengo a ringraziare tutti i miei maestri che mi hanno accompagnato e che mi hanno trasferito parte della loro conoscenza fin dalle elementari all’università.

Gli ultimi che voglio ringraziare sono i miei più importanti maestri che vengono al pari della mia famiglia e che hanno riconosciuto in me delle capacità come mai nessuno aveva fatto prima, e che hanno creduto in me. Gliene sarò sempre grato.

Il primo è il Professor emerito Giuseppe Cantore, un vero uomo accademico un grande insegnante; mi ha fatto capire che nella vita serve anche la forma oltre che la sostanza, ne avevo bisogno.

Il Professor Enrico Mattarelli, l’unica persona che ho incontrato nella mia vita che va ben oltre all’insegnamento della materia, insegna la passione. Un esempio per tutti coloro che hanno la fortuna di incontrarlo. E’ ed è stato un vero maestro per me; tra le tantissime qualità che lo contraddistinguono credo che l’umanità e la lealtà siano quelle che lo descrivono meglio. Mi ha regalato tanto, e non lo scorderò mai.

Il Professor Carlo Alberto Rinaldini, che mi ha accompagnato per tutto il periodo della tesi, del dottorato, nella mia permanenza in università per quasi 10 anni, anche lui è ed è stato mio maestro, sempre molto presente, sempre trasparente. Lui mi ha insegnato quello che so sulla sperimentazione ,materia che adoro, e che mi ha dato anche la possibilità di praticarla. Gliene sarò sempre grato. Un grande insegnante, oltre che una mente brillante.

Francesco Scrignoli, dapprima un mio studente, poi un dottorando, che mi ha aiutato nella stesura dell’ elaborato con preziosi consigli. Un promettente ricercatore, sempre educato e impeccabile, un amico.

Ringrazio profondamente anche Enrico Salardi, che mi ha sempre aiutato a realizzare i componenti meccanici per poter effettuare tutte le prove al laboratorio, un uomo saggio che ha saputo consigliarmi e indirizzarmi ben aldilà della meccanica, un amico.

Abstract

Nowadays, pollutant emissions represent the main topic in internal combustion engine development. Global warming has increased due to the high emissions of greenhouse gases, in particular CO_2 emissions. Internal combustion engines must increase global efficiency and, at the same time, decrease pollutant emissions in order to be compliant to future legislation constraints.

The high efficiency, reliability and flexibility of modern passenger car Diesel engines makes these power units quite attractive also for steady and quasi-steady application (e.g. aero motive, truck, heavy duty, generators) totally or partially running on fuel blends or different combustion process. The engine cost, which is obviously higher than that of current industrial engines, may not be a big obstacle, provided that the re-engineering work in order to implement dual fuel operation is limited and that performance and efficiency are enhanced.

The goal of this work is to explore the potential of a current state of the art turbocharged Diesel engine running on both Diesel Fuel and dual fuel combustion with the use of a premixed charge of methane or gasoline. This particular combustion process called RCCI (Reactive Controlled Compression Ignition) may improve engine global efficiency and reduce pollutant emissions. In particular, CO2 emissions decrease because of the different origin and nature of the fuel. In this contest, an analysis is made also in a two-stroke engine for aircraft application. This kind of engine can be quite attractive for the fewer constraints in combustion chamber design, rather than a four stroke; furthermore, low combustion pressures lead to fit better RCCI concepts.

The present thesis is focused on experimental and numerical CFD combustion calculation on a modern Diesel Engine; a test bed equipped with an indicating system is used for experimental campaign while a custom version of the Kiva 3V software is used for CFD simulations. Two-stroke engine has been then studied by several CFD calculation campaigns in order to investigate two-stroke potential in RCCI applications.

These different combustion processes may have several advantages in terms of global efficiency and pollutant emissions, but these results can be achieved only with an accurate combustion process calibration and several CFD combustion calculation.

Contents

Abstract....8

List of Figures....12

List of Tables....16

Dissemination....17

List of abbreviations....18

Introduction....20

1. Dual Fuel Engines....23

1.1 Fundamentals of gas fueled engines....23

1.2 Dual fuel operation modes....27

1.3 Application of dual fuel engines....32

2. CFD modelling....37

2.1 Introduction....37

2.2 Kiva 3V introduction....40

2.3 Kiva-3V CFD modelling theory....41

2.4 Combustion Modeling....49

3 Optimization of a Dual fuel (Natural gas-Diesel) for Gen-sets....55

3.1 Introduction....55

3.2 The engine choice....58

3.3 Background of DF operation mode....63

3.4 Pollutant emissions....66

3.5 Engine control system and setup....68

3.6 Test bench installation....73

3.7 Result discussion....79

3.8 Combustion Analysis 84
3.9 Application to gen-set 104
3.10 Numerical Validation and investigation 106
3.11 Conclusions 117
4 Experimental investigation on an engine running in RCCI combustion 119
4.1 Introduction 119
4.2 Engine setup 121
4.3 Experimental setup 125
4.4 Experimental Result 127
4.5 Conclusions 136
5 Design of a 2-stroke SI Hybrid engine for small aircraft 137
5.1 Introduction 137
5.2 Engine design 140
5.3 Methods 146
5.4 Injection system 154
5.5 CFD results 161
5.6 Conclusions 169
6 Conclusions 170
References 175

List of Figures

Figure 1 Typical dual fuel engine scheme 27
Figure 2 Fuel quantity split strategy 29
Figure 3 Alternative fuel split strategy 31
Figure 4 BSFC comparison in dual fuel engine VS diesel engine 34
Figure 5 Kiva structure mesh example 42
Figure 6 VM 428 Diesel Engine 58
Figure 7 NOx and CO vs BMEP 61
Figure 8 PMI and UHC vs BMEP 62
Figure 9 Influence of residual Diesel combustion fraction 65
Figure 10 Methane injector 68
Figure 11Development ETK-ECU 70
Figure 12 ETAS592 module 70
Figure 13 D-GID ECU 71
Figure 14 Engine control unit scheme 72
Figure 15 Apicom FR400 eddy current dynamometer 73
Figure 16 Sketch of the test bench 74
Figure 17 Obi client Indicating Software by Alma Automotive 75
Figure 18 Methane injection system installed after intercooler 77
Figure 19 Dual Fuel engine installed at test bench 78
Figure 20 BTE variation VS Percentage of substitution 81
Figure 21 BTE in optimized operation points 83
Figure 22 In cylinder pressure traces 85
Figure 23 Apparent rate of heat release 86
Figure 24 Cumulative heat release 86
Figure 25 Combustion efficiency comparison 88
Figure 26 Global efficiency comparison 89
Figure 27 CO, HC, CO_2 comparison 90

Figure 28 NOx, Soot emission comparison 91
Figure 29 In-cylinder pressure traces 92
Figure 30 Apparent integral heat release 93
Figure 31 Injected volume 93
Figure 32 Injection Rate and timing 94
Figure 33 In-cylinder pressure traces, apparent heat release 94
Figure 34 Apparent integral heat release 95
Figure 35 Injection rate and timing 95
Figure 36 Injected volume 96
Figure 37 In cylinder pressure traces not optimized points 97
Figure 38 Apparent heat release rate 98
Figure 39 Combustion efficiency comparison 99
Figure 40 BTE comparison 99
Figure 41 CO, HC, CO_2 comparison 100
Figure 42 NOx, Soot comparison 100
Figure 43 In cylinder pressure traces, apparent heat release 101
Figure 44 Apparent integral heat release rate 102
Figure 45 Injection rate and timing 102
Figure 46 Computational grid at TDC 107
Figure 47 Operation points, optimized @3000 RPM BMEP=12 BAR 108
Figure 48 CFD model validation 109
Figure 49 CFD model validation 110
Figure 50 Emissions comparison 111
Figure 51 Predicted Soot emissions 111
Figure 52 In cylinder pressure ROHR and mean temperature 113
Figure 53 Soot emission and IMEP comparison 114
Figure 54 In cylinder pressure ROHR and mean temperature 115
Figure 55 Soot emission and IMEP comparison 116
Figure 56 common PFI injector 121
Figure 57 PFI injector manifold detail 1 122

Figure 58 PFI injector manifold detail 2 123
Figure 59 Injector flow rate 123
Figure 60 NI Drivven control system cabinet 124
Figure 61 In-cylinder pressure traces 127
Figure 62 Rate of heat release 128
Figure 63 Mass fraction Burned 128
Figure 64 BTE comparison 129
Figure 65 In-cylinder pressure traces optimized Cases 130
Figure 66 Rate of heat release optimized Cases 131
Figure 67 Mass fraction Burned optimized Cases 131
Figure 68 BTE Comparison optimized Cases 132
Figure 69 In cylinder pressure High loads 133
Figure 70 Rate of heat release high loads 134
Figure 71 Mass fraction Burned high loads 134
Figure 72 BTE comparison high loads 135
Figure 73 Blu spark engine: whole cad model 143
Figure 74 Numerical validation of the Rotax 850 cfd model 146
Figure 75 BSFC validation 147
Figure 76 Charging efficiency vs Delivery ratio 149
Figure 77 Scavenging efficiency vs Delivery ratio 150
Figure 78 retaining efficiency vs Delivery ratio 150
Figure 79 Scavenging curve 151
Figure 80 Scavenging ports configuration STD vs EVO_1 152
Figure 81 Mass flow rate CFD 3D vs CFD 1D 153
Figure 82 Injectors positioning 155
Figure 83 CFD 1D boundary conditions 157
Figure 84 Mixture formation 160
Figure 85 Scavenging process in function of CAD of “EVO” geometry @6000 rpm 162
Figure 86 Air mass flow through inlet and exhaust ports 163
Figure 87 Scavenging parameters in function of engine speed @ WOT 164

Figure 88 BMEP IMEP and F+P MEP comparison.....165
Figure 89 indicated and BTE vs engine speed 165
Figure 90 Mechanical+Pumping, Adiabatic+combustion efficiency @ WOT.....166
Figure 91 Compressor map with operation points @WOT.....166
Figure 92 Brake torque and Power @WOT vs engine speed.....167
Figure 93 BSFC and Maximum in cylinder pressure peak vs engine speed.....168

List of Tables

Table 1 Lower heating value for common automotive fuels 23
Table 2 Typical GEN-SET engines 56
Table 3 VM 428 Tech specs 59
Table 4 Operating points 61
Table 5 Physical properties of Diesel fuel 78
Table 6 Operation Points 81
Table 7 Results of the optimized operation points 82
Table 8 Main calibration parameters for two different points 88
Table 9 Selected operation points for Gen-set 104
Table 10 Specific emissions for the Gen-set 104
Table 11 Kiva 3V main models 106
Table 12 engine operation points 125
Table 13 Experimental campaign operation points 126
Table 14 Two stroke engine design constraints 138
Table 15 Engine main specs. 142
Table 16 Comparison of injection systems 145
Table 17 CFD 3D vs 1D comparaison 152
Table 18 Injector main characteristics 154
Table 19 Main specification of the computational grid 156
Table 20 Investigated injection strategy 157
Table 21 CFD 3D result of injection strategies 158

Dissemination

1. Caprioli S, Rinaldini C, Mattarelli E, Savioli T, Scrignoli F. Design of a Novel 2-Stroke SI Engine for Hybrid Light Aircraft. In: SAE Technical Paper. ; 2021. Accessed February 3, 2022. https://doi.org/10.4271/2021-01-1179

2. Mattarelli E, Rinaldini CA, Savioli T, Scrignoli F. Optimization of a High-Speed Dual-Fuel (Natural Gas-Diesel) Compression Ignition Engine for Gen-sets. SAE Int J Engines. 2021;14(3):369-386. https://doi.org/10.4271/03-14-03-0022

3. Cantore, G., Mattarelli, E., Rinaldini, C. A., Savioli, T., & Scrignoli, F. (2019). Numerical Optimization of the Injection Strategy on a Light Duty Diesel Engine Operating in Dual Fuel (CNG/Diesel) Mode. International Journal of Heat and Technology, 37(3), 682-688. https://doi.org/10.18280/ijht.370303

4. Mattarelli E, Rinaldini CA, Savioli T. Dual Fuel (Natural Gas Diesel) for Light-Duty Industrial Engines: A Numerical and Experimental Investigation. In: Srinivasan KK, Agarwal AK, Krishnan SR, Mulone V, eds. Natural Gas Engines : For Transportation and Power Generation. Energy, Environment, and Sustainability. Springer; 2019:297-328. https://doi.org/10.1007/978-981-13-3307-1_11

5. Legrottaglie F, Mattarelli E, Rinaldini CA, Savioli T, Scrignoli F. Experimental investigation on a diesel engine operated in RCCI combustion mode. AIP Conference Proceedings. 2019;2191(1):020096. https://doi.org/10.1063/1.5138829

6. Cantore G., Mattarelli E. , Rinaldini C.A., Scrignoli F., Development of a 360 HP 2-Stroke CI Aircraft Engine TECNICA ITALIANA-Italian Journal of Engineering Science Vol. 64, No. 2-4, June, 2020, pp. 159-166. https://doi.org/10.18280/ti-ijes.642-405

List of abbreviations

- AHRR Apparent heat release rate
- ATDC After top death center
- BDC bottom death center
- BSFC brake specific fuel consumption
- BTDC Before top death center
- CAHR Cumulative apparent heat release
- CAT Three way catalyst
- CE charging efficiency
- CI Compression ignition engines
- DOI Duration of injection
- DOS Diesel oil surrogate
- DR Delivery ratio
- EM electric motor
- EOC end of combustion
- EOI end of injection
- GEN-SET Internal combustion engine for electrical generation
- HCCI homogeneous compression charge ignition
- HD Heavy duties engines
- HEA Hybrid Electric Aircraft
- HPDI High pressure direct injection
- ICE internal combustion engine
- IR ignition retard
- ITE indicated thermal efficiency
- LPDI Low pressure direct injection
- LPSDI Low pressure semi direct injection
- LTC low temperature combustion

- M-H Magnussen-Hjertager model
- ND Normal Diesel
- NDIR Nondispersive Infrared
- NG Natural Gas
- PaSR Partially Stirred Reactor Model
- PFI port fuel injection
- PHAs Polycyclic Aromatic Hydrocarbons
- RANS Reynolds averaged Navier Stokes
- RCCI reactive controlled compression ignition
- RMS root main square
- SE Scavenging efficiency
- SI Spark ignition engines
- SOC start of combustion
- SOI Start of injection
- TDC top death center
- TR trapping efficiency
- WOT wide open throttle

Introduction

The tightening of regulations on exhaust pollutants and carbon dioxide emissions is pushing the automotive industry to further steps in the development of internal combustion engines. Even if modern after-treatment systems are very effective, it is fundamental to reduce engine-out emissions, in order to mitigate complexity and cost of these devices. As far as carbon dioxide emission is concerned, the mission can be accomplished in different ways: by improving engine brake thermal efficiency; by using fuels with low carbon content (or without carbon, such as hydrogen) or by employing the so-called “carbon-neutral fuels”, i.e. biofuels and e-fuels. The last ones have a net-CO2 emission close to zero, since the amount of gas emitted during combustion is about the same absorbed from the environment during their production.

On the other hand, diesel engines and two-strokes are in danger of being replaced by highly sophisticated gasoline engines or electric motors. Unfortunately, this trend will have a quite negative impact on the cost of the new vehicles. Furthermore, the benefits in terms of CO2 of fully electric vehicles can be appreciated only when the production of electric energy will be almost entirely based on renewable sources. Since this ideal situation seems quite far, in the next years the internal combustion engine will probably continue to play an important role, provided that its development is not abruptly stopped.

Conventional diesel engines may reach higher values of global efficiency in comparison to their gasoline counterparts; the gap can expanded by implementing a dual fuel, reactivity controlled compression ignition (RCCI) combustion, that provides the further advantage of ultra-low soot and NOx emissions. Existing diesel engines can be easily modified to operate in this mode. The difficult part is the calibration of the modified engine, that should be carried out at the test bench with the support of CFD simulation.

RCCI combustion can be applied also to the two-stroke cycle, enjoying some typical advantages of this type of engines: high-power density thanks to the double cycle frequency, light and robust construction, low manufacturing cost. Moreover, two-strokes without poppet

valves leave a wide freedom in the design of the combustion chamber geometry, a fundamental advantage when developing a novel combustion system. The main issue that must be addressed is the short-circuit of fresh charge during the scavenging process: for many applications, this problem can be fixed with the adoption of optimized fuel injection systems, and with a specific cylinder design.

Even if the two stroke engine has disappeared from passenger cars, in some fields it remains unchallenged: large steady and marine engines, micro-engines for car and boat models, small units for ultra-light aircraft, snow mobiles, portable tools for forestry and agriculture (chainsaw, sprayer,..), et cetera. Considering the success of these applications, it is interesting to analyze the concept on engines of average size.

The general goal of this research project is to explore the potential of alternative fuels and innovative combustion concepts in internal combustion engines.

A first part of the activity is focused on the study of Dual-fuel RCCI combustion, which can be obtained combining a low reactivity fuel (such as gasoline, natural gas, ethanol, etc.) and a high reactivity fuel (such as Diesel oil, biodiesel, kerosene, ..). The former is injected at low pressure into the intake manifold, so that it can generate a homogeneous and lean mixture within the cylinder before the start of combustion; the latter is injected directly into the combustion chamber, in order to ignite the lean mixture that otherwise it would be impossible to burn. This technology can be easily applied to existing 4-stroke Diesel engines, designing a low-pressure injection system for the low-reactivity fuel.

In this project, a 4-stroke light-duty Diesel engine has been modified in order to permit the injection of 2 different low reactivity fuels (gasoline and methane). The prototype has been tested in Dual Fuel RCCI mode (Diesel/gasoline and Diesel/methane). In particular, the influence of injection strategy has been investigated, along with the effect of different shares of diesel fuel and methane/gasoline. It was found that this combustion process, if properly optimized, can lead to higher brake thermal efficiencies and lower pollutant emissions, at least in terms of soot and NOx. The application of this innovative concept is expected to deliver

strong advantages on commercial vehicles and industrial engines, without significant drawbacks in terms of costs and performance.

Furthermore, the application of RCCI combustion to a two-stroke engine has been theoretically investigated, with the support of CFD simulation and empirical hypotheses.

The presented work is divided into five chapters: after two introductory chapters, in chapter three, the activity carried out on the light Diesel engine modified for dual fuel operation mode is reported, in particular for Natural gas operation. The activity is divided into two parts. The first one regards the experimental campaign carried out at Unimore test bench. The aim was to investigate the performances in terms of pollutant emissions and fuel consumption; first of all, the engine has been tested running in Dual Fuel mode without any modification to the injection strategy; then, an experimental optimization of injection strategy has been made. The second part of the chapter is focused on the numerical analysis of the RCCI combustion, by means of a CFD 3D model: after the calibration of the model, a numerical optimization campaign has been carried out in order to find some guidelines for dual-fuel engine development.

In chapter 4, the experimental campaign carried out on the RCCI engine modified in order to run in Dual Fuel RCCI Diesel/gasoline mode is reported. This engine derives from a light automotive diesel engine fueled with diesel oil and gasoline, the latter premixed with a PFI injection system. The work reviews the engine conversion process and results of the experimental test underlining some key points to better define the combustion process.

The last chapter (5) reviews the development from scratch of a novel two-stroke engine for light aircraft application. The design process starts from a first sketch of the scavenging ports, using previous experience acquired in this field. The second part of the activity is the building of the CFD 1D and CFD 3D models, in order to improve the geometry of the scavenging system and to define the main engine parameters, in order to meet performance targets and constraints.

1. Dual Fuel Engines

1.1 Fundamentals of gas fueled engines

Fuels that are gaseous in ambient conditions (1 Bar, 293 K) are considered gaseous fuels. The main gas fuels adopted in Automotive industries are typically: Natural Gas (a mixture of hydrocarbon gases with more than 90% of methane), LPG (Liquefied Petroleum Gas, a mixture of hydrocarbon gases, mainly propane and butane), and, most recently, hydrogen. In some cases the pressure storage in fuel tank can liquefy, (typically LPG).The usage of gaseous fuels provide some advantages in comparison to liquid fuels; the aim is to ease injection and to ease the mix with air in order to obtain a uniform blend.

Another interesting thing is demonstrated by the fuel cost, taking into consideration low heating values that represent the amount of energy achievable in single units of fuel mass burnt.

LPG is liquid into the tank, this fact leads to have (considering the same amount of energy storage) a bigger tank in comparison to Diesel Oil and Gasoline, about 1.7 times. If we consider Methane, the factor rises up to 4. This evidence shows a limitation in Vehicle autonomy and a rise in vehicle total mass because gas fuel tanks generally have cylindrical tank made of iron, in order to resist at pressure load.

Fuel	Energy storage [MJ/kg]
Gasoline	42.4
Diesel oil	42.5
Methanol	19.7
Ethanol	26.8
Hydrogen (gas)	119.9
Methane	50.0
Lead acid Battery	0.19

Table 1 Lower heating value for common automotive fuels

Table 1 shows typically heating value for common automotive fuels and also for batteries; as it can be observed, batteries are two dimension order of magnitude lower than fuels in general. Common gas fuels can be compared to liquids in terms of specific Heating value.

A limitation feature in the usage of gaseous fuels is the fact that they lead to decrease volumetric efficiency of the engine. In fact, in naturally aspirated engines the fresh charge is aspirated in the cylinder using the piston as a volumetric pump. If the mixture of air and fuel gas is made from a PFI injection system the engine aspirates the air-fuel mixture. This mixture in case of liquid fuel is mainly composed by air in terms of volume, because liquid fuel takes time to evaporate. This is not true if the fuel injected is already gaseous because the fuel gas takes up space into the mixture. Taking into consideration that the engine elaborates the same total volume, cycle by cycle, the volumetric efficiency decreases. Another issue is represented by the latent heat of evaporation of the fuel, in fact, the liquid fuel evaporation decreases the temperature of air (about 20 K for gasoline at stoichiometric conditions). In case of gaseous fuels this phenomenon is not present because there isn't any change of state. Conversely, gaseous fuels frequently have higher octane number, so that higher temperature in fresh charge may less probably lead to knock conditions. Different behavior can be reached if the engine is turbo charged, the less amount of air can be compensated by increasing boost pressure, this can be reached thanks to the high octane number, and can reduce the specific power gap in terms of displacement to power.

Any undesirable substances that may be introduced into an engine with the gas supply vary widely with the type of fuel gas used, the processing it receives, and local operating conditions. For example, "wet" natural gas, which normally contains small concentrations of higher hydrocarbons, will contribute to an increased tendency for the incidence of knocking, valve sticking, and increased deposits. However, "dry" processed natural gas, although it may be considered to be clean, may carry with it some very fine particles, such as those of rust, along the supply lines. In addition, producer and coke oven gases tend to contain some undesirable particles, such as those of carbon black and particles of sulfur compounds, while fuel gases originating from the steel industry can additionally contain some hydrogen sulfide.

The composition of gaseous fuels generally tends to be much simpler in structure in comparison to common liquid fuels, which are made of complex mixtures of a wide range of large molecular weight hydrocarbons. Thus, the properties of a liquid fuel may vary according to the source of the fuel and the processes they have gone through during its refining. The use of liquid fuel could lead to a worse performance than gaseous fuels that require no atomization or vaporization for their combustion [4].

All these considerations explain that gaseous fuels are simple to use into internal combustion engines, because of some key reasons: the easy system to inject fuel, the good mixing with air, the easy cold condition starts (due to no need to evaporate), the availability of the fuel. For electric generator applications, there is no need of fuel tanks because, in case of usage of natural gas, civil methane network can be used.

Last but not least, due to the higher octane number, the compression ratio of the engine can be increased, this fact is directly related to the engine global efficiency in case of Otto cycle. By this evidence, it is quite common to see conversion of diesel engine into dual fuel engines or methane engine, transform the thermodynamic cycle from diesel cycle to an otto cycle (constant volume combustion) increasing the engine efficiency.

Further consideration to take into account are:

- Gas fuel engines in general have higher combustion efficiency; this fact is due to the "perfect" mixing of the charge and the improved flame stability limits.

- The burning of gases is associated to cleaner product gases with hardly any solid pollutant as soot particulates. This fact leads to lower tendency of corrosion.

- Design, operation and control of the fuel injection system is simpler and easier because of the gaseous nature; there is no need of a fuel pump and the injectors for gaseous are simply made by a valve relay.

A huge limitation is associated with the tendency of fire explosion and toxic hazards, in particular when leakage occurs. However, modern tank system has reached a high level of safety comparable to liquid fuel tanks.

1.2 Dual fuel operation modes

The classic dual fuel engine is basically built up by modifying conventional diesel engine direct injected or with a pre-chamber injection system. The engine modifications basically consist in the integration of the gas injection system. This system is composed of gas injector, gas tank, and one or two pressure reductors depending on the tank pressure. As an example, methane tank pressure is close to 250 Bar, so two reduction stages are required in order to reduce pressure near 5 Bar for injection. The injectors are often in the same number as the cylinders placed into the intake duct; this configuration is chosen mainly for two reasons; the first one is the control of the air-to-fuel ratio, the second one is the fast response of the engine in transient conditions.

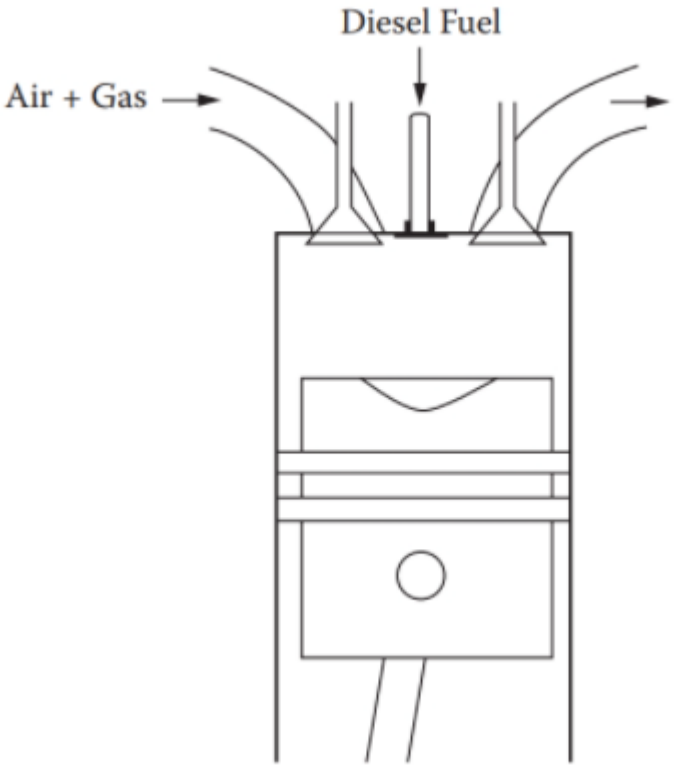

Figure 1 Typical dual fuel engine scheme

Figure 1represents the typical dual fuel engine layout, with PFI gaseous injection system. Dual-fuel engines often derive from diesel engine as mentioned above. The original direct injection system is not modified in hardware components but several differences in injection strategy are necessary. In particular, the diesel fuel is injected in a small quantity to ignite the charge, this usage is called “liquid spark”. Alternatively, injectors can be substituted by classical spark plug, even though maintaining the original diesel injection system may be preferable for the following reasons:

- The liquid spark can ignite very lean mixture; this is very useful for pollutant emissions regulation. Moreover, a “quality” control of the load can be adopted, avoiding the installation of a throttle valve that reduces engine efficiency at low and medium loads.
- The liquid spark reduces the risk of knocking in comparison with traditional spark plug. For this reason, usually, the conversion with spark plugs requires a reduction of the compression ratio of the engine that can be obtained with an expensive substitution of the engine pistons while the engine running on Dual Fuel usually don’t require the same reduction of compression ratio.
- The engine in case of gaseous system failure can run with only diesel fuel, which makes the engine more reliable.
- At high load, the amount of the injection can be reduced because the energy needed to ignite the cargo is less than low loads.
- Methane supply for vehicles is not widespread all over the European country, so that the adoption of a dual fuel engine is required or maybe suggested.

In other words, diesel injection system makes the dual fuel engine more flexible, but the engine control is usually more complex. Spark plug are used in case of engine for energy conversion, because this kind of engine works at fixed engine speed and load, and the fuel supply is taken form the civil network (no need of tank). If the engine derives from a conversion of an old diesel engine (like bus for city transport), it is convenient to leave the

original injection system in order to have some advantages, in other cases the adoption of a spark plug is recommended for simplicity.

Obviously, also the intake throttle valve control is mainly different from diesel engine operation, if present. The intake throttle, generally speaking, must be less open in comparison to the diesel operation mode. This fact leads to decrease efficiency at low loads because the intake pressure drops increase; in this case, the trade-off is the ignition limit of lean charge. The dual-fuel engine at low loads is hybrid concept between a premixed combustion engine (otto-cycle engine) and diffusive combustion (diesel cycle), so if the load of the engine is low and the engine has got no throttle body, the huge amount of air aspirated by the engine must burn for a fraction. According to this evidence, the gas mixture needs to be very lean which decreases the flame propagation and the ignition limit of the charge. In this particular conditions throttle must be used in order to control the air mass flow in a mixture between quantity of charge VS quality of charge.

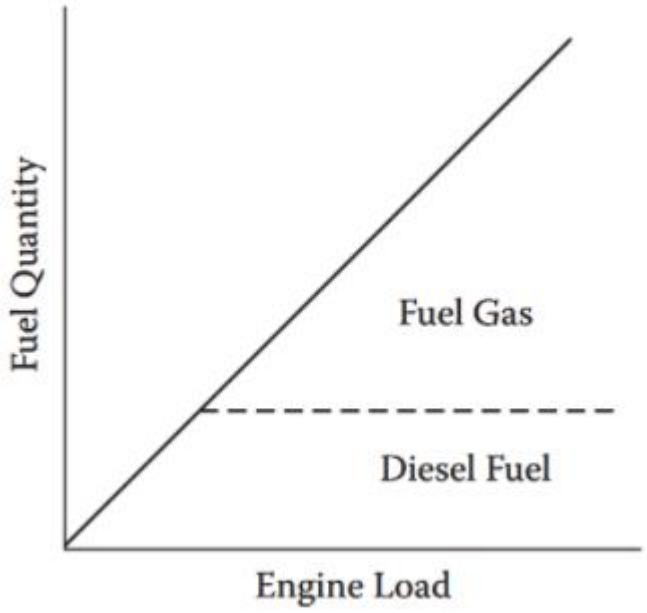

Figure 2 Fuel quantity split strategy

In Figure 2, fuel quantity distribution according to the engine load is represented. The key is to keep diesel fuel consumption constant in order to shift energy balance to gas fuel. The diesel fuel as described above is used as “liquid spark”, so the amount of energy needed to ignite the charge at a fixed air to fuel ratio can be, in first approximation, constant. This approximation can be overcome and the amount of energy in the liquid spark ignition can be quietly reduced. This fact can be explained taking into account the physical conditions in the combustion chamber at high engine load instead of low engine load. At high load gas temperature increases, due to the supercharger compression. Furthermore, the turbulence in terms of momentum of motion quantity increases; this evidence leads to less energy needed to ignite the charge. Consequently, diesel fuel injection can be progressively decreased as engine load increases (Figure 2) .This strategy allows to reach higher engine efficiency in terms of emissions and global efficiency, but on the other hand the calibration of control strategy and the software implementation effort increases.

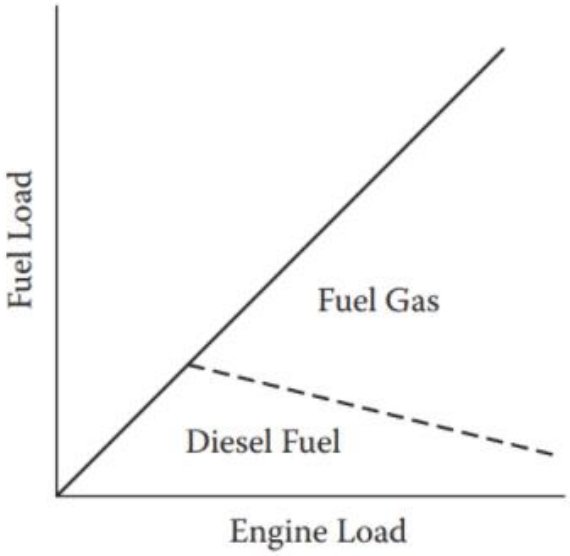

Figure 3 Alternative fuel split strategy

Dual-fuel strategy can also be used in two-stroke engines. In modern engine field there are several applications of two-stroke engine, first of all boat engines; application of this kind of engine also can be seen in snowmobile application, small engine powered tools, energy conversion systems. In particular, two-stroke diesel engines are very efficient but they are characterized by a huge amount of pollutant emissions. Therefore, the fuel supply conversion to gas fuel can be helpful to reduce pollutant emissions and increase performance. In case of loop-scavenged engines, there is an issue due to the charge exchange process; some of the fresh charge pass through the cylinder and flows into the exhaust system, increasing the hydrocarbon emissions. In uniflow-scavenged engines this problem is not present. In conclusion also in two-stroke engines the conversion using natural gas as fuel instead of diesel can be attractive but the described-above constraints have be taken into account when approaching the design of the conversion system.

1.3 Application of dual fuel engines

The applications of dual-fuel engines is widely spread in numerous applications. In particular engine for power generation, driving compressor, water pumps, cogeneration. As described above, the use of this technology can be found in automotive industry for passenger transportation, for example for driving fleet vehicles, heavy duty trucks, buses, locomotive, small medium and heavy boats; last but not least in agricultural applications. Often the application starts from a flexible conversion system applied to a diesel engine. This system can fit a "family" of engines after a calibration process. Common diesel engines tend to ensure successfully long operation life. This makes their conversion to gas fueled operation quite demanding, in particular when high performance is required. There is, for example, a consistent need to develop operational approaches in conjunction with the gaseous fuel combustion characteristics, for instance by a careful choice of pilot fuel size and its injection timing so as to reduce oxides of nitrogen emissions. Moreover, the operation of these engines, especially when employing some gaseous fuel mixtures, can be seriously limited by the onset of knocks. Its avoidance, while retaining the high-compression ratios of the efficient diesel engine, with some gaseous fuels, often remains a challenge and requires proper expertise. The employment of dual-fuel engine for power production despite the above description, has not seen as much wider applications in the past as it could be expected. A number of factors can be suggested to explain their application mostly in stationary engines instead of transport sector[5]:

- The combustion process is more complex than diesel, there is a mixture of issues associated with direct injection diesel combustion and at the same time problems related to premixed combustion.
- The exhaust emissions can decrease in comparison to diesel engine, but this result can be obtained easily if the engine runs at constant loads and speed. If the engine runs in transient conditions, it can affect pollutant emissions. However, many improvements in terms of combustion process have been made, making it easier to deal with these difficulties.

- To obtain all potential benefits with the adoption of dual fuel engine, the engine control system has to be properly implemented and calibrated in order to fit all the operation conditions. This evidence increases development costs a lot, which become bigger as engine flexibility increases.

- There has been a continuing need to retain the capacity of gas-fueled engines to revert to the diesel operational mode promptly and smoothly when needed. This facility must be retained without undermining the performance of the engine as a diesel. This sometimes represents a challenge since diesel engines are required to satisfy increasingly stricter and more challenging requirements of performance and controls.

- Large displacement stationary engines, normally employed for power electric generation, consume very large quantities of fuel. Taking into account this evidence, fuel cost represents one of the higher costs in the entire engine life compared to maintenance operations. This kind of engine is already turbocharged and the performance is well optimized, but gas fuel can furtherly improve performance with an effective cost reduction, with sustainable conversion costs.

- One of the negative effects in the engine gas fuel conversion is related to the gas physic nature; in the intake manifold, some of the air is displaced by gas fuel in terms not negligible. This fact leads to reduce the volumetric efficiency (as described above). The volume decrease is near to 9.51% for methane in stoichiometric conditions. Therefore, the power output may have a little decrease, but the higher thermodynamic efficiency and the higher knock resistance of methane, which allow the usage of higher compression ratio, might reduce this issue.

- The low efficiency and sensitivity to changes in the fuel gas composition of the low-compression-ratio spark ignition gas engine makes it fall increasingly out of favor in comparison to the gas-fueled diesel engine. However, diesel engines, with their continued improvements in the control of their emissions, efficiency, and reliability,

tended to relegate the dual-fuel engine to a secondary role, confining it increasingly to special applications where economic advantages can be assured through the exploitation of much cheaper gaseous fuels.

As a result of all the considerations made in this chapter in Figure 4 we can see the comparison of BSFC (brake specific fuel consumption), in terms of [MJ/kWh] in a typical diesel engine fueled with normal diesel fuel and converted into natural gas fuel. The evidence is a non-negligible improvement in efficiency, especially at medium and high loads, (at low loads combustion speed is lower and very lean mixture can decrease combustion efficiency).

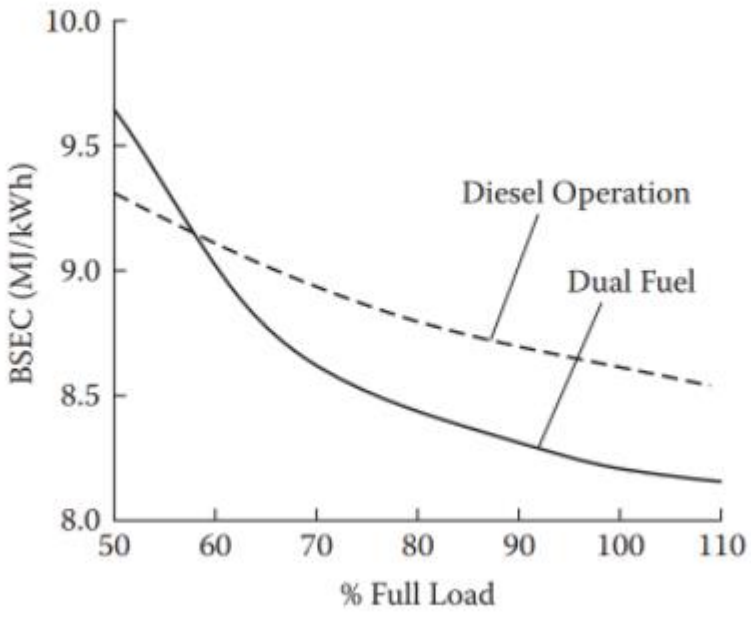

Figure 4 BSFC comparison in dual fuel engine VS diesel engine

The BSFC is directly related to engine efficiency by the relation written below:

$$BSFC = \frac{1}{ki * \eta g}$$

The reduction that can be reached in this application may be up to 10%. This result is the main responsible of the diffusion of this kind of engines as retrofit kits or complete design from the scratch. The particular constraints into automotive application instead of electric power generation or naval engines, have favored first fix applications. However, in the latest years the development made especially in engine control systems and the development in innovative combustion process have paved the way to automotive applications, and they have also opened new research field to be investigated by researchers[6].

2. CFD modelling

2.1 Introduction

As described above in the abstract of this work the aim of this research program is to study the effect of non-convectional combustion process in ICE, in particular into modified diesel engines. The approach is to study the process from a numeric point of view supported by experimental analysis at the test bench. Its first aim is to find a good agreement of calculation results in comparison to measurements at the test bench; secondly, simulations are used to develop an optimized strategy to reach the best results. In order to reach the research target the adoption of CFD (Computational Fluid Dynamics) technique is necessary.

CFD is the study of systems involving fluid flow, heat transfer and associated phenomena such as chemical reactions by means of computer-based simulation. The technique is very powerful and spans a wide range of industrial application fields. Some examples are:

• aerodynamics of aircraft and vehicles: lift and drag

• hydrodynamics of boats

• power plant: combustion in internal combustion engines and gas turbines

• turbomachinery: flows inside rotating passages, diffusers etc.

• electrical and electronic engineering: cooling of equipment including microcircuits

• chemical process engineering: mixing and separation, polymer molding

• external and internal environment of buildings: wind loading and heating/ventilation

• marine engineering: loads on off-shore structures

• environmental engineering: distribution of pollutants and effluents

• hydrology and oceanography: flows in rivers, estuaries, oceans

• meteorology: weather forecast

• biomedical engineering: blood flows through arteries and veins

The first usage of the CFD techniques started from aerospace industry in 1960s, into designing, R&D and manufacturing of aircraft and jet engines. This method has recently been applied to the design of ICE, in particular for the simulation of the flow field into the cylinder and the combustion process into the combustion chamber. Furthermore, vehicle manufacturers now routinely predict drag forces, under-bonnet air-flows and the in-car environment with CFD. Increasingly CFD is becoming a vital component in the design of industrial products and processes. The ultimate aim of development in the CFD field is to provide a capability comparable with other CAE (computer-aided engineering) tools such as stress analysis codes. The main reason why CFD has lagged behind is the tremendous complexity of the underlying behavior, which precludes a description of fluid flows that is at the same time economical and sufficiently complete. The availability of affordable high-performance computing hardware and the introduction of user-friendly interfaces have led to a recent upsurge of interest, and CFD has entered into the wider industrial community since the 1990s.

The CFD as described above is widespread in a lot of industrial fields. The results achievable compared to experimental campaigns lead to diffuse CFD simulations. In particular, there are several advantages:

- Time reduction in component design
- Ability to study complex fluid domain where experimental campaign can be expensive or difficult to run
- Unlimited levels of detail
- CFD can generate huge amount of results with no added costs
- Parametrical geometry optimization

Anyway, CFD requires qualified people in order to manage CFD calculation and to interpret results or to implement different calculation models or strategy.

In fact, the first diffusion of CFD historically starts from academic research before being applied to the industry field. We have to consider the main classification of CFD code: commercial code and open code. The first one is born to fit industry requirements, typically the source code cannot be modified by the user and the calculation grid is a result of an automated process. This fact perfectly fits industry time-to-market needs but it does not match academic research field, if the problem is not “convectional”. For academic research, both types of CFD codes can be used. When the research field or activity is focused on studying different combustion processes or in general problems that are related to physical models, open codes are preferable; they allow to modify the code and to implement new models. On the other hand, if the research activity is focused only on engine design (e.g. combustion chamber design, inlet ports design, etc.) with conventional combustion processes, a commercial code can be useful for achieving the objective. In this work, results obtained by the adoption of both codes are presented, according to the activities and taking into account the above-mentioned considerations. In particular, the open code used is a modified version ok KIVA-3V developed by a collaboration between Unimore and Chalmers University.

2.2 Kiva 3V introduction

The main CFD software adopted in the analysis of combustion process either for methane blended with diesel and gasoline blended with diesel is a custom version of Kiva 3V. This custom version has been developed in Chalmers University in collaboration with Unimore University. Kiva 3V is an open-source code Fortran based; it has been developed in Los Alamos National Laboratory. The first version of the software dates back to 1970 and derives from the previous Los Alamos National Laboratory experiences in the CFD field, mainly related to the Manhattan Project, in which the very early CFD code were used to study nuclear weapons. The first version of the code was able to solve reactive flows for generic application, but, in 1976, Dan Butler, Los Alamos CFD team leader, realized that the program, if properly adapted, could have simulate reactive flows in internal combustion engines [7].The development of the application for internal combustion engine starts and was carried to the birth of the first version of Kiva3V, presented in a SAE paper in 1985 [8].

2.3 Kiva-3V CFD modelling theory

As mentioned above, Kiva 3V is a Fortran based Code. The code is open and therefore, in the research field, many modifications have been made in years in order to adapt simulations to specific problems (e.g. Diesel Combustion, Hydrogen combustion, Dual fuel combustion). In particular, the department of University of Modena and Reggio Emilia in collaboration with the Chalmers University in 2006 developed a detailed chemistry reaction in order to simulate Diesel combustion[9]. The model has been calibrated by several experimental and numerical validations. The fluid calculation domain is discretized by a block-structured mesh. The block-structured mesh and the solution models for transport equations on it are preferred by consideration of the fluid flow problems with high Reynolds and Grashof numbers and turbulence[10]. The advection of heat and of species is also easier computed on the structured mesh. This particular mesh allows to achieve the required resolution in the boundary layers using fewer elements than with the unstructured ones. The higher mesh resolution results in the application of the mesh cells with high aspect ratio. The structured mesh is build up with numerical blocks. Each numerical block is a polygon with at least 4 corners which mark 4 block sides which are pairwise opposite to each other. The structured mesh inside of the block consists of two systems of the mesh lines. The number of the mesh elements at the opposite sides should be equal. In the figure below, an example of structural mesh is represented (two stroke engine):

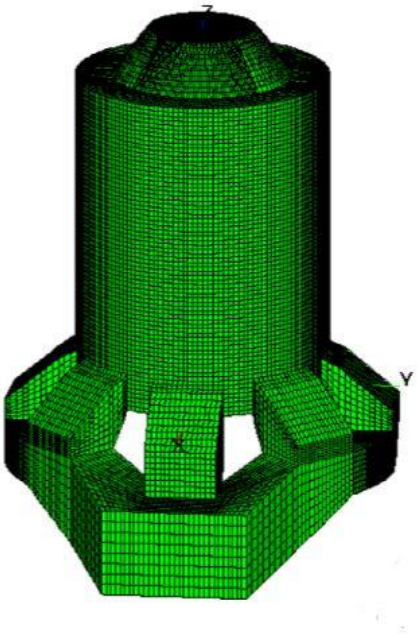

Figure 5 Kiva structure mesh example

Kiva also provides a pre-process software K-3PREP that is used to generate the calculation grid starting from block coordinates. This software is quite good when it is necessary to generate parametrical geometry analysis, because it can generate an algorithm that automatically generates a calculation grid. This feature is especially useful when the geometry studied is not so detailed in order to investigate macro geometrical parameter for first design [11]. The mesh represented in Figure 5 has been generated by K3-PREP, we can observe that geometrical details are quite poor, in that case the base geometry has been used for a parametrical optimization.

2.3.1 RANS equations

Kiva code adopts RANS (Raynolds Avarage Navier Stokes) method for the resolution if the flow field into the engine fluid domains. These equations are time-averaged equations of

flow. The method is adopted to solve turbulent flows and it can be applied to approximate the solution of Navier Stokes equations, represented in figure below:

$$\rho\frac{Du}{Dt} = -\frac{\partial p}{\partial x} + \text{div}\,(\mu\text{grad}\ u) + S_{Mx}$$
$$\rho\frac{Dv}{Dt} = -\frac{\partial p}{\partial y} + \text{div}\,(\mu\text{grad}\ v) + S_{My}$$
$$\rho\frac{Dw}{Dt} = -\frac{\partial p}{\partial z} + \text{div}\,(\mu\text{grad}\ w) + S_{Mz}$$

(2.1)

The main characteristic of this method is the application of Reynolds decomposition to Navier Stokes equations. RANS's method divides flow variables into mean component (u), and fluctuating component (u'). The mean component is a Reynolds operator; these operators have several properties. One of these properties is that the mean fluctuating component is zero12. Therefore, taking the Navier stokes equations into account, and adding this hypothesis and considering the continuity equation div(u)=0, we first note that div u = div U. This yields the continuity equation for the mean flow:

$$\text{div}\ \mathbf{U} = 0$$

(2.2)

A similar approach can be adopted in x- momentum equation. The time average of the individual terms can be written as:

$$\frac{\partial \bar{u}}{\partial t} = \frac{\partial U}{\partial t}$$
$$\frac{1}{\rho}\frac{\partial}{\partial x} = -\frac{1}{\rho}\frac{\partial P}{\partial x}$$
$$\frac{\text{div}\,(u\mathbf{u})}{v\text{div}\,(\text{grad}\,(u))} = \text{div}\,(U\mathbf{U}) + \text{div}\left(\bar{u'\mathbf{u}'}\right)$$

(2.3)

Adding these results to the time-average x-momentum we obtain:

$$\frac{\partial U}{\partial t} + \text{div}\,(U\mathbf{U}) + \text{div}\left(\bar{u'\mathbf{u}'}\right) = -\frac{1}{\rho}\frac{\partial P}{\partial x} + v\text{div}\,(\text{grad}\,(U))$$

(2.4)

Executing the same process for y-momentum and z-momentum, and algebraically manipulating the three equations we obtain:

(2.5)

$$\frac{\partial U}{\partial t} + \text{div}\,(U\mathbf{U}) = -\frac{1}{\rho}\frac{\partial P}{\partial x} + v\text{div}\,(\text{grad}\,(U)) + \frac{1}{\rho}\left[\frac{\partial\left(-\rho\bar{u'^2}\right)}{\partial x} + \frac{\partial\left(-\rho\bar{u'v'}\right)}{\partial y} + \frac{\partial\left(-\rho\bar{u'w'}\right)}{\partial z}\right]$$
$$\frac{\partial V}{\partial t} + \text{div}\,(V\mathbf{U}) = -\frac{1}{\rho}\frac{\partial P}{\partial y} + v\text{div}\,(\text{grad}\,(V)) + \frac{1}{\rho}\left[\frac{\partial\left(-\rho\bar{u'v'}\right)}{\partial x} + \frac{\partial\left(-\rho\bar{v^2}\right)}{\partial y} + \frac{\partial(-\rho\bar{v}'w')}{\partial z}\right]$$

(2.6)

$$\frac{\partial W}{\partial t} + \text{div}\,(W\mathbf{U}) = -\frac{1}{\rho}\frac{\partial P}{\partial z} + \nu\text{div}\,(\text{grad}\,(W)) + \frac{1}{\rho}\left[\frac{\partial\left(-\rho\overline{u'w'}\right)}{\partial x} + \frac{\partial\left(-\rho\overline{v'w'}\right)}{\partial y} + \frac{\partial\left(-\rho\overline{w'^2}\right)}{\partial z}\right] \tag{2.7}$$

The equations system formed by (4.2 ,4.5-7) is called Raynolds-Avarage Navier Stokes Equations. These equations are written in the hypothesis of incompressible flow. For clarity in table below, the set of valid equations is reported in case of compressible flows.

Continuity

$$\frac{\partial\bar{\rho}}{\partial t} + \text{div}\,(\bar{\rho}\tilde{\mathbf{U}}) = 0 \tag{2.8}$$

Reynolds equations

$$\frac{\partial(\bar{\rho}\tilde{U})}{\partial t} + \text{div}\,(\bar{\rho}\tilde{U}\tilde{\mathbf{U}}) = -\frac{\partial\bar{P}}{\partial x} + \text{div}\,(\mu\text{grad}\;\tilde{U}) + \left[-\frac{\partial\left(\bar{\rho}\overline{u'^2}\right)}{\partial x} - \frac{\partial\left(\bar{\rho}\overline{u'v'}\right)}{\partial y} - \frac{\partial\left(\bar{\rho}\overline{u'w'}\right)}{\partial z}\right] + S_{Mx}$$

$$\frac{\partial(\bar{\rho}\tilde{V})}{\partial t} + \text{div}\,(\bar{\rho}\tilde{V}\tilde{\mathbf{U}}) = -\frac{\partial\bar{P}}{\partial y} + \text{div}\,(\mu\text{grad}\;\tilde{V}) + \left[-\frac{\partial\left(\bar{\rho}\overline{u'v'}\right)}{\partial x} - \frac{\partial\left(\bar{\rho}\overline{v'^2}\right)}{\partial y} - \frac{\partial\left(\bar{\rho}\overline{v'w'}\right)}{\partial z}\right] + S_{My} \tag{4}$$

$$\frac{\partial(\bar{\rho}\tilde{W})}{\partial t} + \text{div}\,(\bar{\rho}\tilde{W}\tilde{\mathbf{U}}) = -\frac{\partial\bar{P}}{\partial z} + \text{div}\,(\mu\text{grad}\;\tilde{W}) + \left[-\frac{\partial\left(\bar{\rho}\overline{u'w'}\right)}{\partial x} - \frac{\partial\left(\bar{\rho}\overline{v'w'}\right)}{\partial y} - \frac{\partial\left(\bar{\rho}\overline{w'^2}\right)}{\partial z}\right] + S_{Mz}$$

(2.9)

Scalar equation

$$\frac{\partial(\bar{\rho}\widetilde{\Phi})}{\partial t} + \text{div}\,(\bar{\rho}\widetilde{\Phi}\widetilde{\mathbf{U}}) = \text{div}\left(\Gamma_{\Phi}\text{grad}\ \widetilde{\Phi}\right) + \left[-\frac{\partial\left(\bar{\rho}\overline{u'\varphi'}\right)}{\partial x} - \frac{\partial\left(\bar{\rho}\overline{v'\varphi'}\right)}{\partial y} - \frac{\partial\left(\bar{\rho}\overline{w'\varphi'}\right)}{\partial z}\right] + S_{\Phi} \tag{2.10}$$

2.3.2 Kiva Turbulence Modulation

Turbulence modelling is of fundamental importance in order to study combustion process, in particular Kiva-3V adopt a modified version for compressible flow of k-ε model called RNG k-ε proposed by Han and Reitz[7]. The compressible flow is take into consideration with an extra term added to the dissipation equation witch change in the main strain rate, and compressibility of the flow is accounted for. In the next equations reported below, the RNG k-ε method is described.

$$\frac{\partial \rho k}{\partial t} + \nabla \cdot (\rho u k) = -\frac{2}{3}\rho k \nabla \cdot u + \tau : \nabla u + \nabla \cdot (\alpha_k \mu \nabla k) - \rho \varepsilon + \dot{W}^s$$

(2.11)

$$\frac{\partial \rho \varepsilon}{\partial t} + \nabla \cdot (\rho u \varepsilon) = -\left[\frac{2}{3}C_1 - C_3 + \frac{2}{3}C_\mu C_\eta \frac{k}{\varepsilon}\nabla \cdot u\right]\rho \varepsilon \nabla \cdot u + \nabla \cdot (\alpha_\varepsilon \mu \nabla \varepsilon) + \frac{\varepsilon}{k}\left[(C_1 - C_\eta)\tau : \nabla u - C_2 \rho \varepsilon + C_s \dot{W}^s\right]$$

(2.12)

$$C_3 = \frac{-1 + 2C_1 - 3m(n-1) + (-1)^\delta \sqrt{6} C_\mu C_\eta \eta}{3}$$

(2.13)

$$\delta = 1; \quad \text{if } \nabla \cdot u < 0$$
$$\delta = 0; \quad \text{if } \nabla \cdot u > 0$$

(2.14)

$$C_\eta = \frac{\eta(1 - \eta/\eta_0)}{1 + \beta \eta^3}$$
$$\eta = S\frac{k}{\varepsilon}$$

(2.15)

In Equations (4.8-10), we find the variables reported below:

- K : turbulent kinetic energy
- ε : turbulent kinetic energy dissipation rate
- ρ, u, τ, μ : are respectively density, velocity, stress tensor and effective viscosity
- η : the ratio of the turbulent to mean strain scale
- $S = \left(2S_{ij}S_{ij}\right)^{1/2}$ is the magnitude of main strain $S_{ij} = \left(\partial\bar{u}_i/\,\partial x_j + \partial\bar{u}_j/\,\partial x_i\right)/2.$
- Constants : $m = 0{,}5, n = 1 c_\mu = 0.0845, C_1 = 1{,}42\,, C_2 = 1{,}68, \alpha_k = \alpha_\varepsilon = 1{,}39, \eta_0 = 4{,}38, \beta = 0.012$

Source terms involving the quantity $\dot{W}^s$ account for the interaction between the gas and the spray. Physically W * is the negative of the rate at which the turbulence eddies do work in dispersing the spray droplets. Cs is suggested to be 1.5 [1]. The Cj term accounts for the non-zero velocity dilatation which is closed based on a rapid distortion analysis [36]. Notice that the value of C? varies from 1.726 during compression to -0.9 during expansion [36], which covers the range of values suggested in the previous literature.

2.4 Combustion Modeling

The kiva-3v version used for the calculation campaign is a custom version developed by Unimore and Chalmers University in Sweden. The team integrated Fortran based code CHEMKIN-II in order to obtain a detailed chemistry mechanism to simulate diesel combustion. The model has been calibrated as described in [9]. Obviously in CFD 3D internal combustion engine simulations the physical process is well emulated if the code is well calibrated; in other words code can be predictive if the models implemented into the code fits the combustion process that has to be emulated. This can be traduced in implement detailed chemistry and custom reaction for the specific fuel. Kiva 3V solves fuel spray evaporation coupled with turbulent fluid dynamics of compressible, multiphase, multicomponent, reactive gases in combustion chamber geometry. Kiva 3V calculation code includes detailed combustion chemistry linked to a comprehensive oxidation mechanism of diesel oil surrogate (DOS) [13], turbulence\chemistry model in terms of PaSR (Partially Stirred Reactor Model) [14]. In the modified version of kiva Senkin code of the Chemkin-2 a validated mechanism of combustion for Diesel Oil has been finally build and calibrated. .

2.4.1 Diesel Surrogate Model

In order to simulate properties of diesel oil, a DOS has been implemented in the CFD code. The fuel vapor is modeled by simulating a multicomponent nature of the fuel vapor, regardless that the fuel is assumed to be constructed by one component. Because real diesel oil composition and properties are quite complex in KIVA-3V fuel library, this information was used in the modeling and only the specified chemical formula of the fuel was selected as $C_{14}H_{28}$. Nevertheless, the oxidation models of real fuel Diesel oil are not known; fuel is assumed to be decomposed into n-heptane C_7H_{16} and toluene C_7H_8:

$$1.5C_{14}H_{28} + 0.5O_2 \Rightarrow 2C_7H_{16} + C_7H_8 + H_2O$$

(2.16)

Then detailed chemical sub-mechanism for the other components were constructed. The complete set of equations is composed of 70 species participating in 310 base, global and surface kinetic stage. N-heptane, was chosen to be in excess, since the cetane number is 56 (similar to the original Diesel Oil). Conversely, mechanisms for aliphatic substances and aromatics, which quantify a large part of diesel oil composition, are not well developed. Taking the last observation into consideration ,the existing detailed mechanism did not reach a good agreement in terms of combustion prediction; in this scenario a refinement of the toluene kinetic model was needed to improve performance and to match experimental data. Here below we report the new set of reactions including double ketone $C_6H_4O_2$:

$$C_6H_5 + O_2 = C_6H_4O_2 + H$$
$$C_6H_4 + O_2 \Rightarrow 2CO + C_2H_2 + CH_2CO_2$$
$$C_6H_5O + O \Rightarrow C_6H_4O_2 + H$$
$$C_6H_5O + HO_2 = C_6H_4O_2 + H_2O$$

(2.17)

As a result of the calibration campaign the model matches the experimental data. The calibration process has been performed running several CFD 3D simulations in a constant

volume and adiabatic conditions, at different pressures and temperatures. The results are reported in the figure below [15].

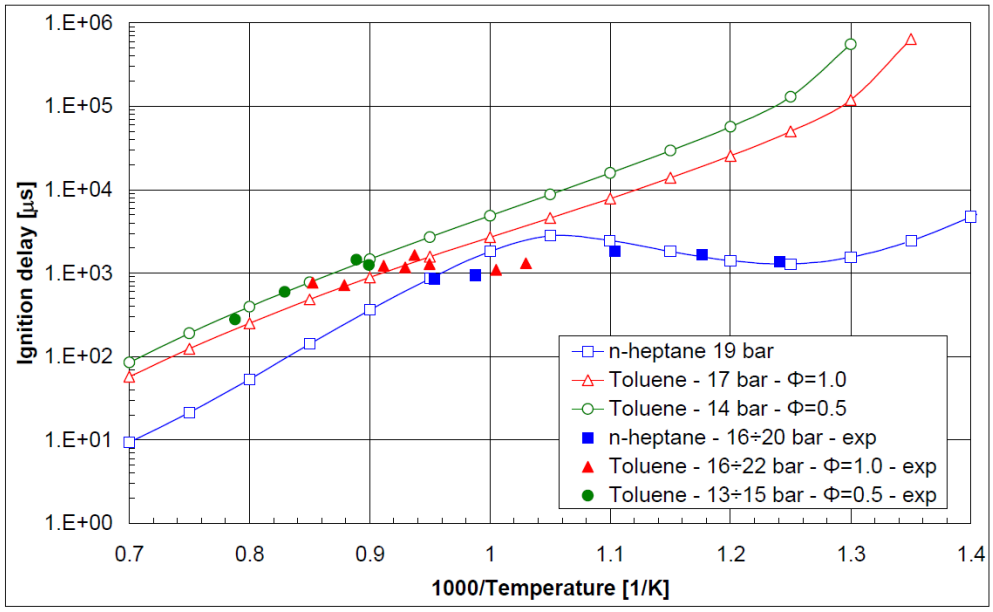

Figure 15 Ignition delay calculated for different mixture and temperature VS compared with the stock-tube data at low pressure

2.4.2 Turbulence/Chemistry interactions

Most methods in CFD 3D simulations involve solving RANS equations. In turbulent combustion modelling, itis of fundamental importance to insert models which take into account macro and micro scale in terms of mixing. In order to show the effects of imperfect mixture, the PaSR model is used.

Assuming that chemical reactions proceed in such a way that a shortest chemical time for a particular species in the reaction is constrained by the micro-mixing time, the PaSR equations read:

$$\frac{dc^1}{dt} = \frac{c^1 - c^0}{\tau} = -\frac{c}{\tau_c}, \frac{c - c^1}{\tau_{mix}} = -\frac{c}{\tau_c} \tag{2.18}$$

Where τ is the time step, τ_{mix} is the micro-mixing time and τ_c is the chemical reaction time. The model can distinguish between: concentration in reactor zone c, reactor exit c^1 and in the feed c^0. With some manipulations, the equation can be written as below:

$$\frac{c^1 - c^0}{\tau} = -\left(\frac{c^1}{\tau_c}\right) \cdot \kappa = -\frac{1}{2} H\left(\frac{c^1}{\tau_c}, \frac{c^1}{\tau_{\text{mix}}}\right) \tag{2.19}$$

where $\frac{k=\tau_c}{\tau_{mix}+\tau_c}$, and H is a harmonic mean

The equation reported above (4.20) shows that the turbulent combustion time is the total of mixing plus reaction times, in case the process is represented in terms of reactor parameter. This fact is due to PaRS modulation. For the detailed chemical mechanism, the net production

rate of the reference species due to the chemical reaction with accounting for the micro mixing effect can be given in a form:

$$\frac{c_s^1 - c_s^0}{\tau} = f_r(c^1) \cdot \kappa = \frac{c_s^0 f_r^0}{c_s^0 + \text{ term } \bar{r}\,\tau + \text{ term } \bar{r}\,\tau_{mix}} \tag{2.20}$$

Where term $\bar{r}$ and f_r^0 are the terms representing mass depletion rate and net chemical production rate.

The above written equation (4.20) is deduced in the hypothesis that chemical reaction times are defined as characteristic times of the species destruction rates, when the production terms are reported in equation below (4.21)

$$f_r(c) = (v_r'' - v_r')\dot{\omega}_r(c) = \text{ term } \overset{+}{r} - \text{term } \bar{r} = \\ = \text{term } \bar{r} - c_s/\tau_c \tag{2.21}$$

The 4.22 v_r'' and v_r' are stoichiometric of the backwards of stages, $\dot{\omega}_r$ is the rate progress variable of the reaction, respectively. Equation 4.21 can be founded if τ_c (chemical reaction time) is defined as characteristic times of the species destruction rates, when the species production are presented as in 4.22. Micro mixing phenomena is described in terms of Kolmogorov's time definition [16]. References species are defined as the species which have smallest concentration among those defining the depletion rate in the linear form 4.22. This definition is similar to Magnussen-Hjertager (M-H) model. This approach introducing such a reference species for each reaction helps to better simulate non -linear expression term $\bar{r}$ by the linear one c_s/τ_c. Manipulating expression 4.21 and substituting the expression 4.22 it can be obtained:

$$f_r(c) = (\text{ term}_r^+ - c_s/\tau_c)\frac{\tau_c}{\tau_c + \tau_{\text{mix}}} = \\ = \text{term}_r^+ \frac{\tau_c}{\tau_c + \tau_{\text{mix}}} - \frac{c_s}{\tau_c + \tau_{\text{mix}}}$$

(2.22)

For the chemical equilibrium conditions $f_r(c)$=0 , term $_r^+ = c_s^{eq}/\tau$c , the final equation with $\tau_c \to 0$ of PaSR can be written in the follow form:

$$\lim_{\tau_c \to 0} f_r(c) = \frac{c_s^{eq} - c_s}{\tau_{\text{mix}}}$$

(2.23)

That perfectly complies with the classic expression of the Magnussen-Hjertager Model.

3 Optimization of a Dual fuel (Natural gas-Diesel) for Gen-sets

3.1 Introduction

The focus of this research activity is to investigate and develop an efficient engine for electric generation (gen-set). The target power of this generator is set to 80 kW. In the Internal combustion engine for gen-set scenario, typical adopted engines are for heavy duties applications (HD). In the GEN-SET applications, engines typically runs at 1500 rpm or at 1800 rpm depending on the electrical frequency. In the table below some typical engine generators are reported..

Manufacturer	DEUTZ	VOLVO PENTA	Cummins	HIMOINSA/ FPT_IVECO	MOTEURS Baudouin
Engine Type	CI	CI	CI	CI	CI
Cylinders arrangement	In-line	In-line	In-line	In-line	In-line
Number of cylinders	6	4	4	4	4
Turbocharger	✓	✓	✓	✓	✓
Injection type	DI	DI	DI	DI	DI
Bore x Stroke [mm]	102 x 132	108 x 130	107 x 124	104 x 132	105 x 130
Displacement [L]	6.47	4.76	4.46	4.49	4.50

Compression Ratio	n.a.	18.0:1	n.a.	17.5:1	18.0:1
Rated rpm@50 Hz	1500	1500	1500	1500	1500
Max. Prime Power at rated rpm [kW]	93.1	76.0	82.0	88.6	74.0
BMEP at max. Prime Power, rated rpm [bar]	11.51	12.76	14.71	15.80	13.15
Fuel consumption at max. Prime Power, rated rpm [L/h]	23.4	21.1	22.0	22.0	18.6
BSFC at max. Prime Power, rated rpm [g/kWh]	209	231	223	206	209
Specific Prime Power at rated rpm [kW/L]	14.39	15.95	18.39	19.75	16.43

Table 2 Typical GEN-SET engines

The engines reported in the table are, as described above, HD engines, so they are very reliable, robust and with a high efficiency near to 200 g/kWh. Nevertheless, the specific power is too low, which leads to have bulky power units. Another evidence to take into consideration for the future of these engines are pollutant emissions, from this point of view in the GEN-SET field the non-road emission standards are close to euro-5 regulations. Therefore, during next years the design of the whole exhaust system and in particular the design of the after-treatment system must be reinvented. The development of an after-treatment system and the

calibration of the new GEN-SET is very expensive. It can be worthwhile running these engines with natural gas NG (Methane); this adoption can drastically simplify after-treatment systems, a simple 3-way catalyst can be used, because of the stoichiometric ratio imposed by spark plug natural gas engines. In addition, the adoption of natural gas is more eco-friendly, also a percentage of this gas can derive from a sustainable sources, furthermore NG is normally less expensive than diesel oil.

However, the adoption of a spark plug engine, decreases engine efficiency, which is due to low compression ratio reachable at knock limit and to the increase of gas heat exchanges into the cylinder during combustion process. A possible different scenario can maintain compression ignition engines (CI), operating in dual fuel mode. In this way, theoretically, it is possible to generate a low reactivity fuel mixed with a PFI system ignited by a high reactivity fuel (diesel oil) directly injected into the combustion chamber. The idea is to ignite a lean charge with a small amount of Diesel Oil; this concept is called “Liquid Spark”.

Converting a direct injected diesel engine into dual fuel engine is quite easy because the only mandatory modification is the adoption of a methane injection system, which is quite cheap (this evidence will be described in the further section). Obviously, there are further improvements that can be added in order to better optimize the whole system (e.g. combustion chamber design, piston bowl design, compression ratio). Maintaining the original compression ratio of the CI engine can lead to reach the same global efficiency of the unmodified engine.

Engine efficiency is related to diesel substitution rate: the more the amount the better is the efficiency increase possibility, but huge amount of NG can lead to knock phenomena.

In order to investigate the substitution rate limit an experimental campaign has been carried out on an experimental engine with several operation points. Every operation point and every step of Diesel substitution needs a specific calibration process. This result can be reached only with a specific and modern control system, so the adoption of a modern diesel engine[17] is mandatory.

3.2 The engine choice

According to all the consideration made in the sections above, the engine chosen is a light-duty diesel engine directly injected, fully-electrical controlled with a development ECU (see next section). This engine is designed for automotive field, basically developed by VM motors in Cento (FE Italy) Figure 6. The main characteristic of the engine are reported in the table below.

Figure 6 VM 428 Diesel Engine

Engine	HSDI 4-S Diesel, EURO IV
N. of cylinders and arrangement	4 in-line
Total displacement [L]	2.78
Bore x Stroke [mm]	94 x 100
Compression ratio	17.5:1
N. of valves per cylinder	4
Air Metering	VGT + Intercooler
Injection system	Common Rail
Max. Injection press. [MPa]	160
Injector hole diameter [mm]	0.153
Number of injector holes	6
EGR system	High Pressure with EGR cooler
Max. brake power [kW @rpm]	130@3800
Max. brake torque [Nm @rpm]	440@1750
Max. Peak cylinder pressure [bar]	150
Max. engine speed [rpm]	4600

Table 3 VM 428 Tech specs

This engine can normally run over 4000 rpm due to the common rail high pressure injection system and the relative small stroke of the pistons. The highest rpm reachable with this engine lead to say that running this engine at 3000 rpm is very easy and not onerous for this power unit. The BMEP reached at this revs is near to 12 BAR, so the power output is near to 80 Kw, similar to engines reported in Table 1 Table 3. Furthermore, there are several advantages with the adoption of this engine:

- The overall dimensions of the GEN-SET power unit are quite small in comparison to the typical engines adopted
- The total weight is significantly reduced
- The global thermal load in terms of BMEP in comparison to HD engines is lower than 25%

The main focus of the calibration process is to minimize, as already mentioned in the previous section, the Diesel oil mass flow trying to maintain the same global efficiency and/or trying to find some improvements. All these hypothesis have taken into account pollutant emissions constraints; in other words any increase of pollutant emission is tolerated in order to obtain a homolog able configuration of the operation point considered, only an increase of CO and HC can be tolerated, due to the different combustion process. The new process is an hybrid between diesel and otto-cycle, so the higher the percentage of substitution of diesel oil, the higher CO and HC emissions are expected. As far as NOx emissions are concerned, the goal of calibration is to keep them lower or equal to the stock Diesel engine in order to reduce the cost and complexity of the after-treatment system.

The most important operating point typically investigated for the development of the GEN-SET engine are the follow:

- Rated speed 1500 rpm ; for the new application 3000 rpm at maximum load
- Rated speed a 75% of the maximum load.

In this research activity investigated BMEP are more than the two points normally studied. Low load conditions were investigated in order to reach NG substitution limit and also a medium load, because in normal use of the GEN-SET load can be fluctuating in time and cover all operating condition at fixed engine speed. In this way it is important to demonstrate not only two operation points but the whole operation field in order to investigate limitation in NG substitution. In the table below the operation points analyzed in this study are reported.

RPM [rev/min]	**Engine Load** [Nm]
3000	44
3000	88
3000	177
3000	265

Table 4 Operating points

Figure 7 and Figure 8show the pollutant mass flow rate in function of the engine load, measured on a reference diesel engine @ 3000 rpm. No EGR is present because the EGR valve is closed, in order to distinguish emission only in terms of load instead of load VS EGR mass flow rate. The graph demonstrates that it is not necessary to run in dual fuel mode in all operating points: at low loads, engine can run only with diesel oil.

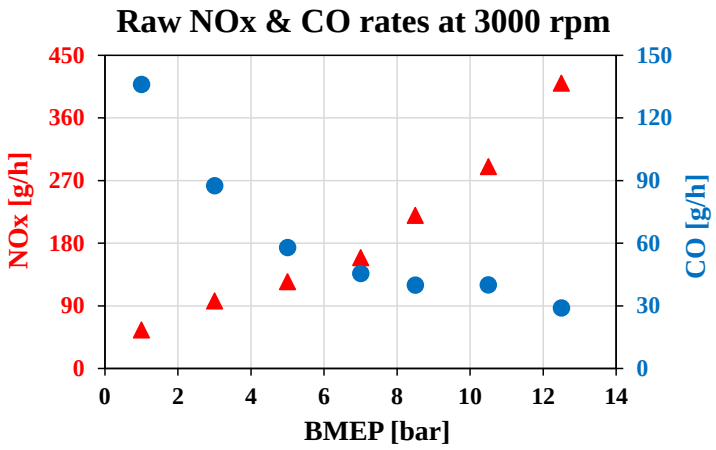

Figure 7 NOx and CO vs BMEP

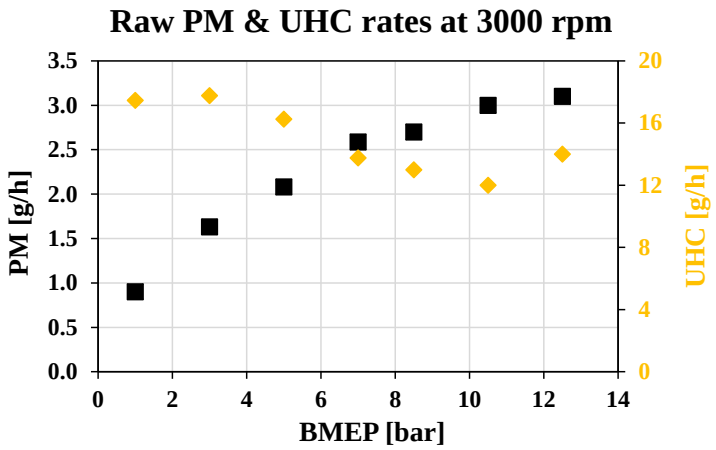

Figure 8 PMI and UHC vs BMEP

This experimental study due to the deep insight of the combustion process is suitable also as a guideline to set up strategies for other applications (e.g. for passenger cars without FAP, boats trucks).The experimental campaign is followed by a CFD 3d calculation campaign in order to validate numerical results and to set the baseline for next developments of the concept for other applications.

3.3 Background of DF operation mode

The engine test has been carried out, first of all, choosing the operation points running dual fuel operation. In the table 5 we can observe the investigated operating points. Engine speed is fixed at 3000 rpm, because one of the main advantages in dual fuel operation is to convert engine for electric generation, as already described in the previous section.

Above all, when running in dual fuel operation mode it is necessary to define some variables. Considering a specific operating point running in standard diesel operation, m_d defines the mass injected for each engine cycle. When running in dual fuel operation this amount decreases due to the increase amount of NG; the Diesel oil flow rate in this case is called m'_d . The ratio between this two quantities is defined as Diesel combustion fraction:

$$x = \frac{m'_D}{m_D} \tag{3.1}$$

In this condition the amount in terms of injected mass per cycle of NG needed (in hypothesis of combustion efficiency equal to 1) can by expressed by:

$$m_{NG} = \frac{(1-x)m_D LHV_D}{LHV_{NG}} \tag{3.2}$$

Where LHV are low heating value of Diesel and NG respectively

$$\lambda_{NG} = \frac{(\alpha - x\alpha_{s,D})LHV_{NG}}{(1-x)\alpha_{s,NG}LHV_D} \tag{3.3}$$

In dual fuel combustion mode, it is important to have an estimation of the air-to-fuel ratio of the premixed charge λ_{NG} . In order to calculate this parameter several hypotheses have been made:

- The air mass delivery is supposed to be constant
- The amount of diesel injected is low in comparison to NG
- Diesel complete combustion ends before NG combustion process according to the higher reactivity
- Diesel subtracts to the premixed charge air mass equivalent to $(m'_D \alpha_{s,D})$, $\alpha_{s,D}$ is the stoichiometric air fuel ratio of Diesel fuel

Considering all the hypotheses above, the relative air-to-NG ratio obtained from a given residual Diesel combustion fraction may be expressed as:

$$\lambda_{\mathrm{NG}} = \frac{(\alpha - x\alpha_{\mathrm{s,D}})\mathrm{LHV_{NG}}}{(1-x)\alpha_{\mathrm{s,NG}}\mathrm{LHV_D}} \tag{3.4}$$

Where:

- $\alpha = \mathrm{m_a}/\mathrm{m_D}$ is the mass ratio of air to Diesel in standard diesel combustion mode
- $\alpha_{s,NG}$ is the stoichiometric air-to-fuel ratio of the NG

The equation reported is valid only if x is a small value. When there is a big amount of diesel, a big portion of Natural Gas burns together with diesel, in this condition it is not possible to estimate the portion of air burnt by the single fuel. This equation is reported in the Figure 9.

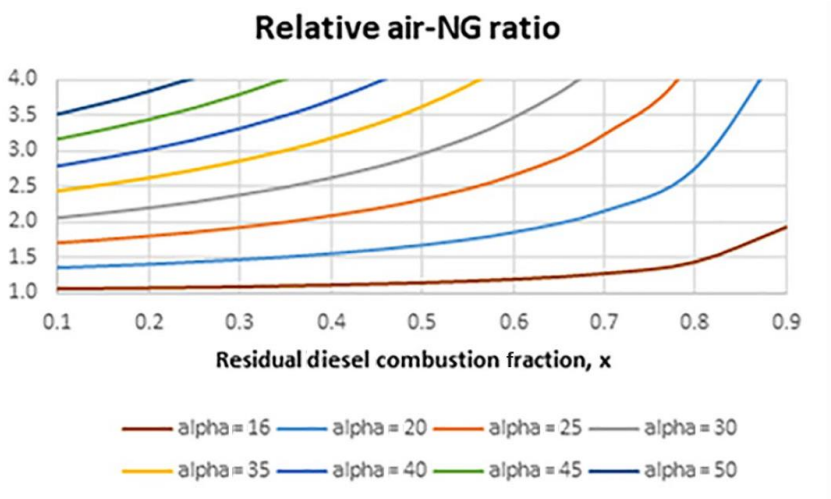

Figure 9 Influence of residual Diesel combustion fraction

Observing Figure 9 we may observe that a big amount of substitution is critical at high loads, because in this case, risk of knocks increases due to the high AFR= 16-20 and to the high compression ratio of the engine. In this scenario, a safe threshold can be set to $\lambda_{NG} = 1.5$, the minimum value of x is 0,4 and 0.8 with respectively α== 20 and 16. In percentage, this means a 60% reduction of diesel oil and 20% respectively[18].

Conversely, when the load is low α is very high, this leads to have unburnt gases because too lean mixtures have a huge decrease in combustion speed. One possible alternative can be to increase the amount of EGR or to control boost pressure. When the amount of NG is enough, DF combustion process is near to a conventional spark ignited engine, however the distribution of the mass fraction burned in comparison to a SI engine is slightly different in the first phase; in the DF operation the first part of the combustion is faster. This fact is due to the amount of Diesel oil injected for the ignition of the charge in the first part of the process.

3.4 Pollutant emissions

In terms of pollutant emission the application of dual fuel process can determine several advantages in terms of exhaust pollutant emissions, and also some disadvantages.

In literature, there are several works that explain that the main advantage of the introduction of Dual fuel combustion process is represented by the soot reduction [19–27]. The main reason for this assumption is that soot is a product in the diffusive combustion process of the Diesel fuel. However, in DF operation this amount is drastically reduced and this evidence demonstrates the soot reduction. Another evidence is the absence of Polycyclic Aromatic Hydrocarbons (PHAs)in NG, which are precursors of PM formation[28].

The second advantage in DF introduction is the reduction in of CO_2 [21,22,29], this is due to the higher Hydrogen element in Methane molecule. Unburned Hydrocarbon emissions slightly increase when passing to diffusive to pre-mixed combustion[30,31].The main reasons are:

- In lean mixtures combustion speed is lower than stoichiometric mixture, fuel far from the injector can not react
- Some fuel may be lost because NG is injected in engine Port, so fuel can by-pass combustion chamber when intake and exhaust valve are open.

Another negative difference in DF and CI is the increase in CO emissions, the reasons are similar to HC emission increase, in addition we can add:

- HC oxidation reactions are faster than CO oxidation, as result the CO concentration can freeze
- Combustion partial products contain a huge percentage of CO, this reaction tends to freeze during the expansion phase

As regarding NOx emission in literature discordant conclusions are reported, in some cases it is reported a reduction[19,26]; in others works, though, an increase is observed [22,24,27]. In the former case, we can consider the following hypotheses for the NOx decreasing:

- Premixed charge made of NG and Air has a higher heat capacity than air, this leads to have a lower temperature at the end of compression, and consequently to a reduction of NOx
- The increase of temperature due to DF operation mode is smaller especially when the premixed charge is lean.

Nevertheless, if a relatively large volume of air and NG is ignited by the injection of Diesel fuel, the local temperature tends to rise abruptly, along with the formation rate of NOx.

Global efficiency is related to the operation point and at high value of λ_{NG} emissions we can observe:

- Decreasing of Combustion efficiency due to not complete combustion
- High heat losses due to the slow combustion process in DF operation mode when the mixture is lean

In conclusion, when passing from a standard Diesel combustion process to a DF process with a premixed charge of Methane, taking into account the same operation point (speed and load), CO_2 and SOOT emissions are expected to decrease; CO and HC to increase, and depending on the calibration, operating point and % of substitution NOx emission may decrease, or not.

3.5 Engine control system and setup

In this section, the engine modification is described and also the installation at the test bench at Unimore University.

First of all, the engine has been equipped with a methane injection system . Methane injectors are quite simple compared to diesel injectors. They are composed by a solenoid actuator which drives a gas valve with calibrated hole. The hole diameter is quite huge in comparison to a liquid fuel injector, itis near 1.5 mm; this fact is due to the lower density of the gas fuel instead of liquid fuel. in addition, the injection pressure is low , near 4-5 bar, so it is necessary to enlarge the hole in order to have correct mass flow rate and not to have too big injection time. In the figure below the methane injector is shown :

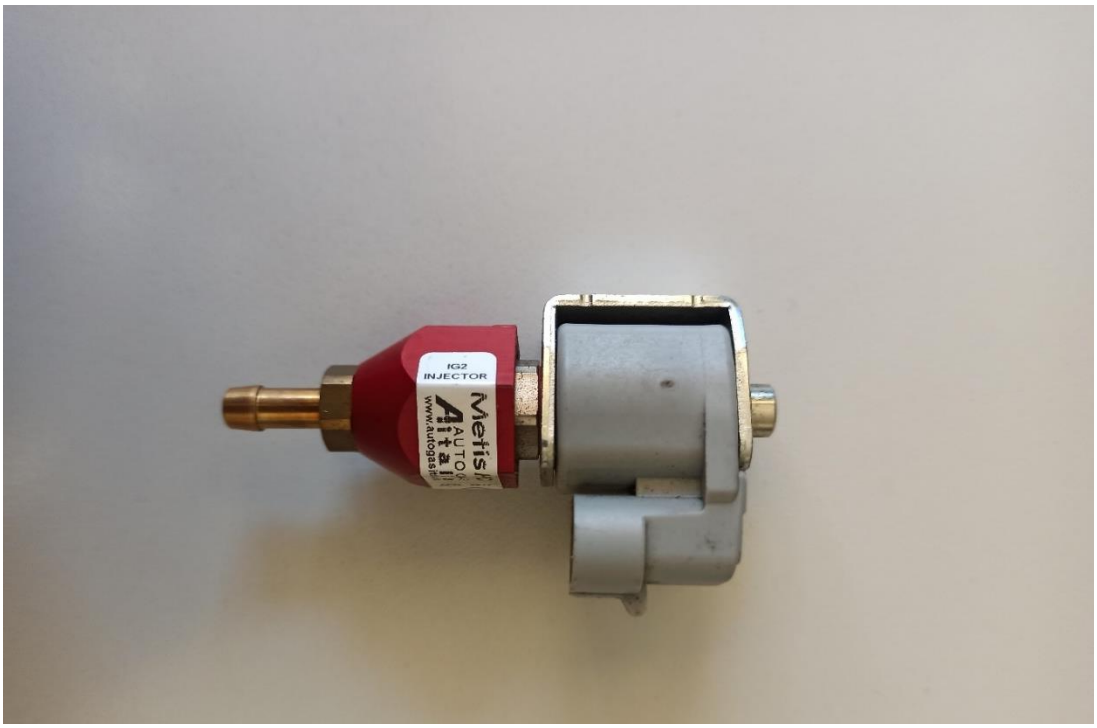

Figure 10 Methane injector

The injector is driven by a development ECU which allows to calibrate the injection phase time in function of several engine parameters such as engine speed, load, intake air temperature, intake pressure etc. .

The original engine control unit does not include dual fuel operation because it is intent to drive only diesel oil engine. The ECU which drives VM428 engine is a MED EDC16, it is a "standard" ECU provided by BOSCH Figure 11. In this case, in order to modify all calibration parameters, the engine is equipped with a specific development ECU; this system drives with the same software as the commercial engine but with the possibility to change instantaneously all calibrations and to switch on and off strategies or diagnosis that could be a source of problems when the engine is in dual fuel operation mode. As an example, in figure 18 an image of a ETK ECU is reported. In order to control ETK ECU it is necessary to have a specific hardware configuration and a specific calibration program. The hardware needed in order to calibrate parameters and measure is provided by ETAS and specifically developed for ETK, the module used is called ETAS592 Figure 12. The software adopted to measure calibration and dataset management is ETAS INCA; this software represents a standard for automotive control calibration.

The controller of the methane injection is directly provided by Ecomotive solution Figure 13. This controller is made for development as it has already been described for BOSCH ETK. Its control parameters can be changed when the engine is running, which is essential for the optimization of the dual fuel combustion process.

Figure 11Development ETK-ECU

Figure 12 ETAS592 module

Figure 13 D-GID ECU

For reason of clarity a scheme of the whole controller is reported. There are two parallel controllers working as stand-alone systems, this can be useful only for testing bed calibration at fixed operating points, not for transient conditions, because in that case a communication between parallel controls via can bus protocol must be realized. For these reasons, it is not necessary to implement this communication.

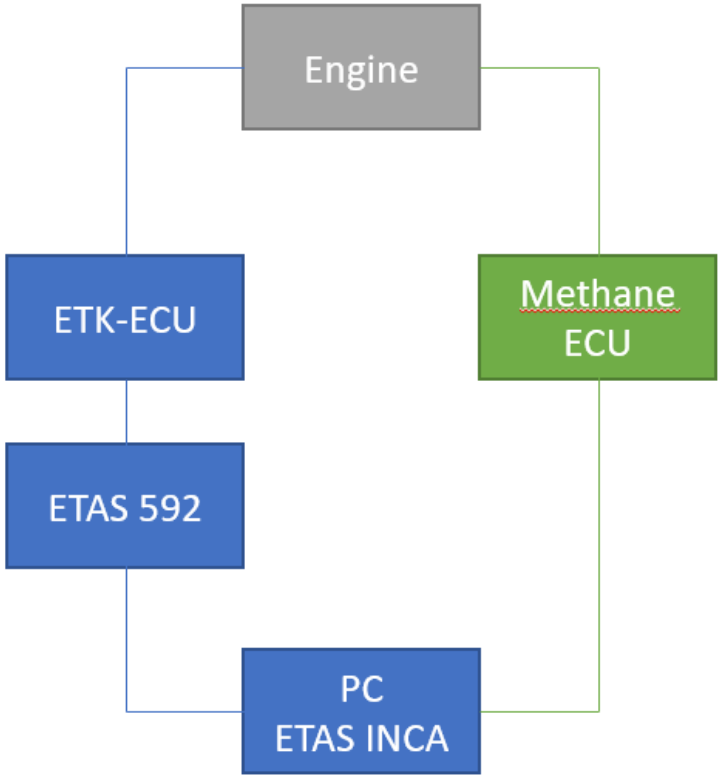

Figure 14 Engine control unit scheme

3.6 Test bench installation

The engine is installed at the Unimore test bed. This bed is provided by Apicom and it is equipped with a Eddy current dynamometer FR400BRP. In Figure 15 the technical specification of the instrument are reported:

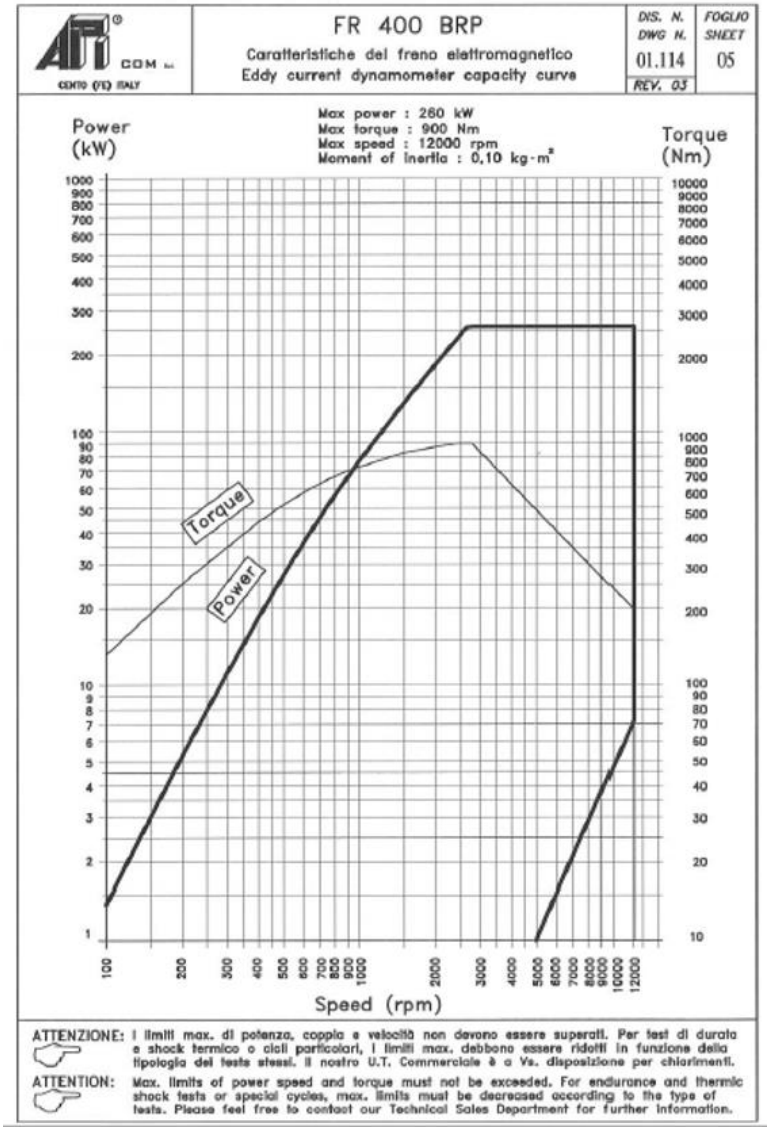

Figure 15 Apicom FR400 eddy current dynamometer

In Figure 16 below a scheme of the test bed installation and measurement equipment is shown.

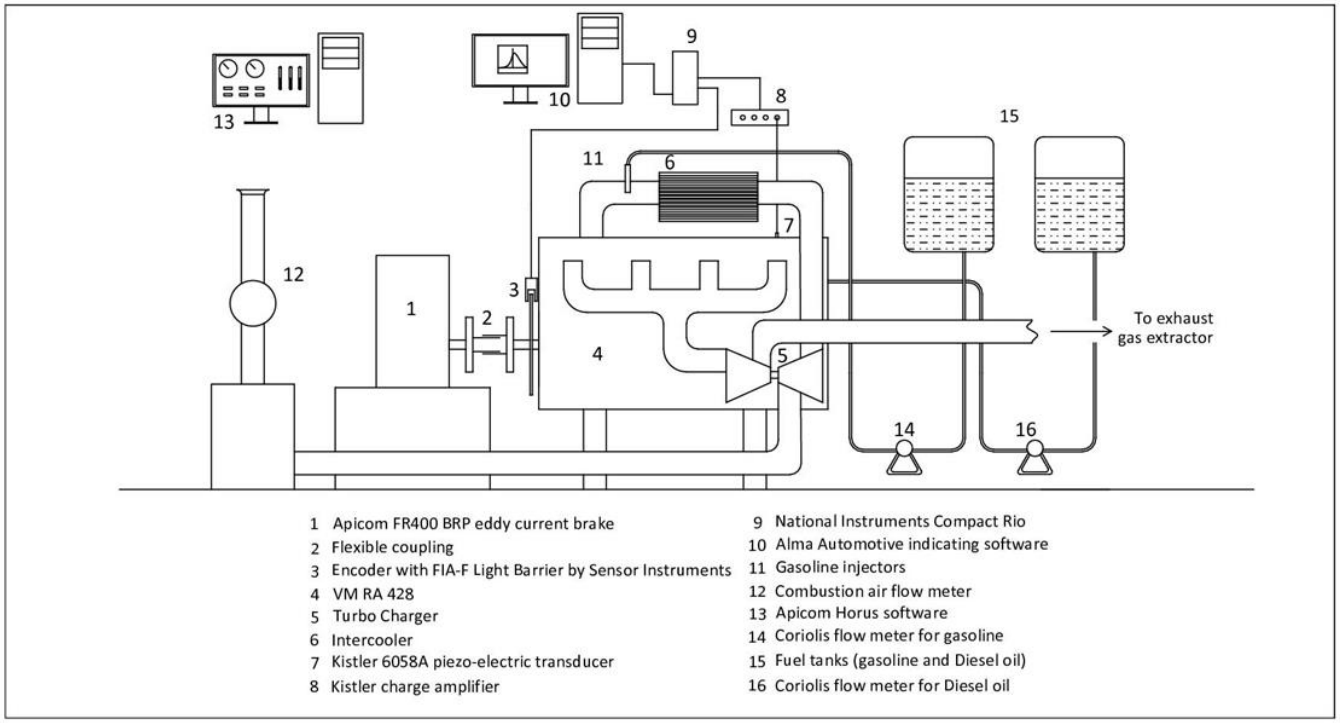

Figure 16 Sketch of the test bench

In order to calibrate combustion process it is fundamental to measure the instant in cylinder pressure. Therefore, the test bed is equipped with an indicating measure system provided by Alma Automotive. The pressure sensor is a Kistler piezostar 6058 transducer and it is installed with a plug adapter instead of the glow plug of one cylinder. An optical encoder provided with 120 teeth and specifically designed to fit the engine provides the crankshaft position detection. The pressure transducer is linked to a Kistler charge amplifier in order to keep the charge Coulomb signal and traduce it in an analog signal 0-10 V. This signal is kept as input into a Compact Crio logger along with the digital signal coming from the crankshaft position sensor. Compact Crio communicates via ethernet cable with a PC where Alma Automotive Software Obi Clinet runs (Figure 17). As an example, a screenshot of this software is reported in the figure below .

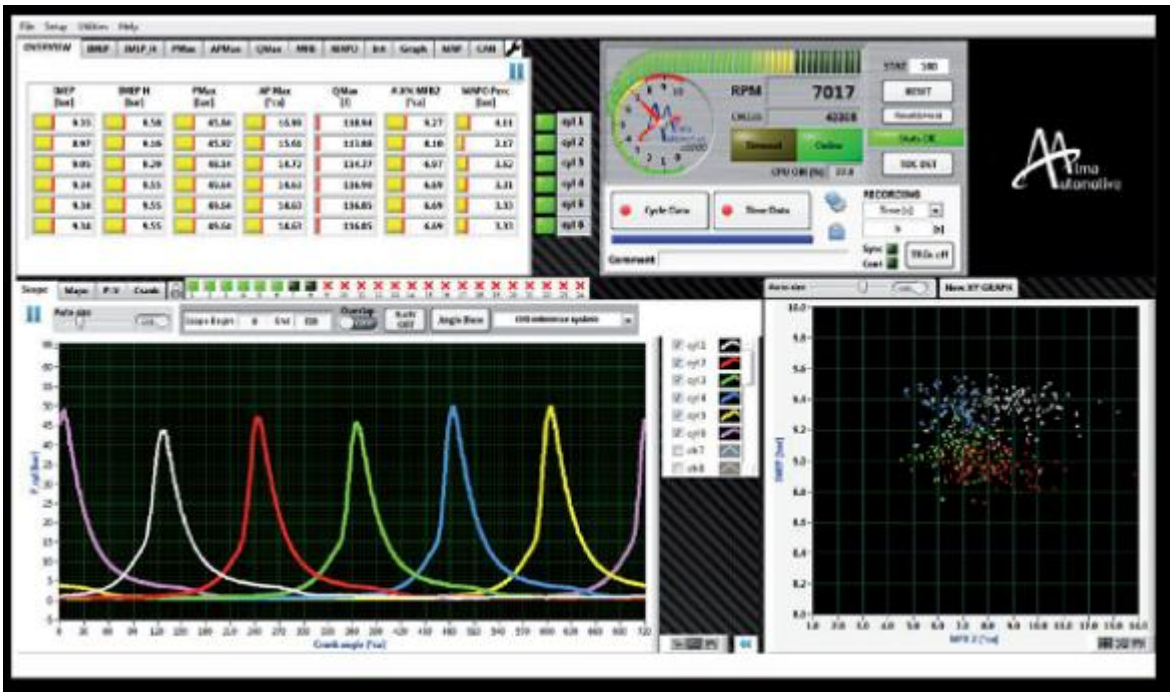

Figure 17 Obi client Indicating Software by Alma Automotive

This software can record a fixed amount of pressure cycle data, calculating all main engine parameters which derive from in-cylinder pressure traces (e.g. IMEP, IMEPH, PMEP, MFB10,50,90, ROHR…). All collected data are post-processed in order to analyze engine combustion process.

The combustion process is slightly different from cylinder to cylinder, especially for gasoline engines; taking these considerations into account, the methane injectors are installed just after the Intercooler system in order to ensure homogeneous mixing of the premixed charge. Intercooler system is different from the original one installed in VM428; at the test bed, the intercooler is an air-to-liquid heat exchanger, and the outlet temperature of the air is controlled by a PID regulator acting to the water flow rate running into the exchanger.

For the measurement of the Diesel flow rate, a Coriolis flow meter is adopted. As for the methane gas flow, a specific flow meter produced by Alicat MCE is applied . This specific transducer is a venturi pipe.

All other measurements and controls of the test bench are acquired from Apicom automation test software Horus, in particular all the 4 states of the operational fluid are measured: pressure temperature and humidity at ambient condition, compressor inlet, compressor outlet, intercooler outlet, turbine inlet and outlet.

For the measurement of the pollutant emissions, MRU Vario plus industrial has been used. The gauge measures O_2, CO, CO_2, NO, NO_2, NO_x, and CH_4 using Nondispersive Infrared technology (NDIR). Soot emissions are measured by a AVL Di Smoke 4000 opacemeter. In the interests of clarity, we have to consider that these measurements are engine-out emissions, without aftertreatment system installed into the engine. This is important in order to evaluate the performance of calibration hint in pollutant emissions. This work does not aim at evaluating aftertreatment system performance and its calibration.

In order to calculate stoichiometric ratio, the test bench is equipped with an air mass flow meter installed before the compressor. The Ecomotive solution injection system drives 4 injectors; in this application, all the injectors are needed in order to supply the right amount of methane for the VM428.The nominal flow rate of the injectors is 1.5 g/s at 3 bar of differential injection pressure. The installation is near the intercooler system and about 500 mm before the plenum. In order to improve mixing, the 4 injectors are installed forming a 30° angle with the radius of the duct cross section passing from the nozzle.

The installation of the methane injectors is reported in Figure 18, it is important to underline that injectors installed in this configurations works like a single point injector. This do not affect results because no dynamic load transition are investigated, in that case injectors must be placed near the intake duct of every cylinder. The number of injectors is kept equal to the number of cylinder only for simplicity because the control system has bee specifically designed for this configuration.

Figure 18 Methane injection system installed after intercooler

Methane injection system is quite simpler than a liquid injection system, substantially it is composed by a pressurized tank at 250 Bar and two pressure reduction stages. The last one determines injection pressure. Injectors, as already described above, are very similar to PFI gasoline injectors.

The whole installation system at Unimore test bed is reported in the Figure 19:

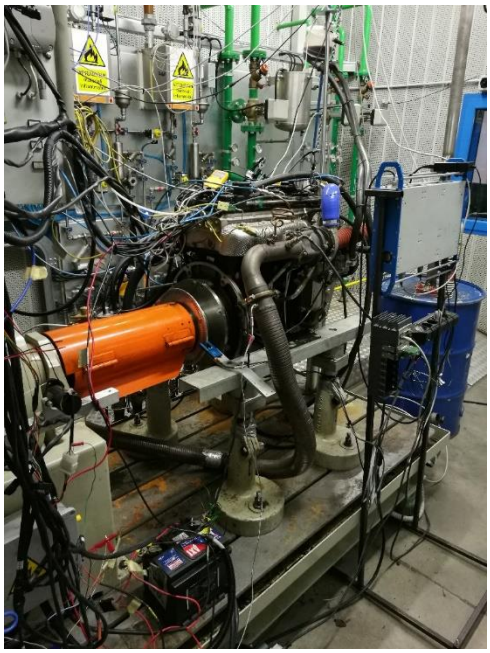

Figure 19 Dual Fuel engine installed at test bench

In

Table 5 main specifications of the Diesel Oil and natural gas are reported

Fuel properties	**Methane**	**Diesel oil**
Lower Heating Value (LHV) [MJ/kg]	49	43.5
Stoichiometric AFR (α_s) [-]	16.84	14.50
Relative Lower Heating Value (RLHV) [MJ/kg]	2.91	3.00
Heating value of stoichiometric mixture [MJ/kg]	2.75	2.81
Research Octane Number (RON) [-]	≈120	-
Cetane Number (CN) [-]	-	52
Autoignition temperature [°C]	650	200

Table 5 Physical properties of Diesel fuel

The natural gas is 95% methane.

3.7 Result discussion

The experimental campaign cover 4 operation points, as already described in the previous paragraph. Here below all the operation points are reported.

- 3000 rpm – 44 Nm/BMEP = 2 bar;
- 3000 rpm – 88 Nm/BMEP = 4 bar;
- 3000 rpm – 177 Nm/BMEP = 8 bar;
- 3000 rpm – 265 Nm/BMEP = 12 bar.

The test bed control system uses two closed loop controls, which are applied in order to control both engine speed and load through the current flowing into the eddy current dynamometer. The controlled engine load has been kept constant by adjusting the load in the Diesel control system. When the dual fuel operation mode is turned on the diesel fuel flow is reduced in order to compensate methane fuel flow.

Regarding the consideration made above, the normal operation in Diesel fuel only is called normal Diesel (ND): m_d is the amount of diesel injected in ND mode. Conversely, the amount of natural gas NG (m_{NG}) increase step by step, while the mass of Diesel injected is reduced. In these conditions, the torque closed loop controller keeps BMEP constant. Two parameters X_{NG} ,X_D are defined in order to assess the amount of energy provided by methane instead of Diesel, and to compare Global efficiency:

$$X_{NG}[\%] = \frac{\mathrm{m_{NG}} \cdot \mathrm{LHV_{NG}}}{\mathrm{m_D} \cdot \mathrm{LHV_D}} 100 \tag{3.5}$$

$$X_D[\%] = \left(\frac{\mathrm{m'_D}}{\mathrm{m_D}} 100\right) \tag{3.6}$$

Comparing these two parameters the difference in terms of Global efficiency is clear. If the amount of energy in terms of methane is higher than the quantity subtracted from Diesel amount, the global efficiency decreases, otherwise it increases.

All the points analyzed are measured at the same engine coolant temperature oil temperature and at the same ambient conditions in terms of pressure temperature and humidity, along with boost pressure and intake temperature (before intercooler). As already described, the EGR valve is kept closed, in order to better control the operation points. In Table 6 all the operation points valuated in this study are reported with the steps in terms of percentage of substitution of Diesel Oil:

Engine load	**Dual fuel cases**	**Percent diesel by energy [%]**	**Percent NG by energy [%]**
3000 rpm – BMEP = 2bar 44 Nm	ND	100.00	0.00
	-20% Diesel fuel +46% NG	63.75	36.25
	-41% Diesel fuel +63% NG	48.81	51.19
	-60% Diesel fuel +132% NG	24.27	75.73
	-80% Diesel fuel +175% NG	9.60	90.40
3000 rpm – BMEP = 4bar 88 Nm	ND	100.00	0.00
	-20% Diesel fuel +36% NG	68.95	31.05
	-34% Diesel fuel +43% NG	60.90	39.10
	-64% Diesel fuel +86% NG	29.82	70.18
	-80% Diesel fuel +148% NG	12.15	87.85
3000 rpm – BMEP = 8bar 177 Nm	ND	100.00	0.00
	-27% Diesel fuel +32% NG	70.00	30.00
	-46% Diesel fuel +55% NG	49.52	50.48
	-60% Diesel fuel +66% NG	38.03	61.97
	-80% Diesel fuel +93% NG	17.47	82.53
3000 rpm – BMEP = 12bar 265 Nm	ND	100.00	0.00
	-28% Diesel fuel +30% NG	70.95	29.05
	-36% Diesel fuel +42% NG	60.43	39.57

	-60% Diesel fuel +63% NG	39.38	60.62
	-80% Diesel fuel +75% NG	21.55	78.45

Table 6 Operation Points

Looking at Table 6, it is clear that, in most cases, the more we increase Xng the more is the total amount of energy per each cycle. That is to say, there is a drop in terms of thermal efficiency.

This result was expected because decreasing diesel flow rate determines the application by the ECU of partial load injection strategy. These strategies are not optimized for dual fuel operation mode.

This first turn of experimental measurements are taken as base for the development of a custom calibration of the injection strategy, in terms of timing, pressure, number of injection, in order to investigate if is it possible to improve performance in terms of global efficiency.

In Figure 20 the BTE variation in the tested cases is reported , without optimization process; we can observe a reduction in BTE in most of the analyzed cases, only one case at high load has a 2%increase. This result is expected as mentioned above[32].

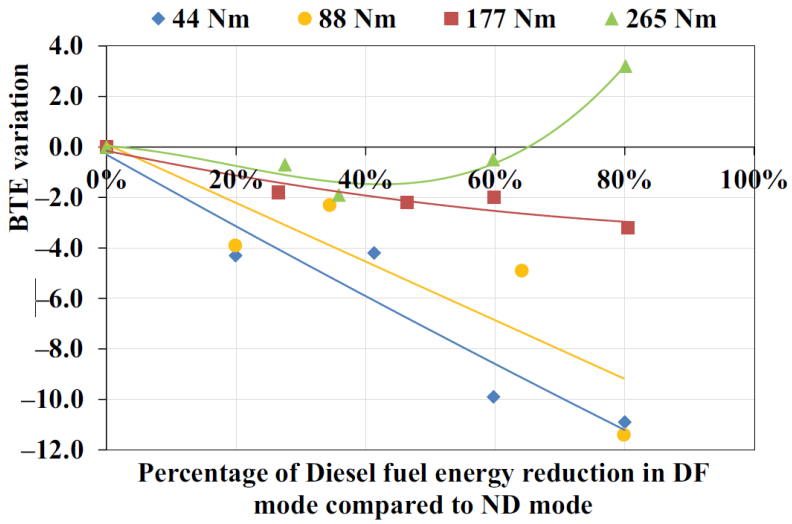

Figure 20 BTE variation VS Percentage of substitution

As a result of the optimization campaign, here in Table 7, the performances in terms of energy conversion are reported.

Engine load	Non Optimized DF	Optimized DF
3000 rpm – BMEP = 2 bar	-80% Diesel fuel +175% NG	-80% Diesel fuel +135%NG
3000 rpm – BMEP = 8 bar	-60% Diesel fuel +66% NG	-60% Diesel fuel +57% NG
	-80% Diesel fuel +93% NG	-80% Diesel fuel +74% NG
3000 rpm – BMEP = 12 bar	-60% Diesel fuel +63% NG	-60% Diesel fuel +52% NG

Table 7 Results of the optimized operation points

In order to summarize results of the calibration process in terms of global efficiency we must consider the cases at high percentage of substitution (the main goal of the activity is to substitute as much Diesel as possible with NG), which are reported in Figure 21

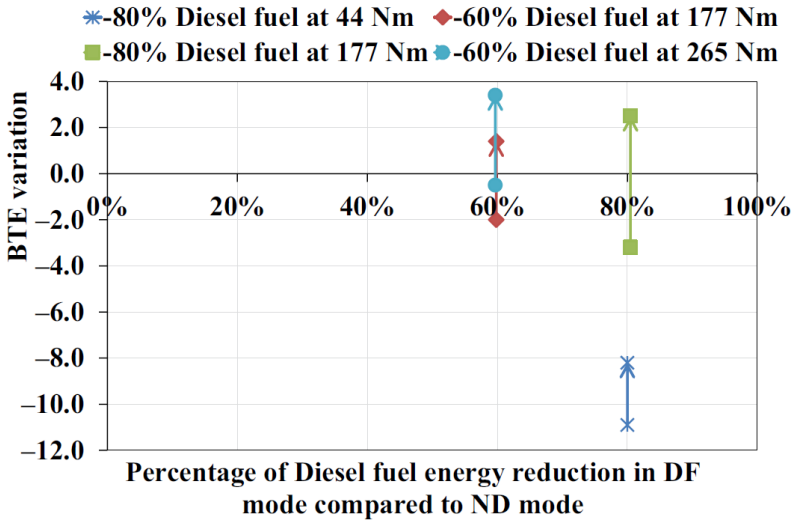

Figure 21 BTE in optimized operation points

The Figure 21 reports in the x and y axis the same reported in Figure 20, the main result is that in almost all cases the engine efficiency increases in comparison to the original diesel operation points. In the case 60% Diesel at 265 Nm, the efficiency rises near 4% (3.8%). Only at the lowest load, which is 44 Nm at BMEP=2 bar, the BTE can not be improved. This fact is due to the high value of air to NG ratio, if the premixed charge is too lean, the reactivity falls down and the combustion process, especially in end gas zone, can not be completed. Therefore, in order to obtain the same load, engine efficiency decreases.

In conclusion, in one hand, it can be affirmed that DF-NG combustion is absolutely convenient if the rate of substitution is grater than 60%, at least from the Brake Thermal efficiency point of view. On the other hand, a drop of the global efficiency is observed; the calibration process partially close the gap, but is not possible to run at the same BTE. Though diesel combustion is quite clean and efficient at low engine loads, so in the hypothesis of an engine conversion in DF mode, a substitution of NG at low load is not mandatory. In addition in GEN-SET operation mode low loads are not particularly interesting. The analysis , which follows in the next paragraph, is focused in the medium high load points.

3.8 Combustion Analysis

The first case of analysis is the 8 bar if BMEP @3000 rpm, the main focus is to compare natural diesel mode with DF mode. Figure 23 shows the apparent heat release rate, it is important to specify that heat release has been calculated by a thermodynamic method starting from the first law of thermodynamic and from the in cylinder pressure traces. So the thermal exchange between in-cylinder gases and coolant liquid can not be estimated, for the sake of simplicity, the specific heat constants are kept constant throughout the engine cycle. This simplification do not lead to e huge errors.

In Figure 22, Figure 23, Figure 24, respectively in-cylinder pressure, apparent heat release and Cumulative apparent heat release are reported, for all percentages of substitution without an optimization of the injection strategy.

In Figure 23 it is clear that, in four out of five cases, the peak in heat release remains the same near 25 Deg before top death center (BTDC); only one case (80% substitution) the charge starts to burn near TDC. For ND mode, the two peaks before the main heat release represent the burn of pre and pilot injection, normally used to warm air for the main combustion process. In the 80% substitution, the huge amount of methane starts to burn along with pilot injection. In Figure 24, we can notice that the amount of heat release is shifted to the TDC, the 50% of the total in case of only Diesel is 22,6° ATDC, for the 80% DF is 16.4° ATDC. This is due to the phenomena described above.

The third peak of heat release is related to the main injection, in the 80% substitution, it is quite small because of the reduction in main injection quantity. In other words, when a lean mixture of NG is introduced within the cylinder, the fist two peaks of AHRR increase at the expense of the third one (it can be better noted in Figure 24 observing integral heat release rate). The rise of the pack release near pilot and pre injection is easily explained because these injections are performed in a gas with a premixed methane, which can ignite when diesel oil starts to burn. The larger is the amount of NG in the premixed charge, the larger is the amount of the heat released[33].

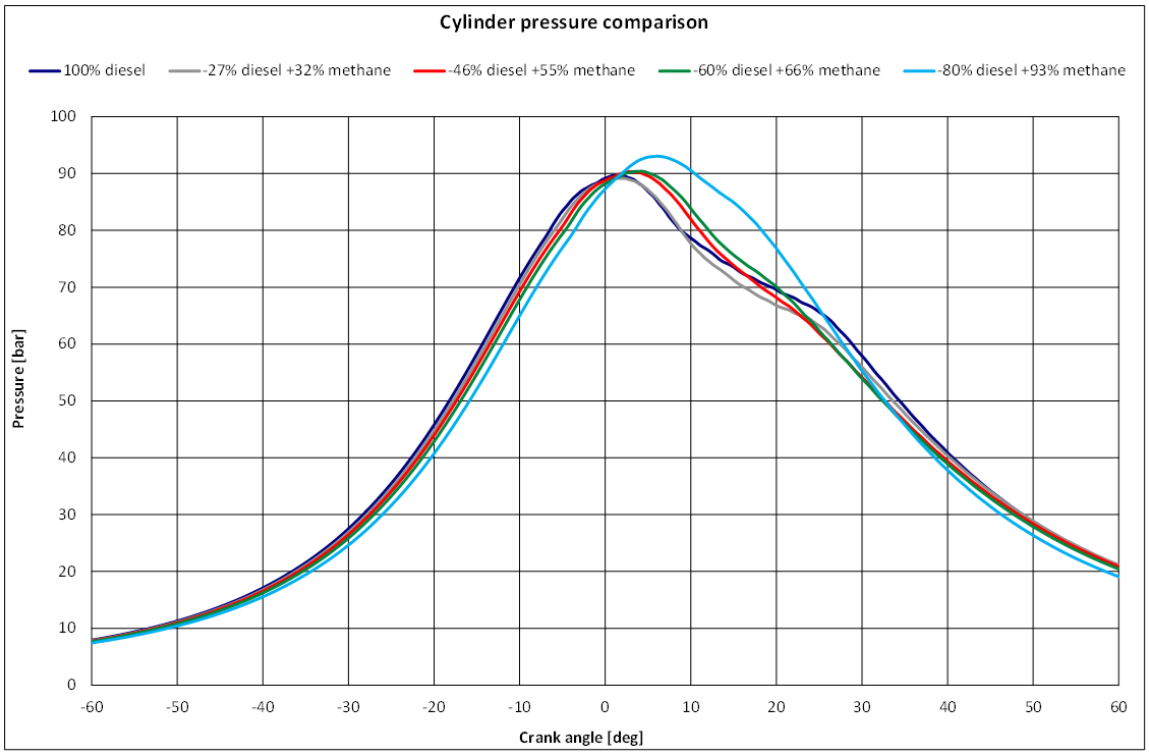

Figure 22 In cylinder pressure traces

In Figure 23 it is evident that maximum heat release peak drops when the amount of NG increases. This parameter is directly related to pressure gradient, this fact leads to a decrease in engine noise and vibrations. Another interesting thing regarding pressure traced in Figure 22, is the slight reduction of pressure in the compression for all DF cases This evidence can be explained by the higher heat capacity of the mixed air with NG in comparison to pure air, so the polytropic index decreases.

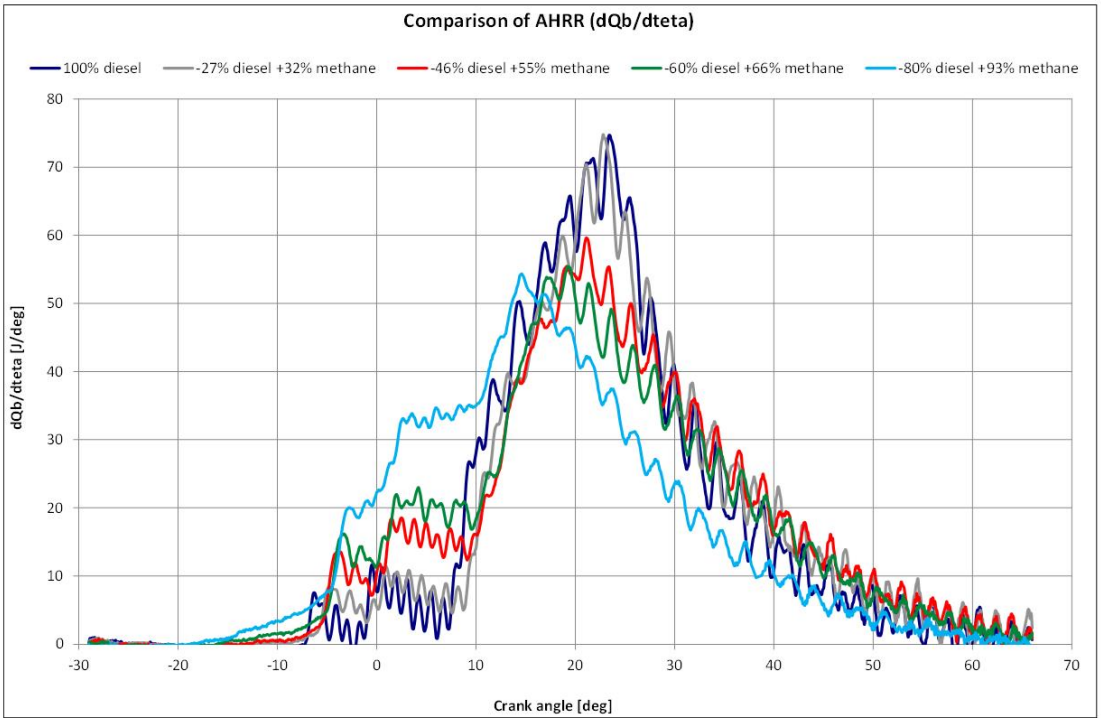

Figure 23 Apparent rate of heat release

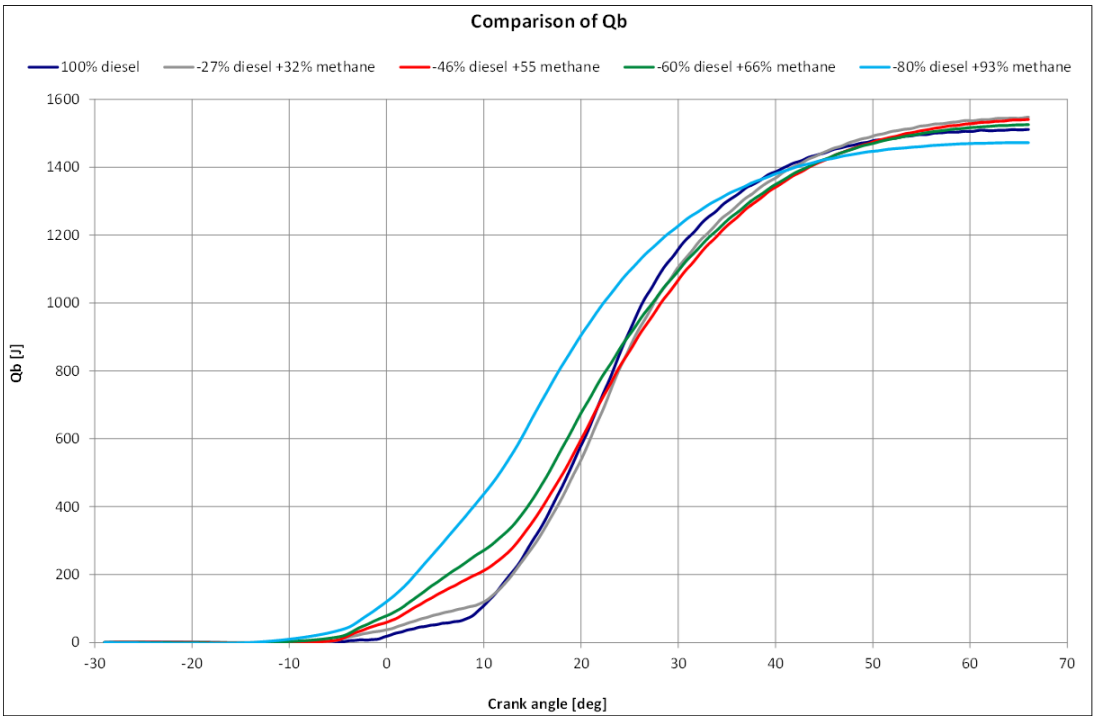

Figure 24 Cumulative heat release

To assess the complete combustion of the fuel injected, a reference is made to combustion efficiency (η_c) calculated with the formula reported below:

$$\eta_c = \frac{\left(\mathrm{P_{in}} - \frac{HC}{10^6}\frac{16}{29}\dot{m}_{air}\,\mathrm{LHV_{NG}}10^3 - \frac{CO}{10^6}\frac{28}{29}\dot{m}_{air}\,\mathrm{LHV_{CO}}10^3\right)}{\mathrm{P_{in}}}100$$

(3.7)

Where :

- $\mathrm{P_{in}} = \dot{m}_{NG} \cdot \mathrm{LHV_{NG}} + \dot{m}_D \cdot \mathrm{LHV_D}$ is the introduced power in [kW]
- $\dot{m}_{NG}$ is he Methane mass flow rate in [g/s]
- $\mathrm{LHV_{NG}}$ is the low heating value of NG [MJ/kg]
- $\dot{m}_D$ is the masso flow rate of Diesel oil in [g/s]
- $\mathrm{LHV_D}$ is the low heating value of Diesel oil [MJ/kg]
- $\mathrm{LHV_{CO}}$is the low heating value of Carbon monoxide [MJ/kg]
- HC is the concentration of NG equivalent unburnt hydrocarbons in [ppmn]
- $\frac{16}{29}$ is the ratio between Methane molar mass and standard air
- $\dot{m}_{air}$ is the mass flow rate of the air in [g/s]
- CO is the concentration of carbon monoxide in [ppm]
- $\frac{28}{29}$ is the ratio between Molar mass of CO to Air

This equation does not contain the contribution of hydrogen which could not be measured during the tests. Despite this approximation, combustion efficiency should be reliable at least in relative comparative.

In Figure 25 and Figure 26 respectively combustion efficiency and global efficiency comparison in all cases not optimized are reported, adding two new points:

- -60% Diesel +57% NG

- -80% Diesel +74% NG

These two points derive from the optimization of the injection strategy in "−60% Diesel fuel +66% NG" and "−80% Diesel fuel +93% NG.

Table 8 shows the main calibration parameters changes:

Engine Load	SOI main [° AFTDC]	Rail pressure [bar]	Boost pressure [bar]
-60% Diesel fuel +66% NG	0.0	800	1.8
-60% Diesel fuel +57% NG	- 6.0	850	1.8
-80% Diesel fuel +93% NG	- 1.0	750	1.8
-80% Diesel fuel +74% NG	- 6.0	1050	1.4

Table 8 Main calibration parameters for two different points

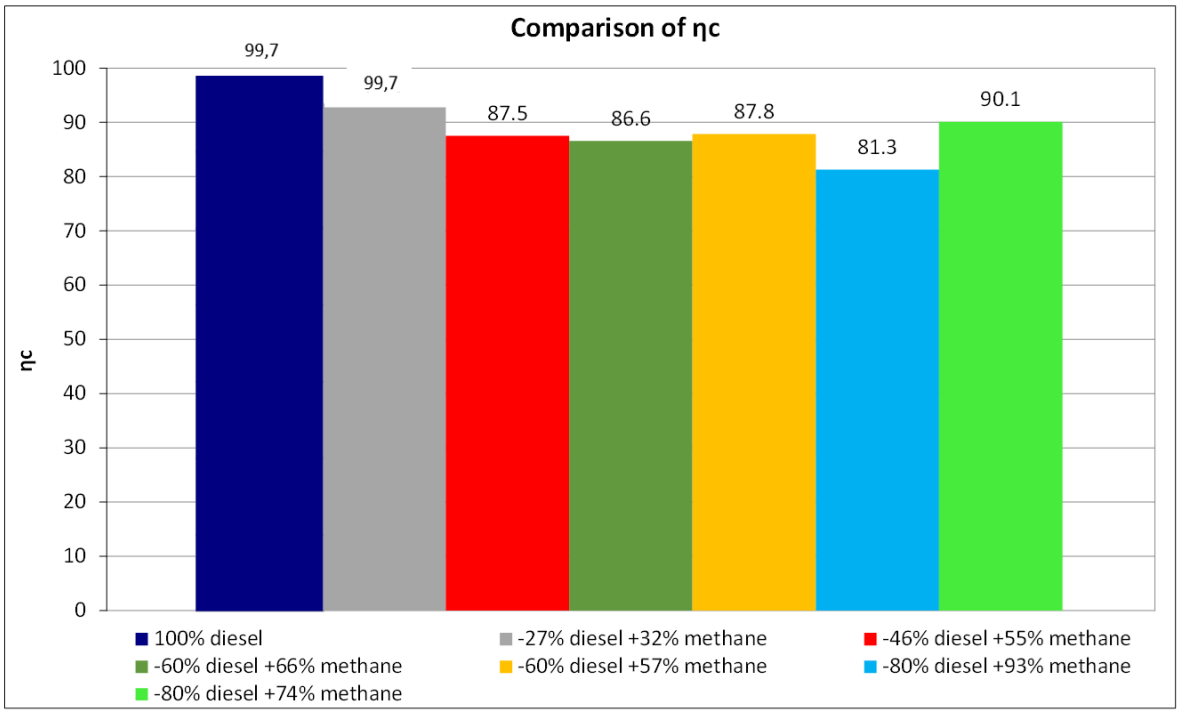

Figure 25 Combustion efficiency comparison

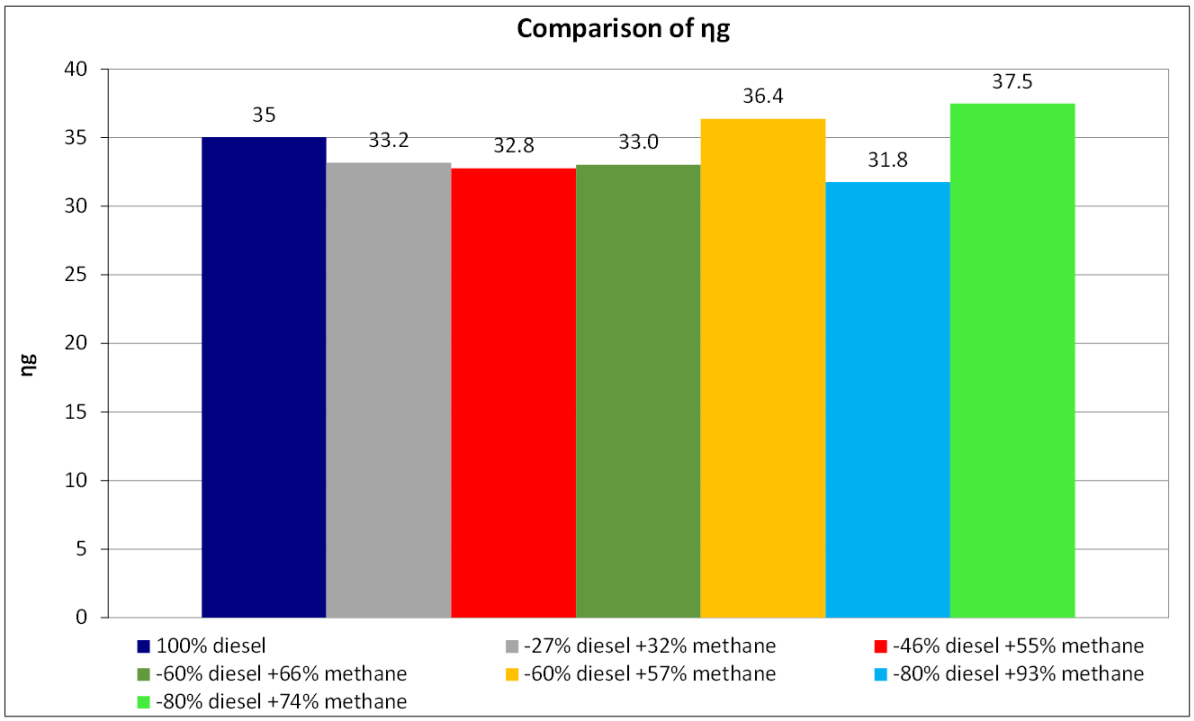

Figure 26 Global efficiency comparison

In order to improve performance, as shown in Table 8, for dual fuel operation mode, the increase of rail pressure and the advance of SOI (start of injection) have been changed, along with boost pressure, so as to recover combustion efficiency, because reactivity is directly related to air to NG ratio.

The enhancement in terms of BTE is shown in Figure 26, this result was expected because premixed combustion maintains the same compression ratio (CR) of the engine have better indicated efficiency because of the combustion speed. Furthermore, the optimization contributes to reduce HC emissions, this is due mainly to injection advance, which takes into consideration the increase on ignition retard in lean mixtures.

Figure 25 shows the combustion efficiency for the whole cases, the worsening of combustion pass from ND mode to "−80% Diesel fuel +93% NG" DF case, the combustion efficiency decreases from 99.8% to 96.8%. This behavior was also expected because high reactivity fuel is substituted with a low reactivity lean premixed fuel; however the optimization process

allows to recover some efficiency percentage point; e.g. from case "−80% Diesel fuel +93% NG" to case "−80% Diesel fuel +74% NG" improve η c of 1,5%.

The increasing injection pressure up to 1050 bar leads to have better fuel atomization and mixing, this fact leads to start combustion process quickly and it involves a larger amount of pre-charge.

Figure 25 shows decrease in Brake thermal efficiency, in particular in all cases except -60% Diesel +57% and -80 Diesel +74%. With the specific calibration activity, the BTE, in the two optimized points rises up to 36,4% and 37,5% respectively. In ND mode the BTE measured is 35%.

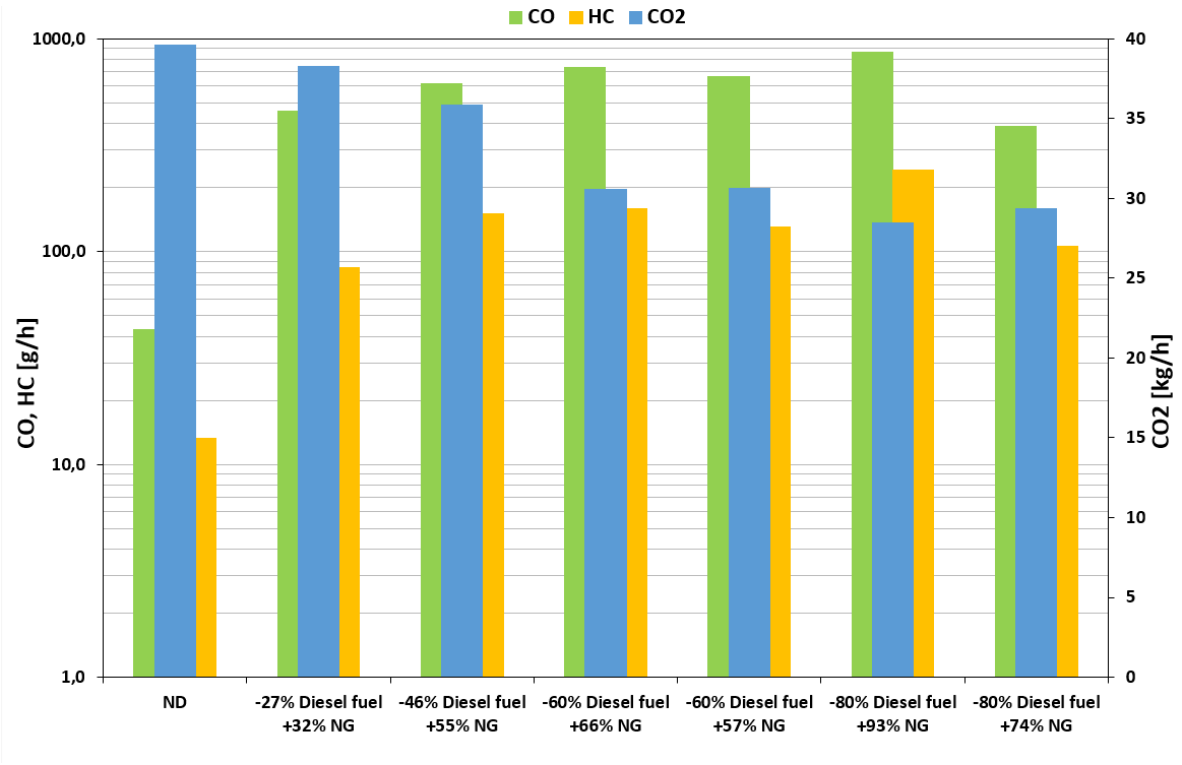

Figure 27 CO, HC, CO_2 comparison

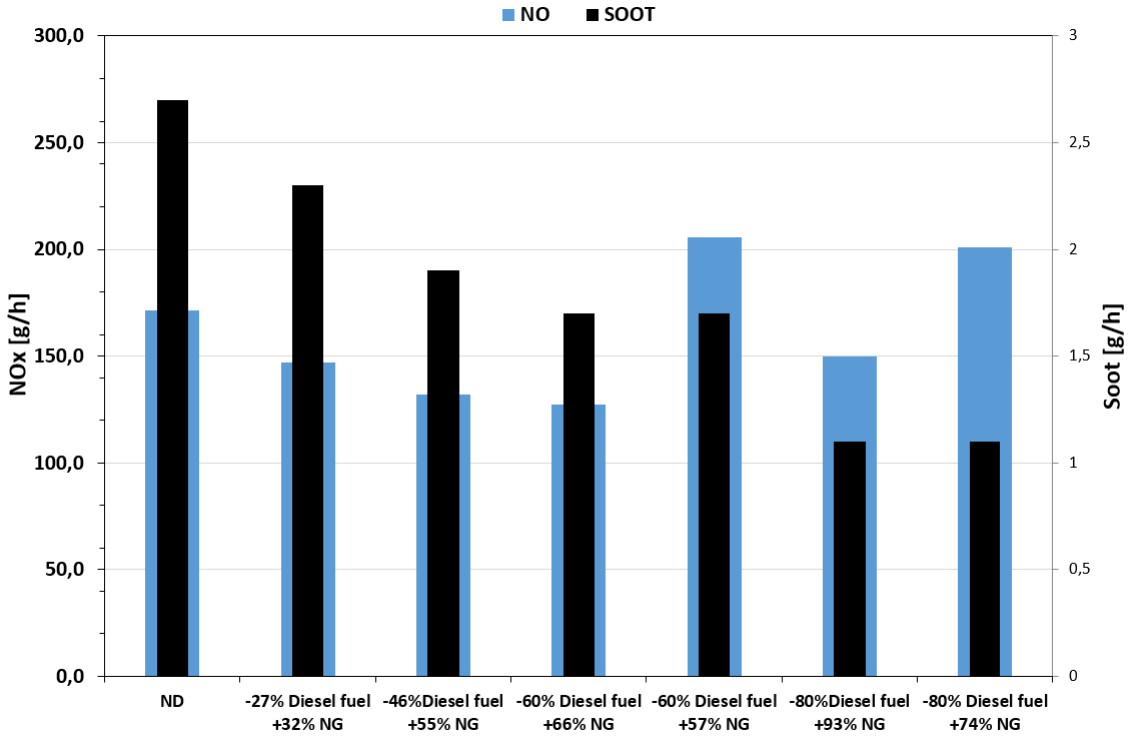

Figure 28 NOx, Soot emission comparison

The emissions analysis introduce further considerations to better understand the previously trends showed above in terms of BTE.

In Figure 27 CO, CO_2, HC emissions are reported for the whole DF operation points. The evidence is a huge increase of CO and HC emissions, of about one order of magnitude. This fact was expected, and this trend is more evident the higher the rate of substitution in terms of DF is. This fact is mainly due to the very low flame propagation especially in lean premixed charge. This trend is confirmed by 34. Furthermore, as diesel fuel is reduced it is more difficult to ignite the NG charge, because of the hot spot generated in Diesel fuel combustion.

On the other hand, a decrease in CO_2 is observed, which is mainly due to the different Carbon-to-Hydrogen ratio of the charge composition. As diesel oil decreases into the charge the ratio lowers; furthermore, the other effect is the increase of BTE, energy conversion is obviously directly correlated. In the two calibrated DF points, the maximum reduction is equal to 30%, obviously this advantage is reduced if a catalyst is added in the aftertreatment system because

the conversion of the HC and CO (higher than ND mode, as described above) increases CO_2 production.

Figure 28 shows a decrease in NOx emissions running in DF mode without optimization. Unfortunately, after the optimization of the operation points the advantage is canceled, and a small increase is observed. Without any calibration, in Figure 23, it is possible to observe that the peak after the TDC in terms of released rate of heat is quite similar in DF in comparison to ND This leads to reduce maximum temperature and, hence, formation of NOx. This effect is compensated by the advance of the main injection timing.

In terms of Soot emissions reported in Figure 28, as expected, these emissions decrease as the rate of substitution increases. The difference is about 50%, comparing ND to DF -80% optimized. Furthermore, NG do not contain PAH , this leads to decrease Soot formation.

Here below, the comparison of the two optimized operation points in terms of in Cylinder pressure, Heat release rate, and injection strategy is reported.

- 177Nm (BMEP=8 bar) @3000 RPM -60% Diesel

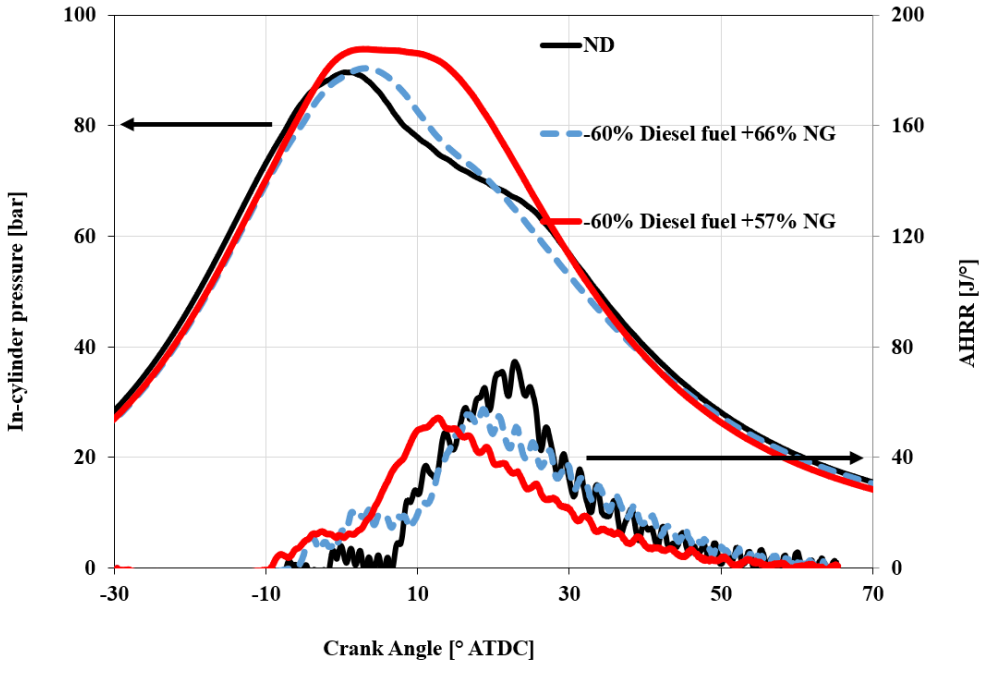

Figure 29 In-cylinder pressure traces

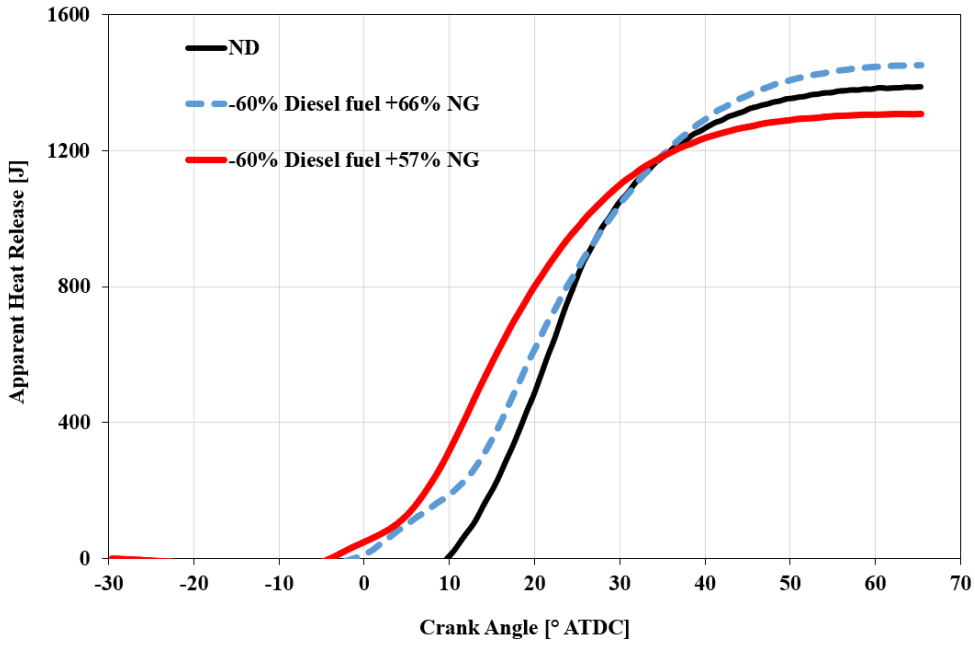

Figure 30 Apparent integral heat release

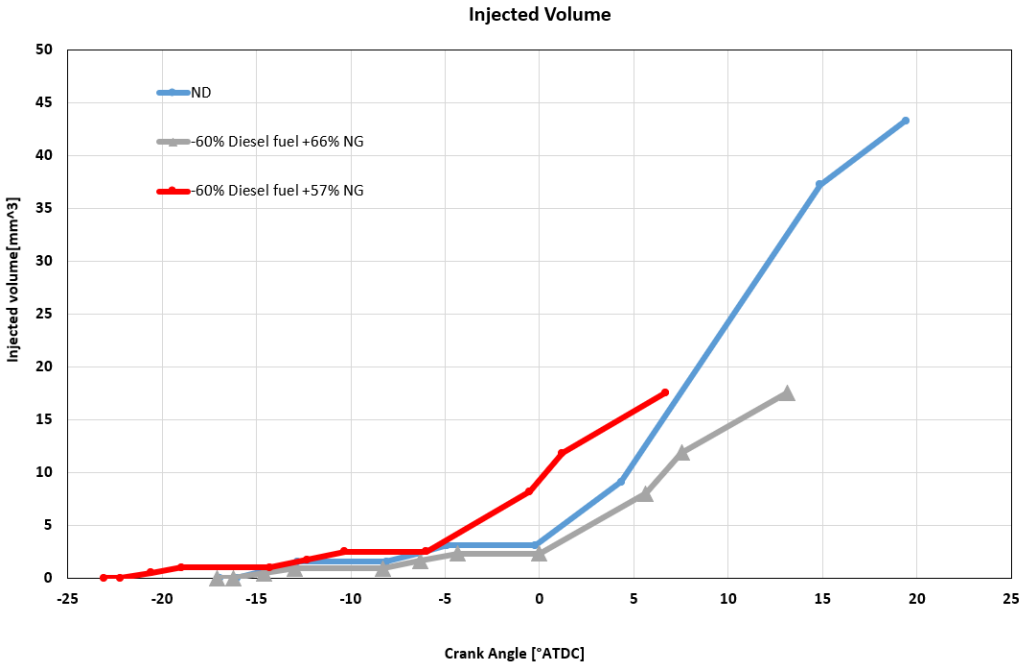

Figure 31 Injected volume

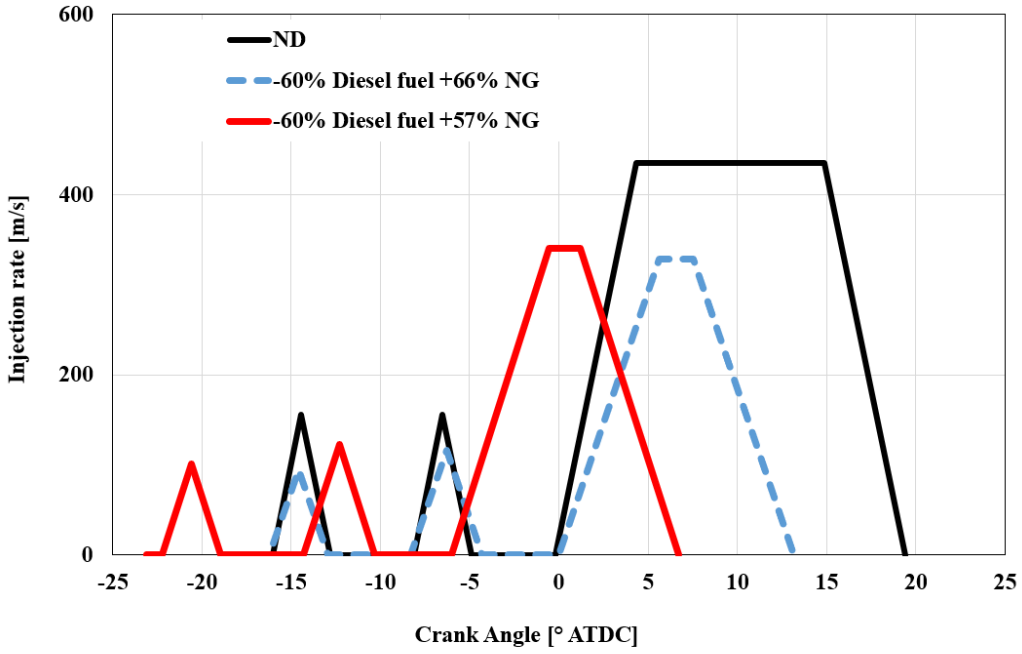

Figure 32 Injection Rate and timing

- 177 Nm (BMEP= 8 BAR) @3000 rpm -80% Diesel

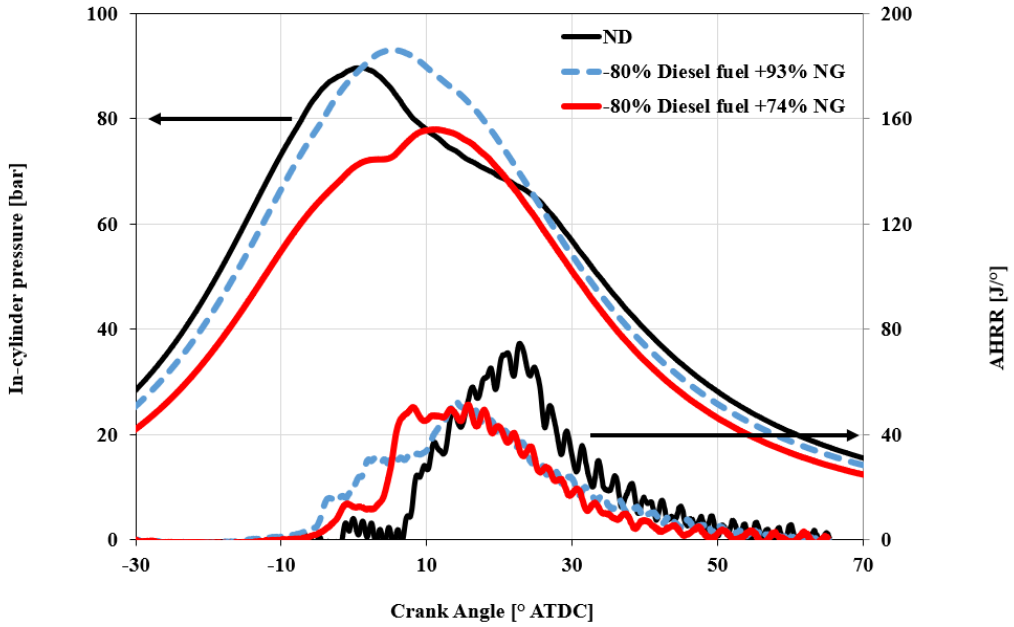

Figure 33 In-cylinder pressure traces, apparent heat release

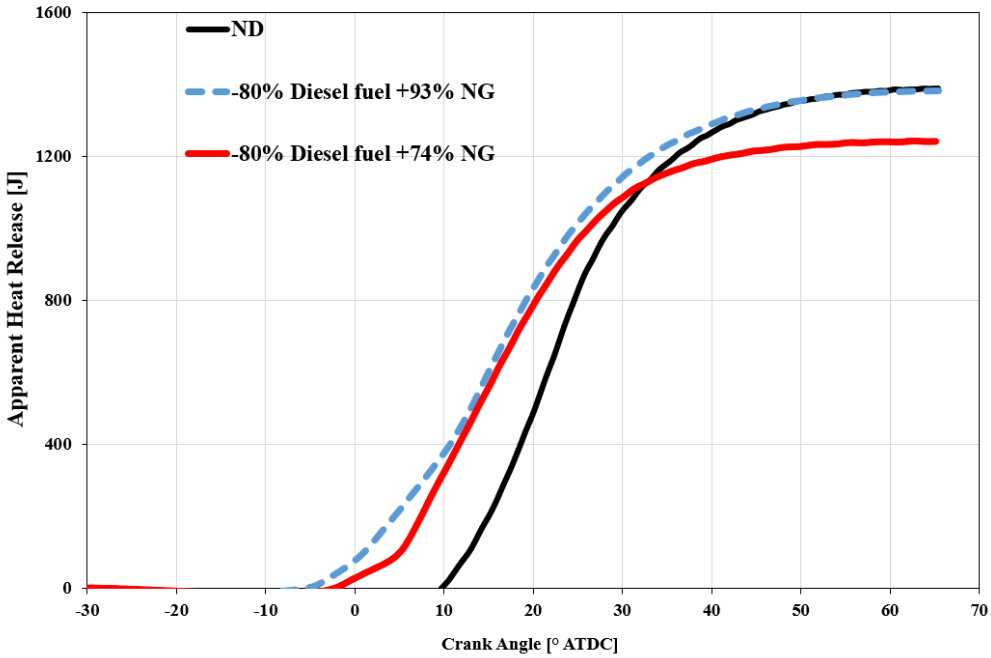

Figure 34 Apparent integral heat release

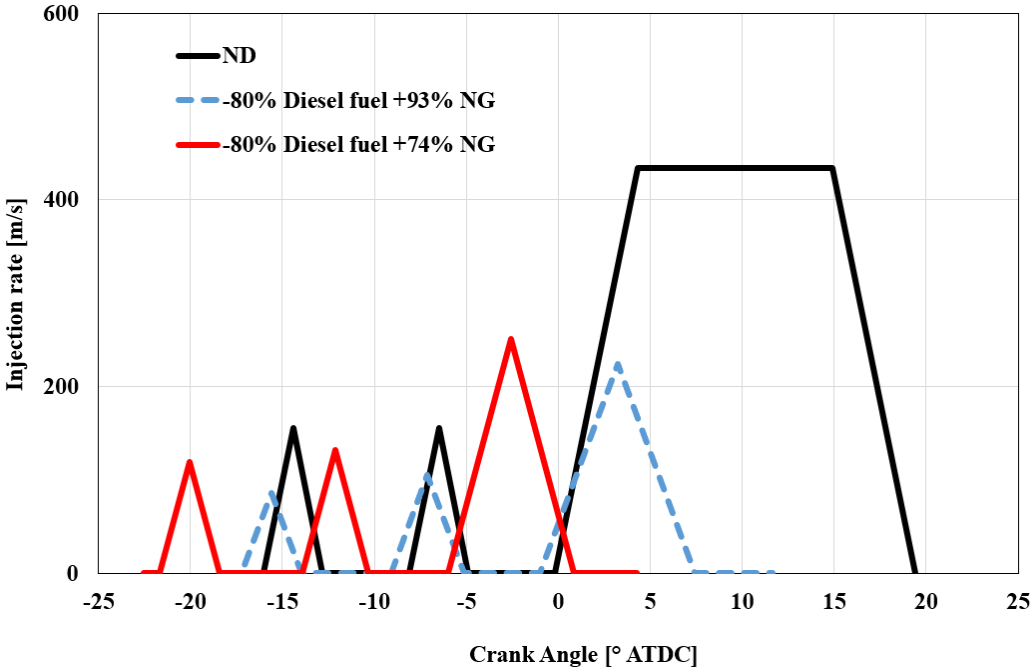

Figure 35 Injection rate and timing

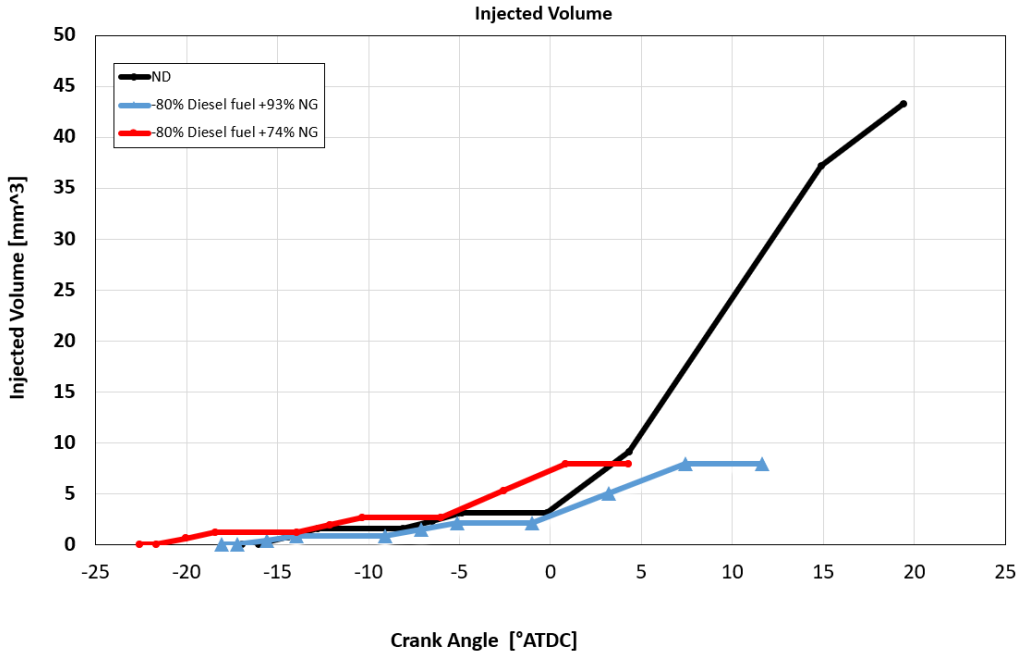

Figure 36 Injected volume

The second operation point corresponding to the higher investigated load (BMEP = 12 bar and 265 Nm) is now discussed.

The first analysis is made comparing in-cylinder pressure traces reported in Figure 37.

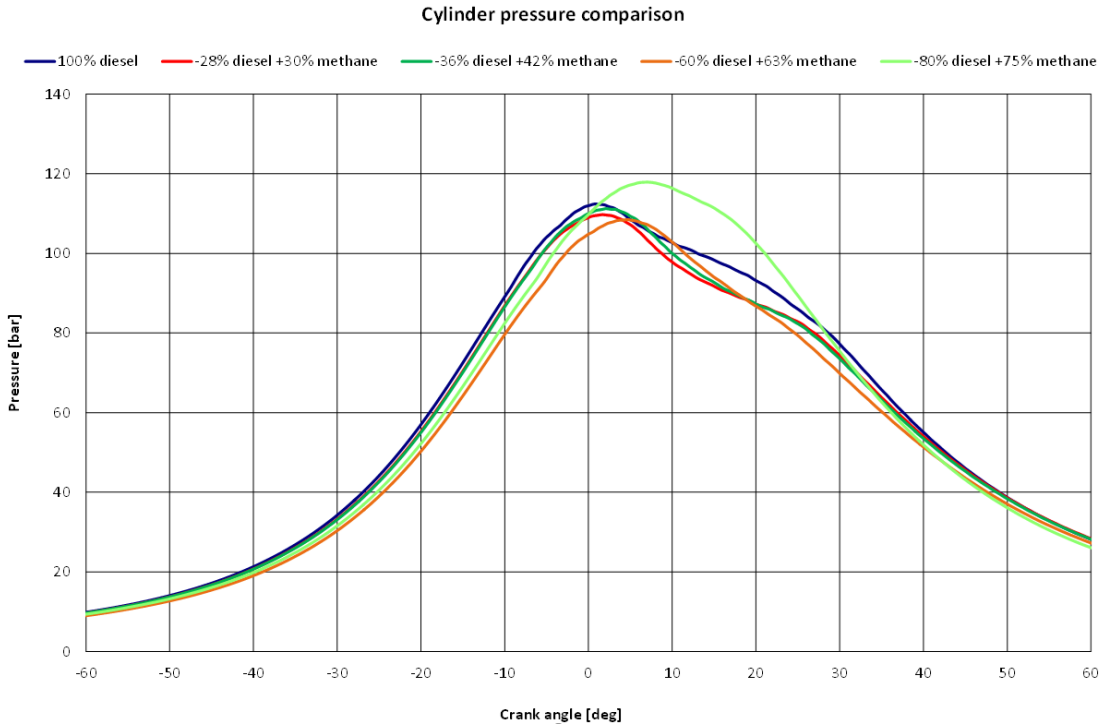

Figure 37 In cylinder pressure traces not optimized points

In Figure 38, the AHRR is reported, we may notice the presence of three peaks for each curve. However, in this case, at high loads the damping of the third peak is observed only in two cases (-60% Diesel fuel +63% NG and -80% Diesel fuel +75% NG. Having a look at Figure 37, dual fuel cases tends to be lower than Diesel operations. Only at the maximum rate of distribution, an increment in cylinder pressure is shown. Observing heat release for this case, we can notice a peak of heat release near 20° ATDC (Figure 38); the heat release in this case is quite in advance in comparison to 100% diesel oil. This behavior has bene already seen in the previous case (Figure 23).

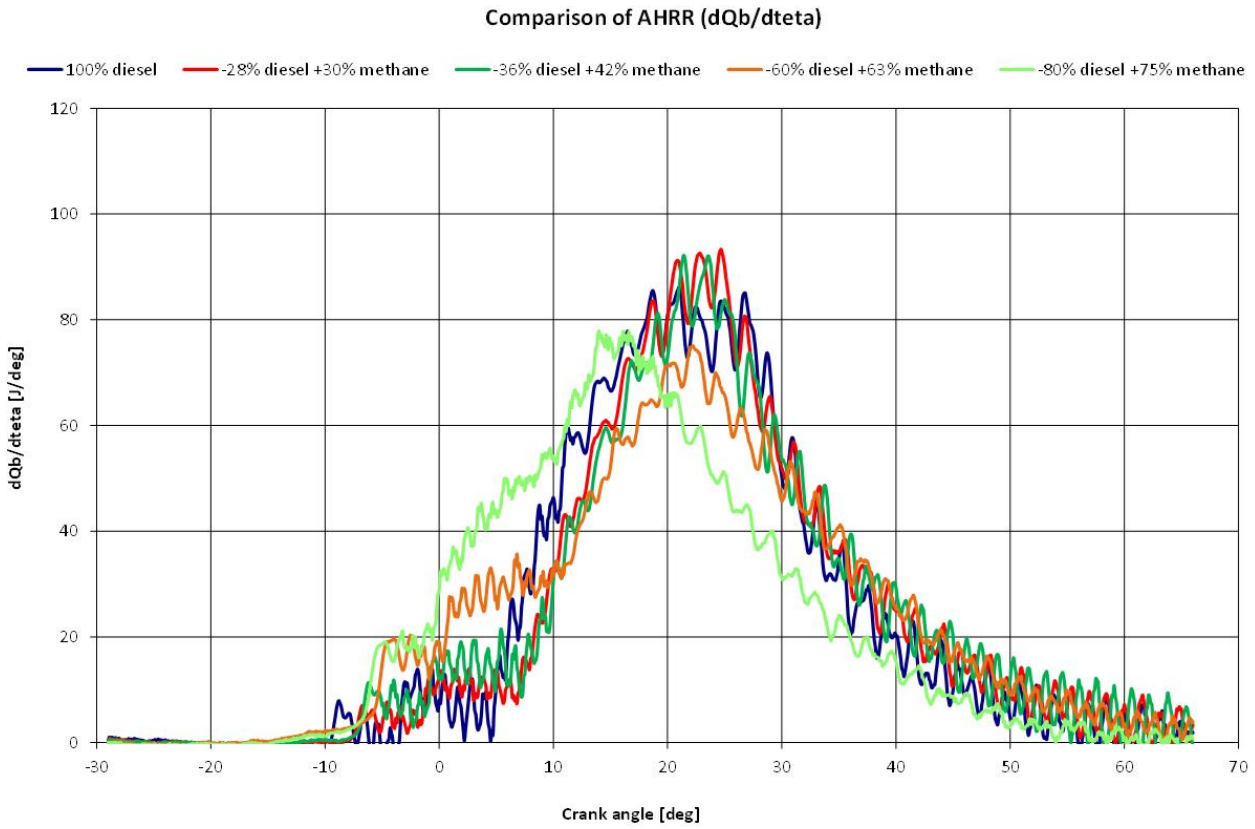

Figure 38 Apparent heat release rate

In Figure 39 and Figure 40 a comparison between BTE and Combustion efficiency is shown for all the cases of substitution analyzed and also optimized cases. As already observed for the previous case, a decrease in terms of combustion efficiency is observed when Diesel substitution rate increases, even though this drop is smaller than the previous case at BMEP= 8 bar. The difference may be due to the higher engine load; in this DF operation, therefore, the air-to-NG ratio decreases, making the premixed charge more reactive. Furthermore, an increase in combustion efficiency is measured in "−60% Diesel fuel +63% NG" to case "−60% Diesel fuel +52% NG", is 0.3% (from 98.3% to 98.6%, respectively).

The main advantages in terms of BTE are plotted in Figure 40, for all cases including optimized ones. The trend observed in the previous optimized case BMEP = 8 bar is confirmed at high loads. In particular "− 60% Diesel fuel +63% NG" to case "− 60% Diesel fuel +52% NG," the improvement of BTE is 3.9% (from 35.3% to 39.2%). Furthermore, in "− 80%

Diesel fuel +75% NG" an improvement of BTE is observed without any modification of the injection strategy.

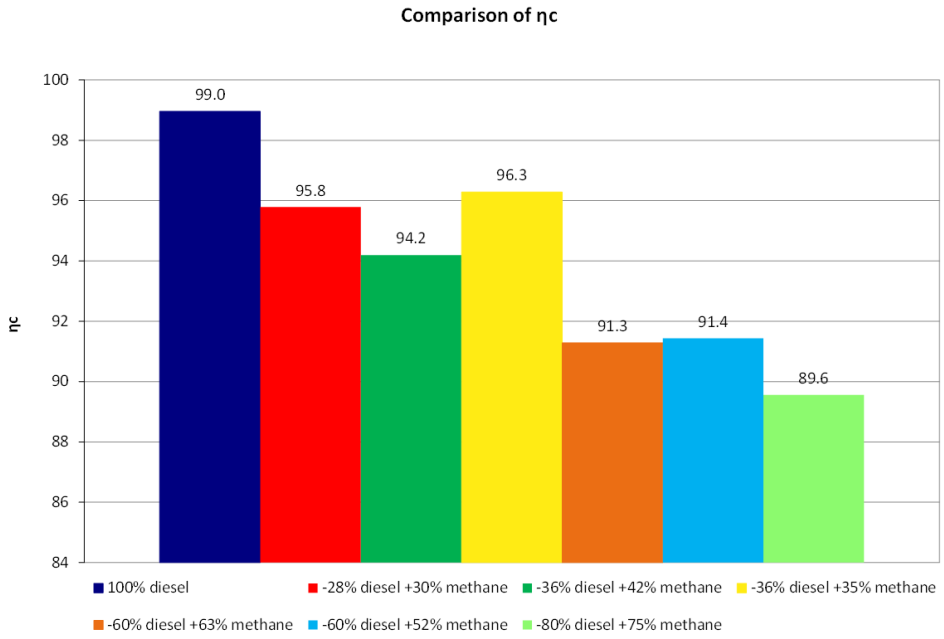

Figure 39 Combustion efficiency comparison

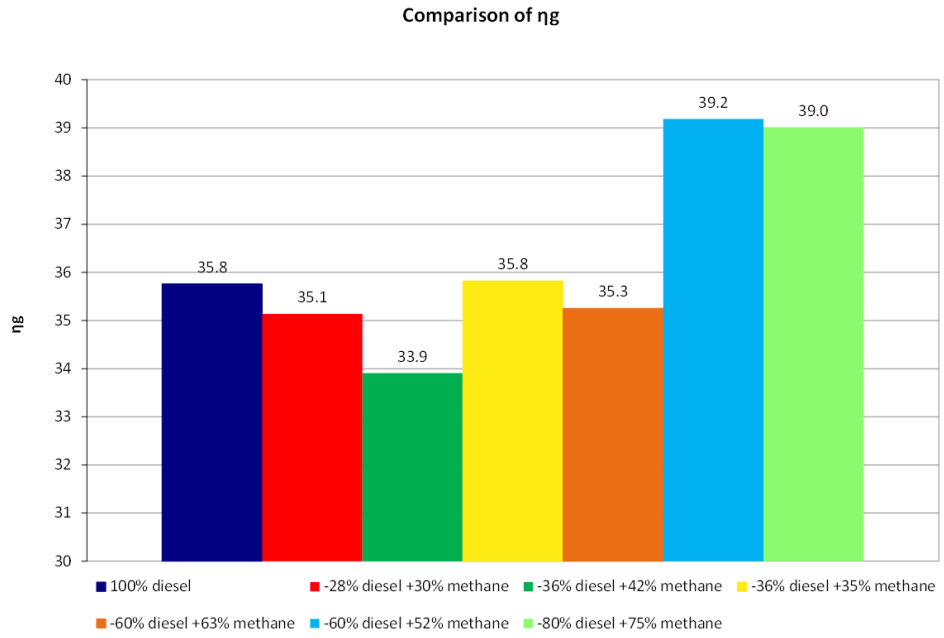

Figure 40 BTE comparison

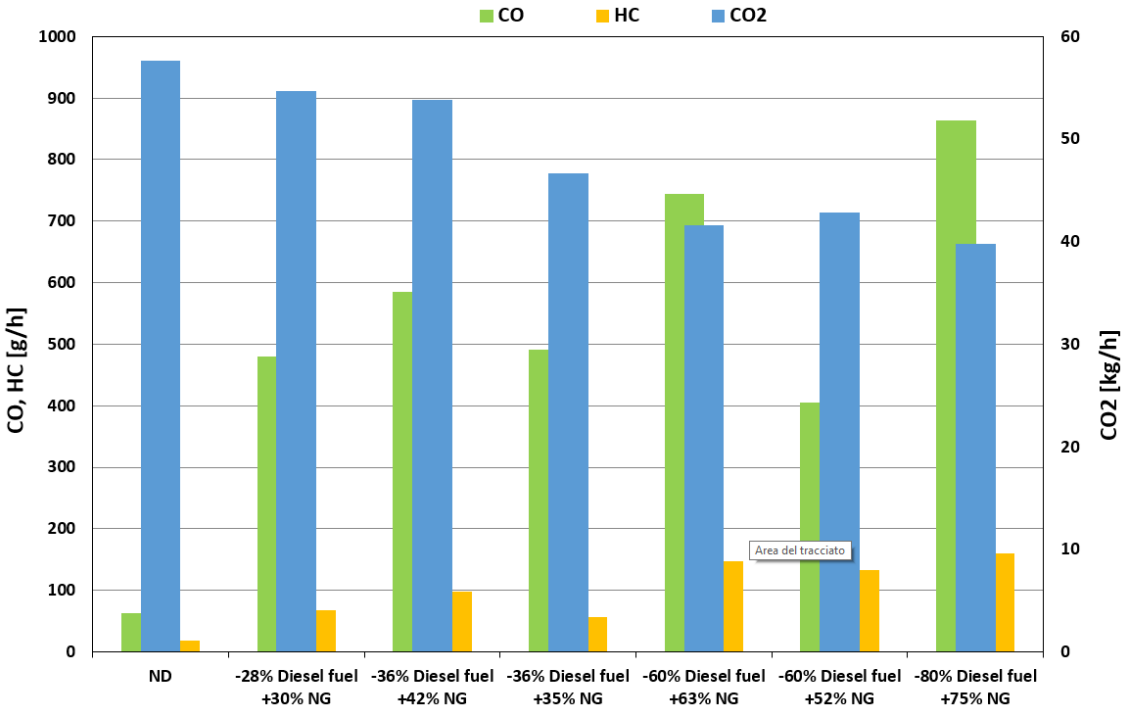

Figure 41 CO, HC, CO_2 comparison

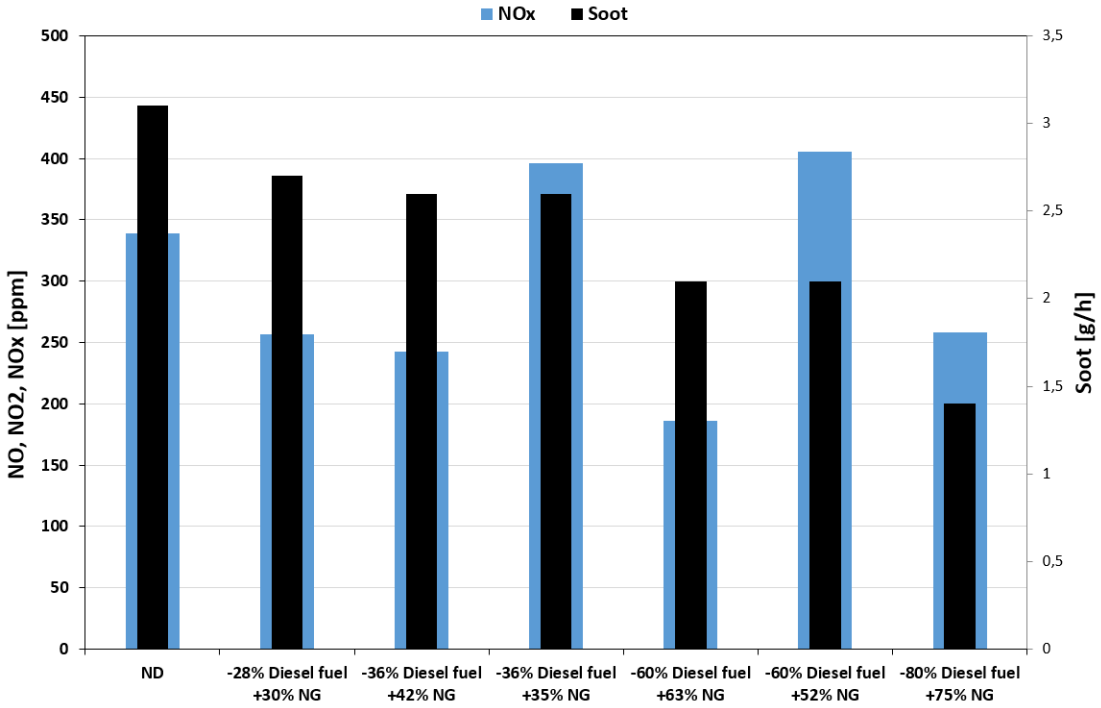

Figure 42 NOx, Soot comparison

The pollutant emissions measured with the analyzer are reported respectively in Figure 41and Figure 42. Regarding Figure 41, CO_2 emissions slightly decrease as the NG percentage increases. This evidence confirms previous analysis performed at 8 Bar of BMEP. This further evidence contributes to affirm the lower impact of the DF combustion in comparison to Diesel combustion. As already seen before, when the rates of distribution are small the advantage disappears.. The difference measured in -28% Diesel fuel +30% NG is comparable to the uncertainty of the instrument, so it is not a accurate measure.

Only "−60% Diesel fuel +52% NG" DF is divergent in comparison to the other analyzed cases. This fact can be explained by the oxidation of a larger amount of CO, after optimization of the injection strategy. In Figure 42 the reduction in NOx emissions can be observed, when the engine is operating in DF mode (the maximum reduction percentage is up to 50)[35]. When the optimization of the strategy is performed, this advantage decreases, in line with the results already discussed above. In Figure 43, Figure 44, Figure 45, reported here below, we can see the results of the optimization.

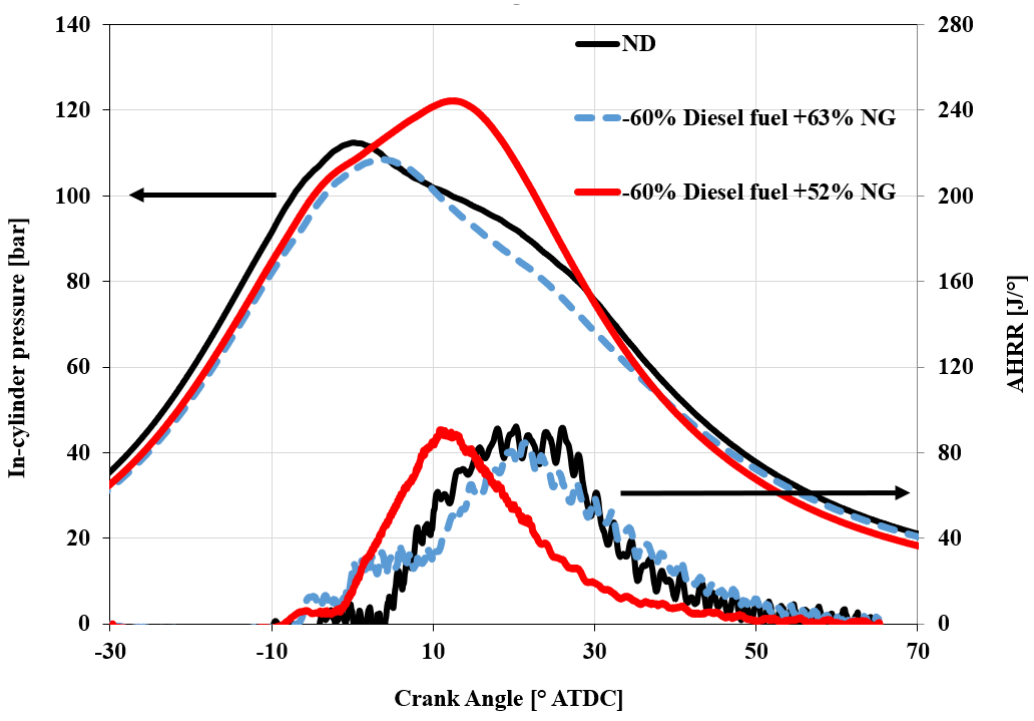

Figure 43 In cylinder pressure traces, apparent heat release

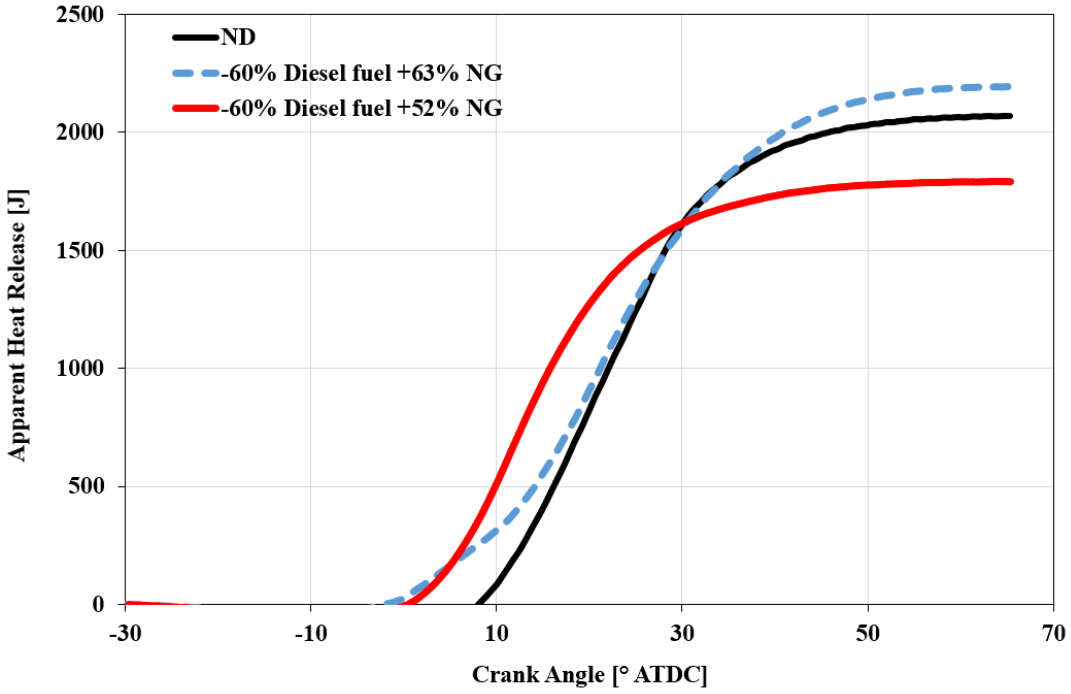

Figure 44 Apparent integral heat release rate

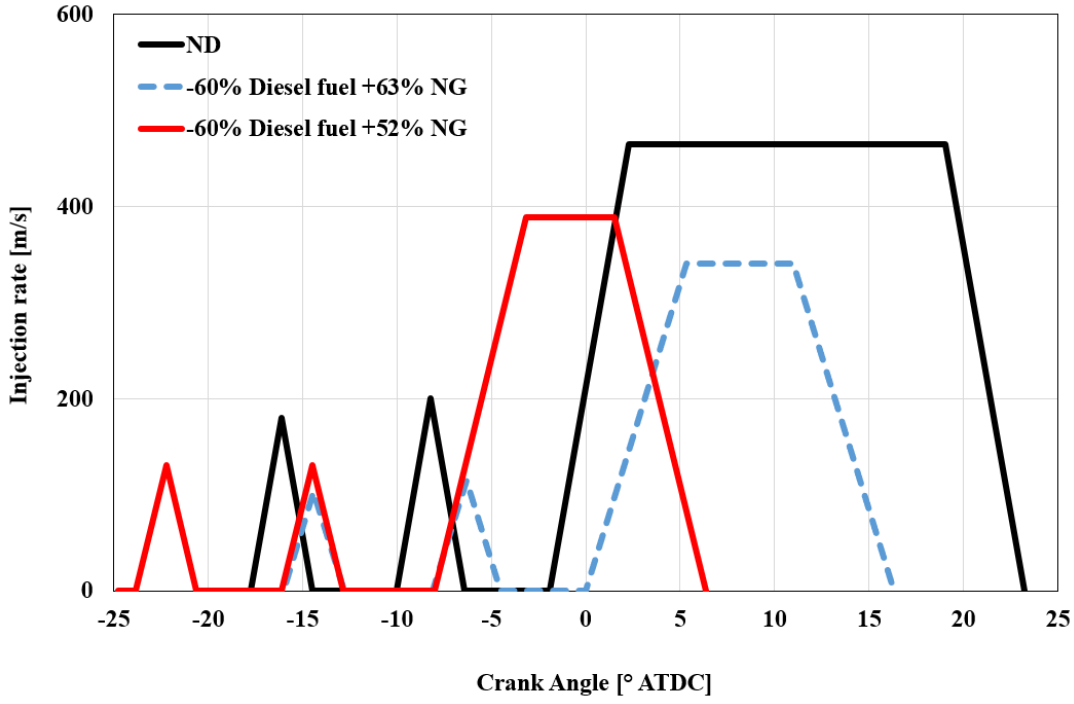

Figure 45 Injection rate and timing

In Figure 44 and Figure 45 it can be observed that the optimization of the injection strategy, in terms of ignition advance, shifts the main release of the combustion toward the TDC. This fact leads to increase maximum peak of pressure and hence temperature, Figure 43. NOx emissions can increase ,Figure 42, conversely, HC and CO emissions decrease according to improvements observed in combustion efficiency (Figure 39, Figure 41). This result is evidence of a strong link between HC/CO emissions and NOx emissions: as the formers increase, the latters decrease, and vice versa. Soot emissions reported in Figure 42 according to the previous analysis performed at BEMP = 8 bar are strongly reduced, especially in the optimized case, the rate of decrease is over 50% regarding "−80% Diesel fuel +75% NG" in comparison to ND. This evidence demonstrates another advantage when DF mode is applied to a ND engine.

3.9 Application to gen-set

The results of this experimental campaign are addressed to develop an engine for electric generation (gen-set), near 80 kW @3000 rpm, as already explained in the first section. The maximum BMEP required in order to reach power target is 12 bar, the partial load considered is set at 75% of the whole power (BMEP= 8 bar). Low loads remain of less interest especially for DF operations, because of the efficiency of the ND engine in terms of BTE and pollutant emissions.

Table 9 reports the operation point selected.

BMEP = 8 bar, 60 kW	**BMEP = 12 bar, 80 kW**
−80% Diesel fuel +74% NG	−80% Diesel fuel +75% NG

Table 9 Selected operation points for Gen-set

These two operation points correspond to the maximum substitution rate in diesel oil with a complete combustion. The amount of energy provided by diesel at high and medium load is about 20%.

	Brake power = 60 kW			**Brake power = 80 kW**		
	ND	DF	Diff [%]	ND	DF	Diff [%]
CO2 [g/kWh]	667	483	-38	719	500	-44
PM [mg/kWh]	45	13.3	-238	37.5	12.5	-200
NOx [g/kWh]	3.33	3.33	0	4.75	3.25	-46
CO [g/kWh]	0.67	0.25*	-167	0.38	0.38*	0
HC [g/kWh]	0.22	0.17*	-30	0.16	0.15*	-8

Table 10 Specific emissions for the Gen-set

*HC and CO are calculated after the catalyst.

In Table 10, specific exhaust emissions for each pollutant are reported, compared to diesel engine. As already mentioned, CO_2 and Soot emissions decrease as expected and a NOx emission decrease can be observed only at high loads. In percentage, CO_2 best reduction is near 44% and Soot is 238%. Conversely, CO and HC emissions in terms of engine-out emissions increase (as expected). However, supposing to adopt a three-way catalyst with a 95% efficiency for CO and 90% for HC, the obtained result is a strong reduction comparable to ND cases.

3.10 Numerical Validation and investigation

After the experimental campaign the second part of the activity has been focused on CFD 3D calculation. In order to further investigate dual fuel combustion without the only support of the experimental data, it is necessary to adopt CFD simulation. The first part of the campaign regards the numerical validation of the CFD model. As already mentioned, the software adopted for this calculation campaign is Kiva-3V code. In the table below, the main models and sub models implemented in the code are reported. It is important to underline that the adopted version is a custom version of the code implemented with Chalmers University with Unimore [14]. This study is a preliminary approach to the investigation of this combustion phenomena in ICE, this is intend as basis for further investigations.

Turbulence Model	RNG k-ε model
Breakup model	Hybrid KH-RT model
Droplet collision model	Droplet trajectories
Combustion	PaSR coupled with chemical kinetics
Flame Propagation	TFC / Premix code for aspirated fuel
Fuel Composition	Natural Gas / Diesel Oil Surrogate

Table 11 Kiva 3V main models

The computational grid has been created with the adoption of the pre processor K3prep , included in Kiva code. The engine has an axisymmetric geometry, so a 60° sector mesh is considered, also because the injector has 6 holes. The geometry is largely simplified, nevertheless, the differences reported in calculation for standard diesel engine vs experimental data are very few. This leads to assume that the simplified geometry introduces a small uncertainty comparable to measurement uncertainties.

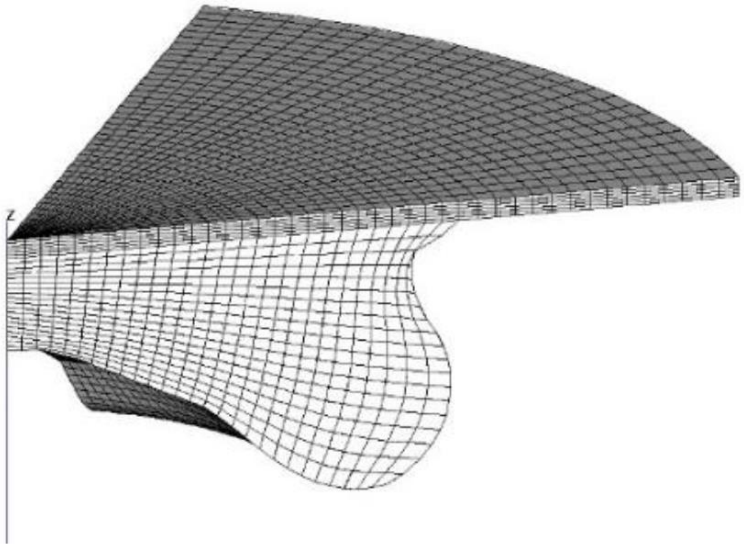

Figure 46 Computational grid at TDC

The computational grid is reported in Figure 46, the mean dimension of the cells is near to 0,5-1,0 mm, the grid consists of 100.000 cells at BDC and 25.000 at TDC . The grid has been built up adopting criteria validated in previous analysis and taken as best practice. These criteria guarantee a good compromise with computational effort and good agreement with experimental data.

Initial boundary condition of the simulations derive from experimental results, for the flow field, previous calculation has been performed[36]. The Natural gas is composed by Methane 95%, propane 4% and nitrogen 1%; Diesel oil is represented by the DOS model, where the liquid properties are the same of the real fuel while fuel vapor is a blend of n-heptane and toluene. The combustion mechanism is composed by 81 chemical species and 41 reactions.

In the figure below, for the seek of clarity, there is a summary of the operation points previously tested and optimized (as already seen in the previous sections of this chapter); in terms of the ratio of energy provided by diesel (XD) and Natural gas (XNG).

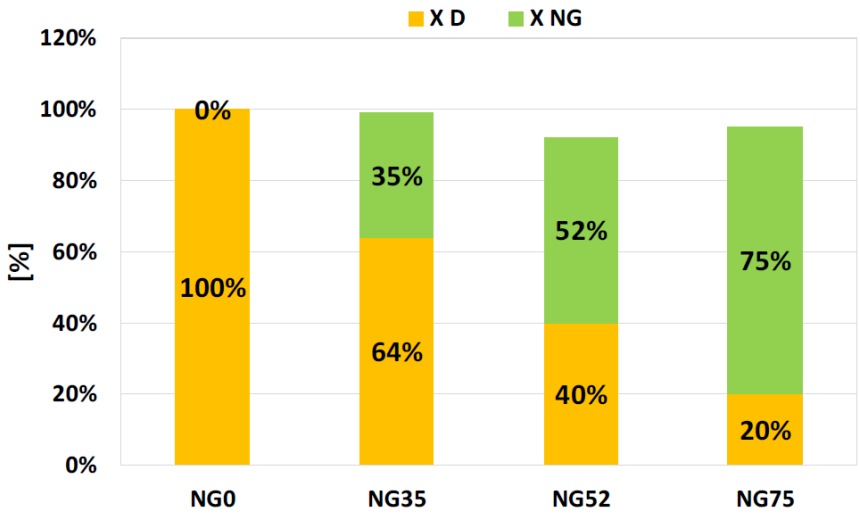

Figure 47 Operation points, optimized @3000 RPM BMEP=12 BAR

In order to get a good accuracy of the model in terms of robustness, for predictability it is necessary to calibrate the model with several experimental data. Obviously, data provided by the experimental campaign are mainly in cylinder pressure trace and rate of heat release. This last one can be calculated starting from the first thermodynamic law. The ROHR calculation is affected by errors because of thermal exchanges passing through the burnt gases and water jacket. This consideration allows to say that ROHR can not be an absolute reference for CFD calculation campaign. The purpose is to adopt parameters which can be directly measured; in this scenario, we refer to exhaust-gas concentration such as NOx, CO, CO_2 and HC.

The main calibration of the model consists in finding a setting in terms of injection curves(rail pressure, start of injection, timing etc.) and of Diesel fuel atomization.

Below in Figure 48 and Figure 49 a comparison between the results of the experimental campaign and the result of the CFD simulation campaign is made after the calibration process of the model.

In terms of agreement, the result of the campaign is satisfactory, for all cases analyzed, which leads to the robustness of the model.

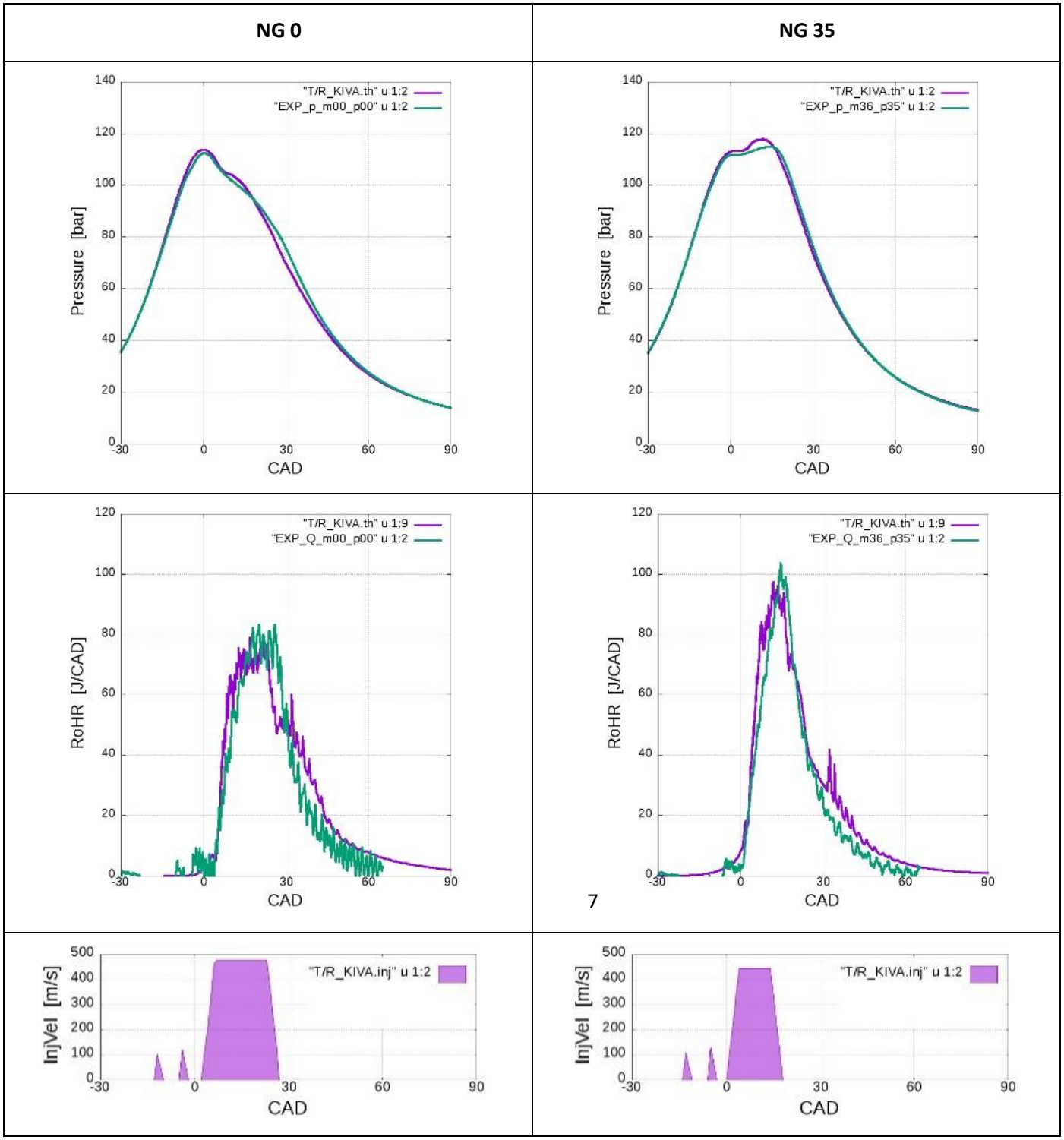

Figure 48 CFD model validation

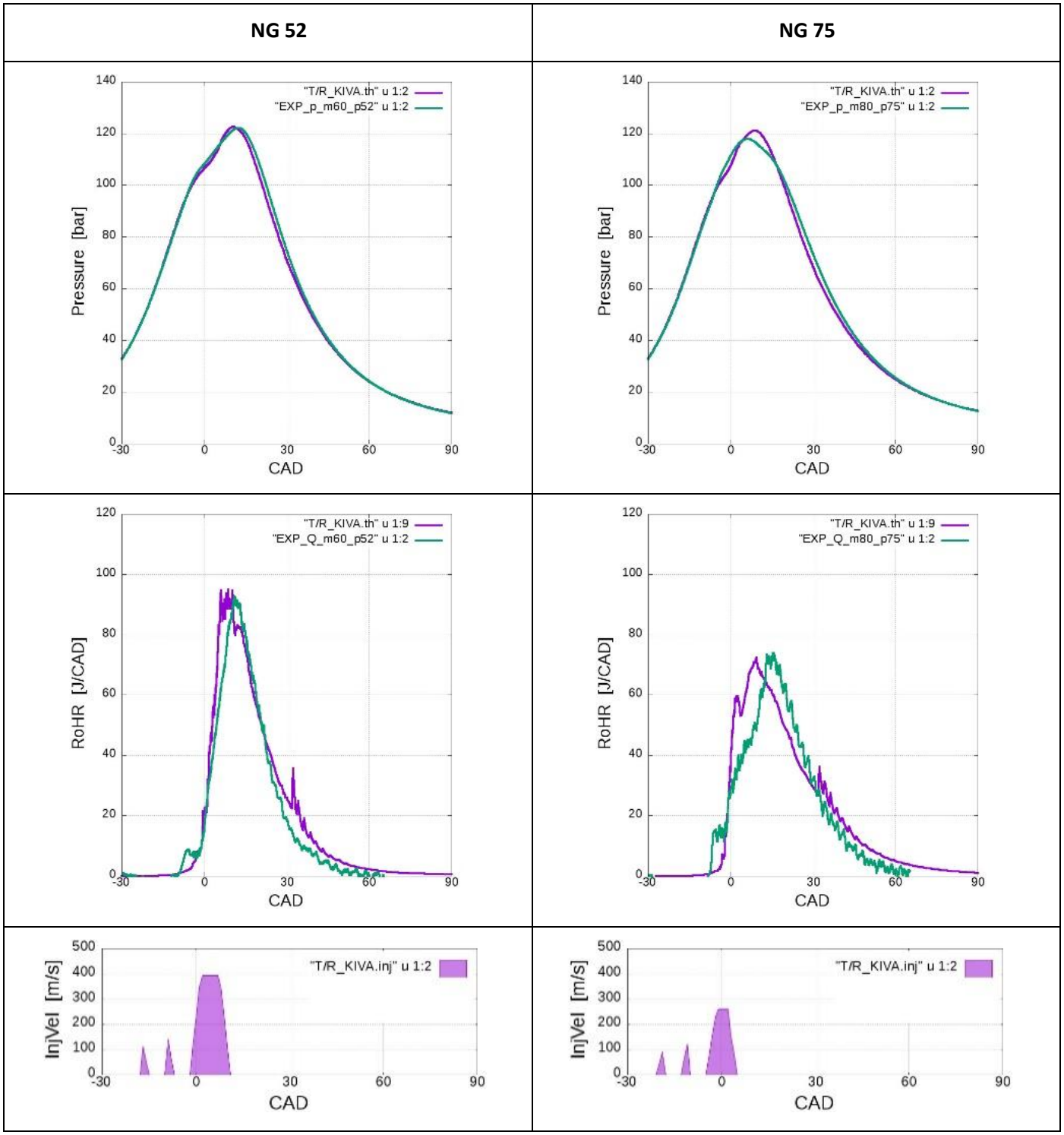

Figure 49 CFD model validation

Furthermore, a comparison between exhaust emissions is made:

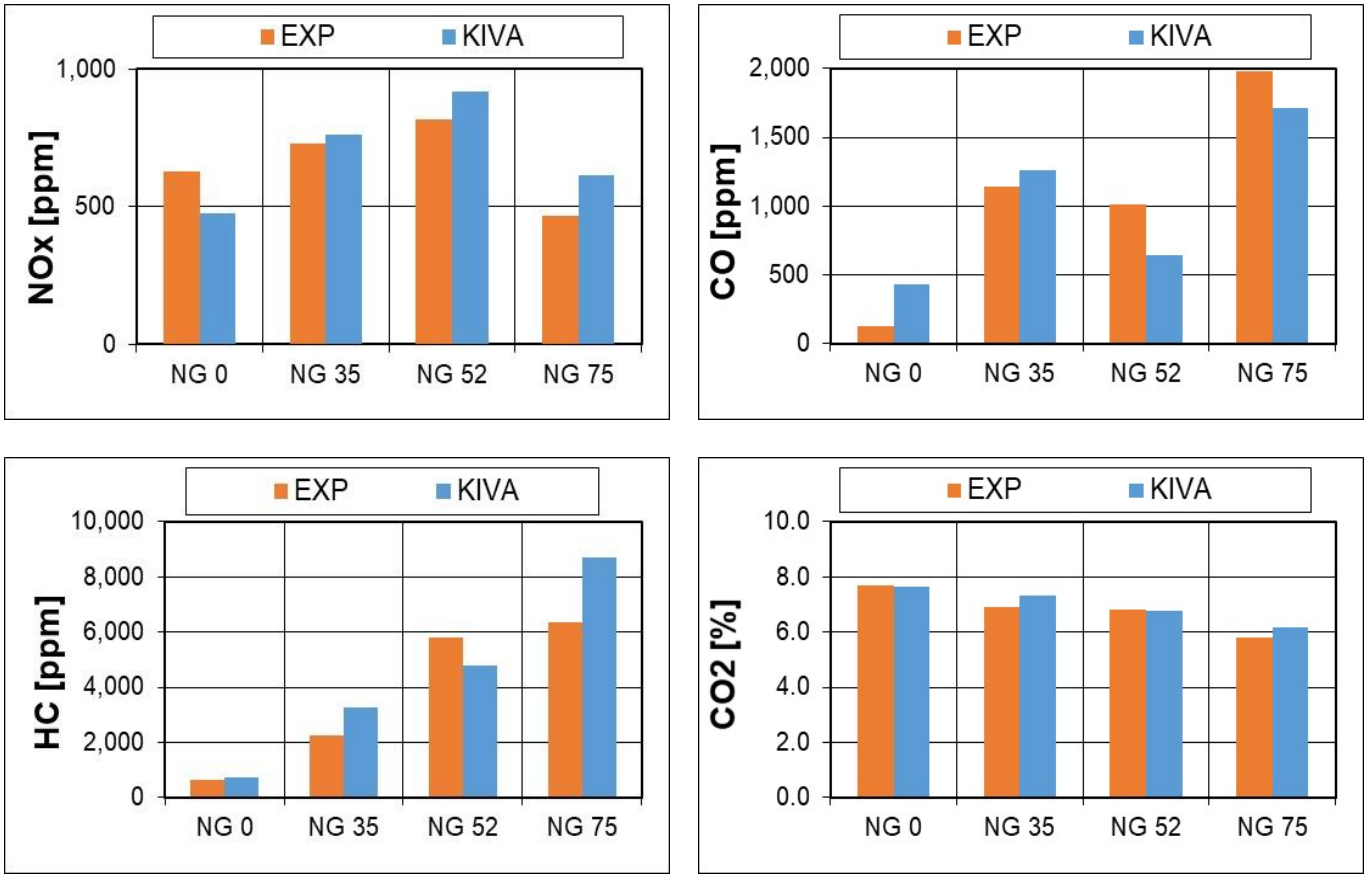

Figure 50 Emissions comparison

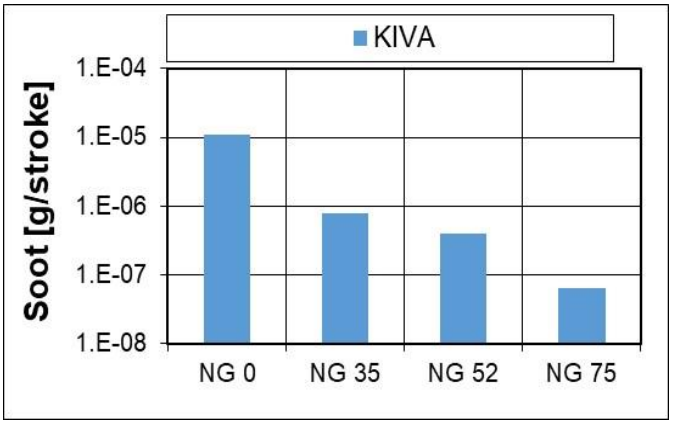

Figure 51 Predicted Soot emissions

In Figure 50 and Figure 51 the results in terms of comparison between CFD simulations and experimental data are reported. Generally speaking, there is a good agreement between the experimental data versus calculations. In particular, CFD model tends to overestimate NOx emissions, but the trend calculated by simulations follows the increment seen in experimental data. On the one hand, this result is particularly interesting in order to estimate a trend for NOx emissions; on the other hand, the absolute value can not be adopted for a good prediction.

The same results can be observed in HC emissions but, in this particular pollutant, there is an important uncertainty, near +/- 10% of the measurement instrument.

However, regarding CO, HC emissions, predicted trends are in line with the trend measured in the experimental campaign, as expected[32]. Even in these cases the absolute value is affected by calculation errors, the trend is significantly followed, in order to predict pollutant emissions trend as function of NG substitution rate.

Soot emissions are only considered by CFD predictions, because of the uncertainty of the opacimeter used for the experimental campaign. However, soot emissions predicted by calculations decrease as the substitution rate of the NG increases. This result trend is in line with the measurements made by the opacimeter[37].

After the validation of the CFD model described above, the model has been used in order to investigate the influence of the injection strategy in terms of performances and emissions, in order to find some guidelines for the development of these typical dual fuel engines[38].

In particular, two different variations of the original injection law are investigated, considering two cases at medium substitution rate i.e. NG52. The first modification regards pre and pilot injection alternatively turned off, and the energizing time of the main injection, which is proportionally increased, in order to maintain the same fuel mass injected. Furthermore, the timing of the main injection is shifted with a 2 CAD steps forward and backward.

In the next figures, the results of the CFD simulation campaign are reported.

Legend:

- Inj 111 (red lines): pre, pilot and main injections

- Inj 001 (green lines): main injection
- **Inj 011** (blue lines): pilot and main injections
- **Inj 101** (yellow lines): pre and main injections

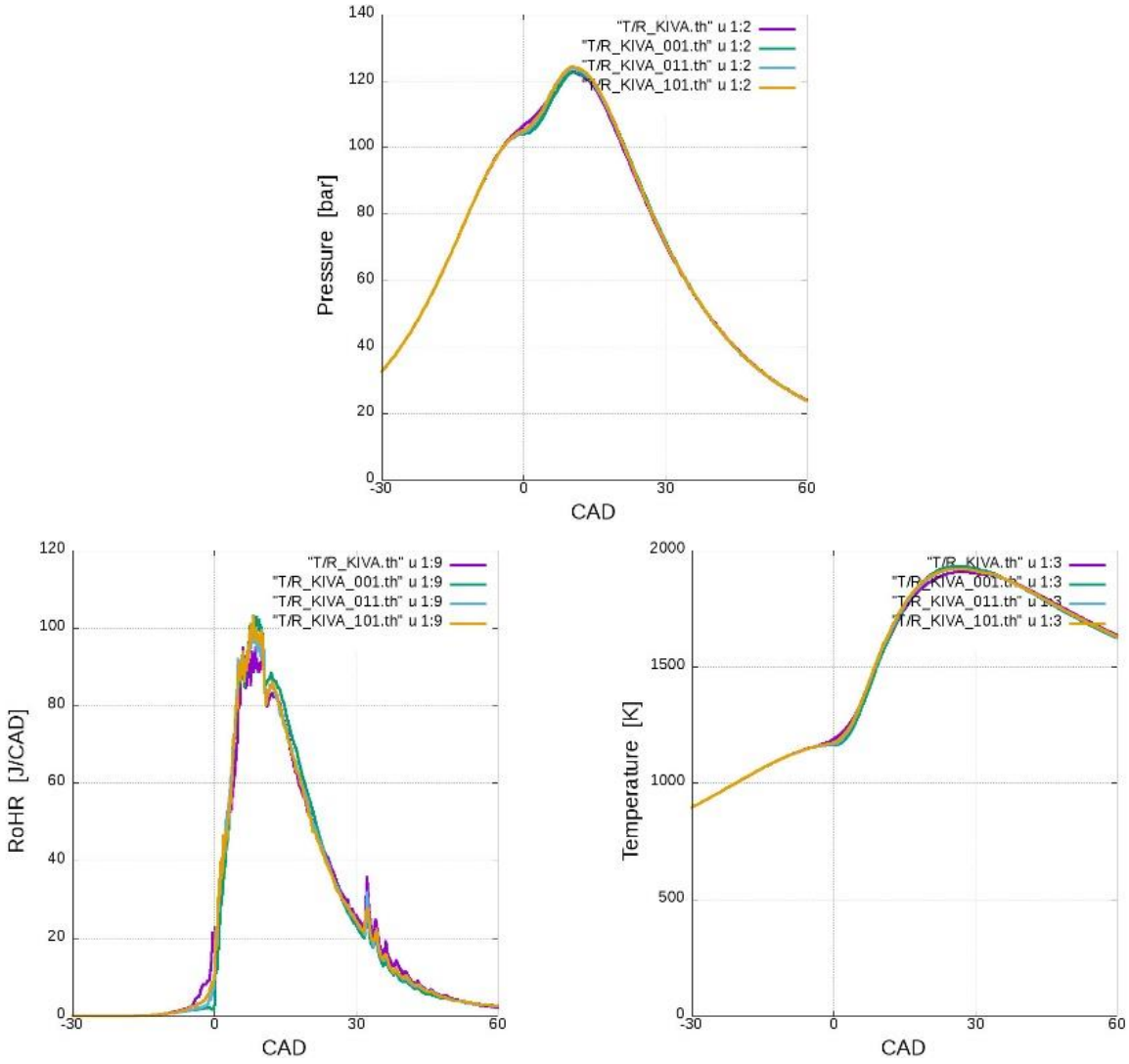

Figure 52 In cylinder pressure ROHR and mean temperature

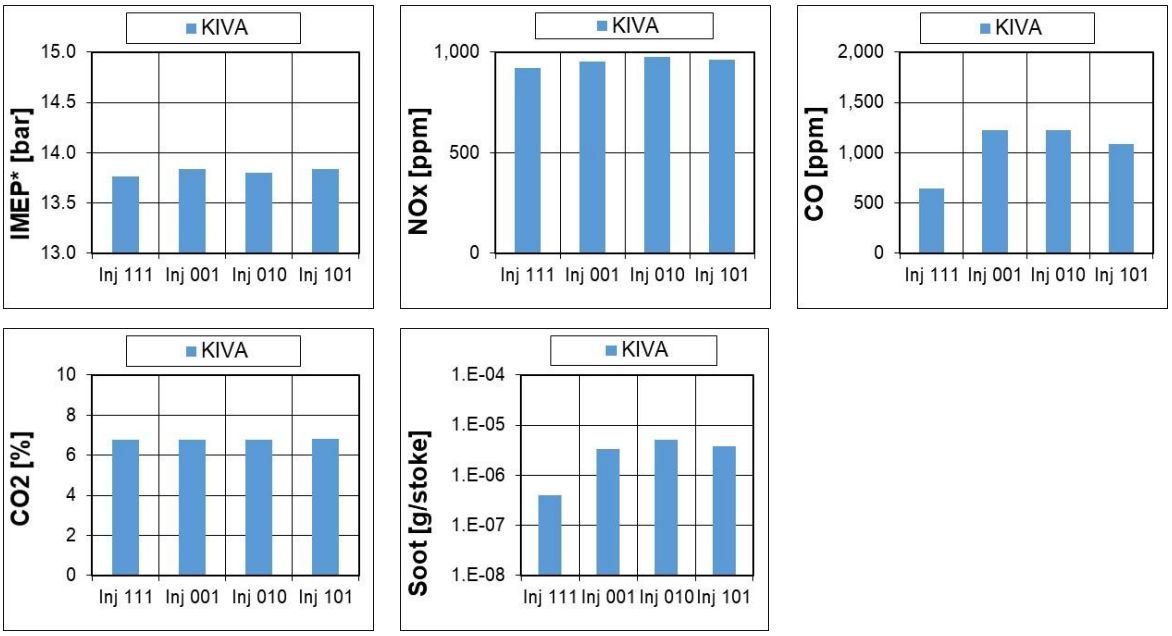

Figure 53 Soot emission and IMEP comparison

In Figure 52, Figure 53, Figure 54, Figure 55 the simulations campaign results are reported in terms of the following indicated parameters: in-cylinder pressure, temperature ROHR,Gros IMEP, and also pollutant emissions.

Looking at the figures, the elimination of pre and pilot injection does not affect in-cylinder pressure and, in particular, maximum peak reached during the combustion The only notable difference is observed in the first part of the combustion regarding the ROHR graph, where there is a small heat release in case of pilot and pre injections. Conversely, turning off these injections, the peak is not present anymore. Therefore, this difference does not affect the process unless pilot and pre injections turned on, which leads to a quite small heat release.

Another difference when pre and pilot is turned off is represented by a small increment of NOx and CO_2 emissions and a small increment of IMEP. Meanwhile, a bigger increment is registered in CO and Soot emissions.

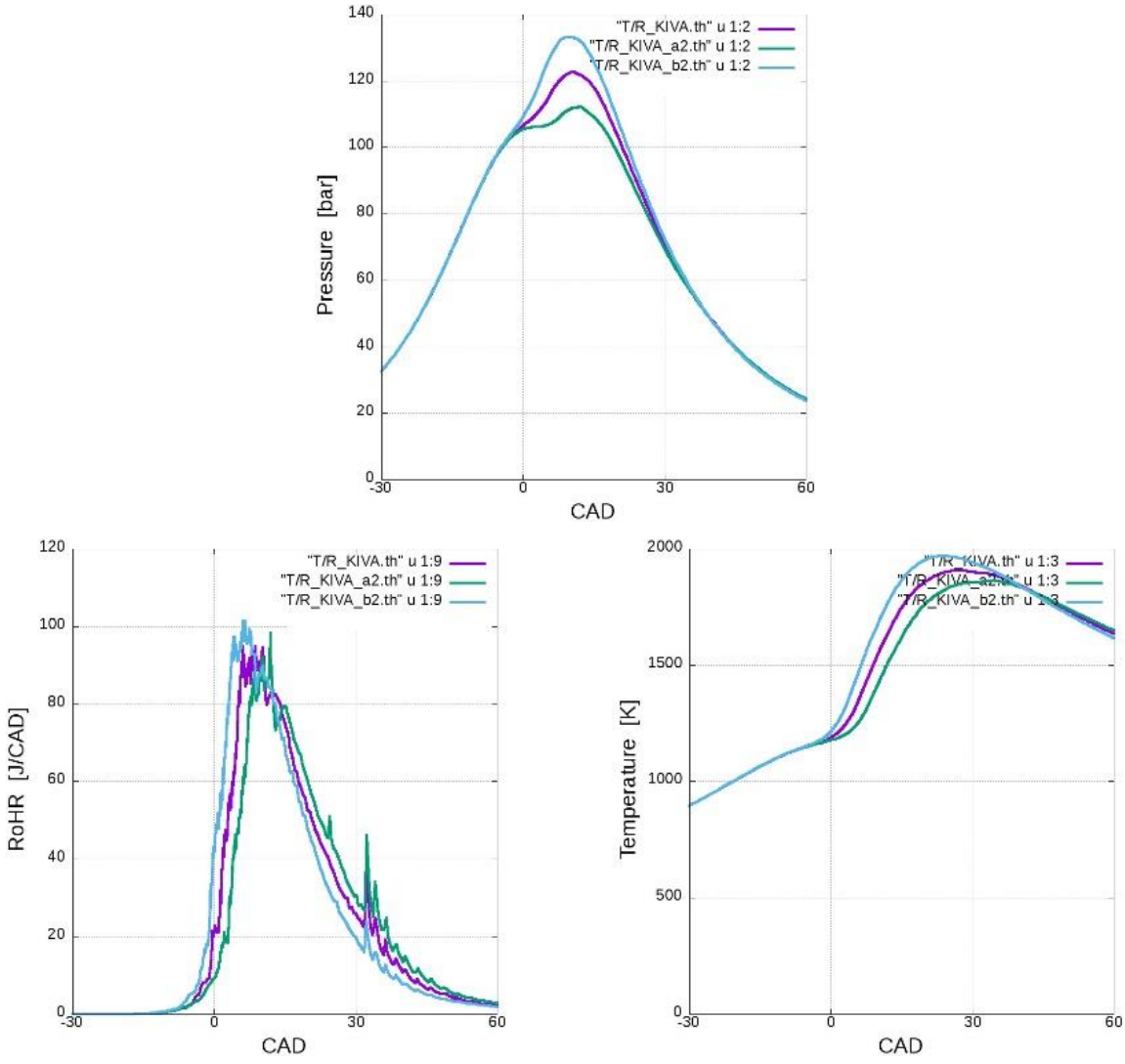

Figure 54 In cylinder pressure ROHR and mean temperature

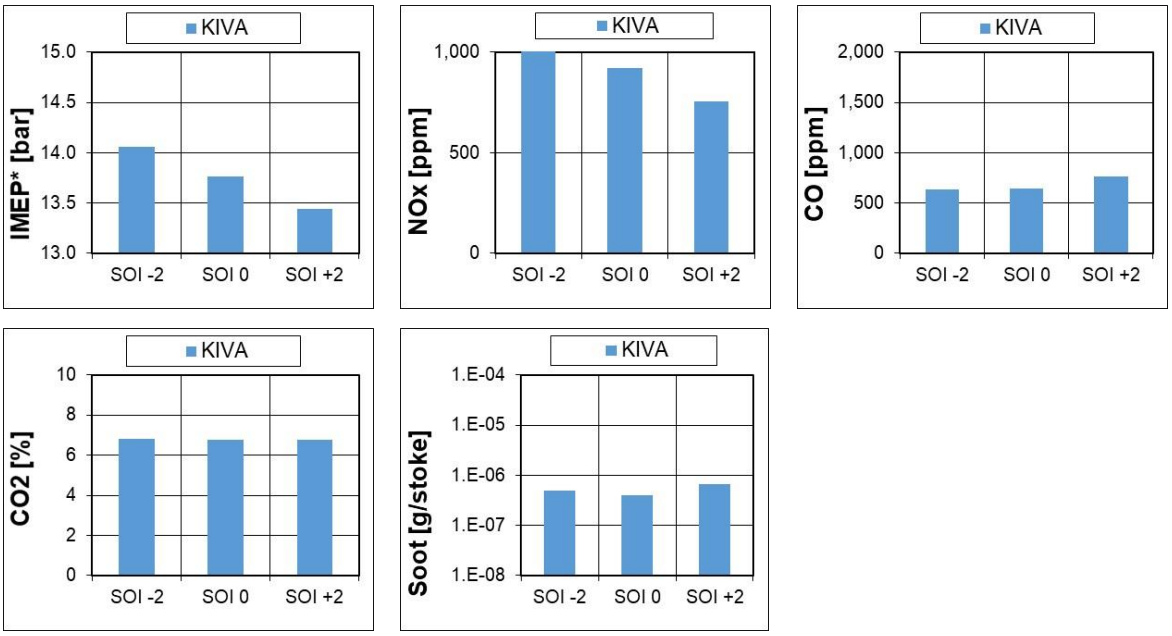

Figure 55 Soot emission and IMEP comparison

Obviously, the delay or the advance of the main injection has a not negligible impact in maximum pressure traces. With a span of + 2 CAD, the maximum peak of pressure slightly increases, about 10 BAR delta. Furthermore, the IMEP increases about 2%. The injection timing affects the in-cylinder temperature, thus NOx emissions decreases if injection is delayed[19,39].

No difference is observed in CO, CO_2 and HC emission when the injection is shifted.

3.11 Conclusions

The study presents the result of an experimental campaign carried out on a four stroke light weight common rail 2.8 turbocharged EURO IV diesel engine. The goal of this research activity is the implementation of a DF system with minimal intervention on the Injection hardware. The modified engine can reach power target imposed by preliminary constraints (80 kW @ 3000 rpm). The study is focused on the main operation points for electrical generation (i.e. 100% and 75% load), respectively 12 and 8 bar of BMEP. For each point, the start condition was the ND; the Dual fuel mode is obtained by substituting diesel with natural gas. In order to run in DF mode an optimization of the injection strategy was performed, as far as injection timing, boost pressure, injection pressure are concerned . The campaign provides some final considerations:

- Without a specific calibration, it is not possible to run DF mode with high substitution of diesel oil, with high BTE and low HC and CO emissions. Conversely, in this case, Soot and NOx emission are always low, while CO_2 tends to decrease.
- If the substitution rate remains the same BTE, HC and CO emissions tend to decrease if load increases.
- Specific calibration of the strategy increases Combustion efficiency, this leads to an increase BTE with advantages in terms of CO_2 emissions.
- The calibration also reduces HC and CO emissions, this is due to the higher combustion efficiency. Conversely NOx emissions may increase, but they remain comparable to ND mode.
- At low loads, it is not convenient to run DF mode, because HC and CO increase for the slow combustion speed due to the high air-to-NG ratio. This result may be reduced adopting a throttle valve in the intake manifold, but a further investigation is necessary in order to assess if the advantages in combustion can compensate intake pressure drop.

For the Gen-Set development DF operation points taken into consideration are 8 and 12 bar in terms of BMEP. At low loads the generator run in ND mode. With this configuration, there are some advantages in comparison to ND mode:

- The diesel fuel is strongly reduced (80%)
- CO_2 is reduced up to 44%
- NOx is reduce up to 46%
- Soot is reduced up to 238%
- Can be compliant to Stage V pollutant emissions regulation for Gen-Set

However, the development of Dual Fuel Natural gas engine requires a specific aftertreatment system (3-way catalyst), and a new calibration of injection parameters. From the engine point of view, there are few modifications for the implementation of the Gas injection system and control (injectors, piping, pressure regulators, ecu, can communication, fuel tank). In comparison to market gen-set, this solution is lighter and more compact, the displacement is about a half, without any significant drawbacks in terms of costs and durability (high value in terms of piston speed, but lower BMEP).

In conclusion, the conversion of an high speed diesel engine into Dual Fuel Natural Gas engine can be a very promising and easy to run solution; this leads to reducing environmental impact of Gen-set maintaining same standard in terms of reliability, efficiency and costs.

After the first experimental study, a numerical validation has been performed in order to investigate how main injections parameters affect the combustion process in terms of heat release maximum pressure peak and Pollutant emissions. The main results of the study may be reduced to some observations:

- Pre and Pilot injection does not affect combustion process, they can make heat release smoother, but with a not significant increment in maximum peak of pressure.
- Turning on pre and pilot injections may lead to a slightly increase of IMEP, NOx and CO_2 but not significantly. Conversely, CO and Soot emissions increase.
- Delaying or advancing significantly injection affects maximum peak of pressure
- SOI affect mean in-cylinder temperature, in case of retard can decrease NOx emissions

4 Experimental investigation on an engine running in RCCI combustion

4.1 Introduction

As described in the previous chapter, the LTC (low temperature combustion) can be a practicable way to reach euro 6 emission target. In chapter 5, we investigate some guidelines for a dual fuel Diesel Natural Gas engine. In this chapter, we investigate the potential of a dual fuel Diesel – Gasoline engine. In this case, the dual fuel mode is different from the previous case. The most spread technique in LTC is the HCCI (homogenous compression charge ignition), where a lean mixture of gasoline or diesel are diluted in air and EGR, during the compression phase the pressure and temperature rise up to ignite the charge. In this case, no flame front is generated; the process is a controlled "knock" combustion. Nevertheless, this process is difficult to control, especially in transient mode and with high loads, because the cycle-to-cycle variations lead not to have precision in charge auto-ignition timing. Furthermore, high loads are not possible because of noise and mechanical loads; raw combustion tends to increase maximum peak of pressure into cylinder.

Conversely, this combustion concepts permits less NOx emissions, Soot, and CO_2, if an optimization is made for specific DF combustion[40].

An alternative is to inject directly a small amount of a high reactive fuel (diesel), as already seen in chapter 5. This HCCI (homogenous compression charge ignition) technique leads to several advantages because this modification has the effect to create a tight correlation between the late fuel injection and the auto-ignition process:

- Improve controllability of the combustion process
- Reduce CO and HC emissions

In literature, this combustion strategy is named in many different ways, the most used are reported as it follows [41–46]

- Premixed Charge Compression Ignition (PCCI) combustion
- Partial Fuel Stratification (PFS) combustion
- Partially Premixed Combustion (PPC)
- Partially Premixed Compression Ignition (PPCI) combustion

This experimental research activity is focused in the development of a dual fuel Diesel oil Gasoline. The low reactivity fuel is premixed with a modification of the engine by a Port fuel injection system driven by a custom control unit. The main advantages are the control of the reactivity of the premixed charge with the air-to-gasoline ratio. As a result, a more controllable combustion process and, consequently, a wider operating range can be obtained, along with higher Brake Thermal Efficiency (BTE) and low NOx and soot emissions [42,47,48]. The experimental activity has been carried out without using external EGR, in order to identify the upper threshold beyond which Diesel injection is no longer sufficient to obtain a regular RCCI combustion[49].

4.2 Engine setup

The engine used for this experimental campaign is the same chosen for the Dual Fuel Gen-Set described in the previous chapter. For the seek of clarity, the engine is a four cylinder diesel directly injected common rail Euro IV diesel engine. The main features are reported in Table 3. The experimental setup of the engine at the test bench is similar to the one adopted for the DF NG engine. The differences in this case regard the gasoline injection system and the controller. In addition, the test bench is the same used before.

The engine has to be modified in order to run in RCCI combustion. The main modifications of the engine obviously regard the injection system. In order to have a homogenous premixed charge (the study does not aim at investigating mixture formation), gasoline injectors are placed just before the intercooler.

Installed injectors are common commercial PFI injectors reported in Figure 56.

Figure 56 common PFI injector

This injectors can run only with quite low injection pressure (near 4 bars). In order not to run into mixing problems due to the low injection pressure, the injectors are far from the intake ducts. This position can not be adopted in a commercial automotive engines because of the slow response in terms of load variation which may cause lambda oscillation. This

phenomenon is not acceptable because three-way catalyst can only work in stoichiometric conditions, high oscillation in lambda value lead to damage the component.

However, in comparison to the NG injectors that inject gas fuel, PFI gasoline injectors inject a liquid fuel, in this case it is fundamental to orient injectors towards the air mass flow predominant direction. This characteristic is required in order to prevent liquid fuel formation in the intake manifold. Fuel film can act as disturbance in air-to-fuel ratio cycle to cycle control.

In order to consider this constraint, a specific spray duct is designed using a free CAD software and realized in rapid prototyping with a FDM printer. The result is reported in Figure 57, Figure 58.

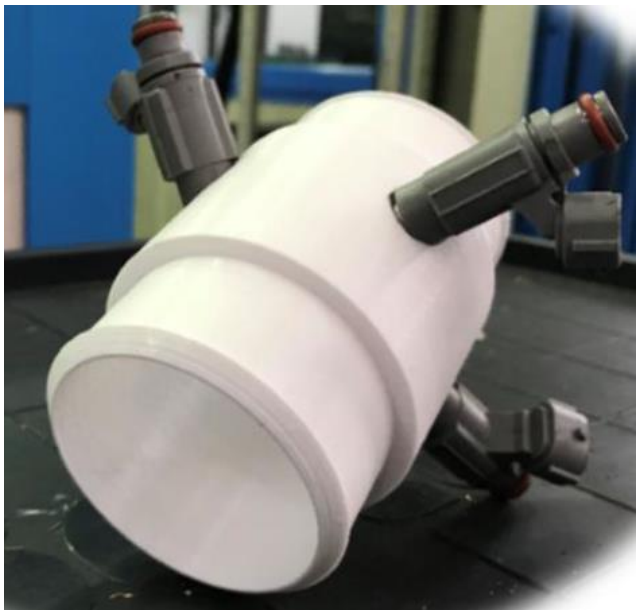

Figure 57 PFI injector manifold detail 1

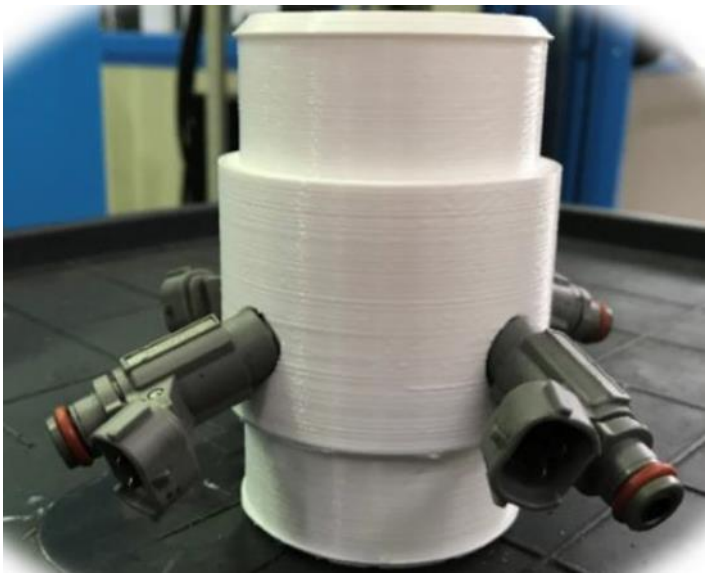

Figure 58 PFI injector manifold detail 2

PFI injectors are tilted 30° towards the main pipe direction and also tilted into perpendicular at the same direction (20°). The second tilt is used to generate a small swirl in the injection pattern in order to ensure a better vaporization and to avoid fuel film generation. Four injectors are used in order to provide the right amount of gasoline. This configuration is equal to a single point injector system, the number of 4 injectors has been chosen because the droplet dimensions decreasing. This fact lead to increase evaporation fuel flow rate.

Injector flow rate is reported in Figure 59:

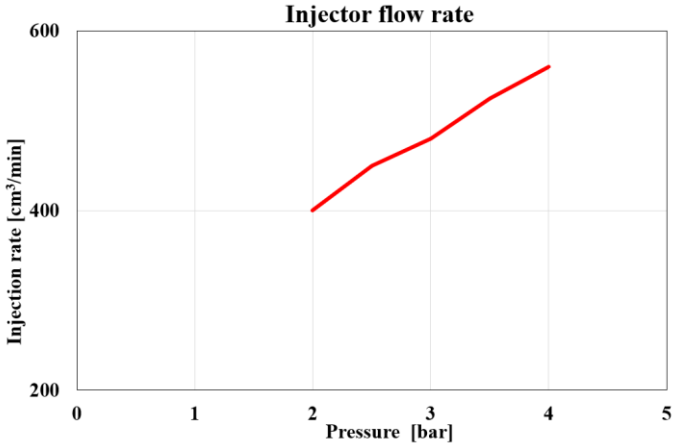

Figure 59 Injector flow rate

As already mentioned in the previous chapter the engine is controlled by a Develop ECU driven by ETAS INCA calibration software. As far as the PFI injection is concerned, it is controlled by “Drivven” control system. This system is a lab view base flexible ECU; this hardware is modular and can fit many requirements: e.g. drive direct injectors , throttle body, hall sensors, phonic wheels, pfi injectors, egr valve , etc.). In this case, the PFI injector module and the crank position sensor are used in order to get right timing injection.

In Figure 60, the Drivven system is reported.

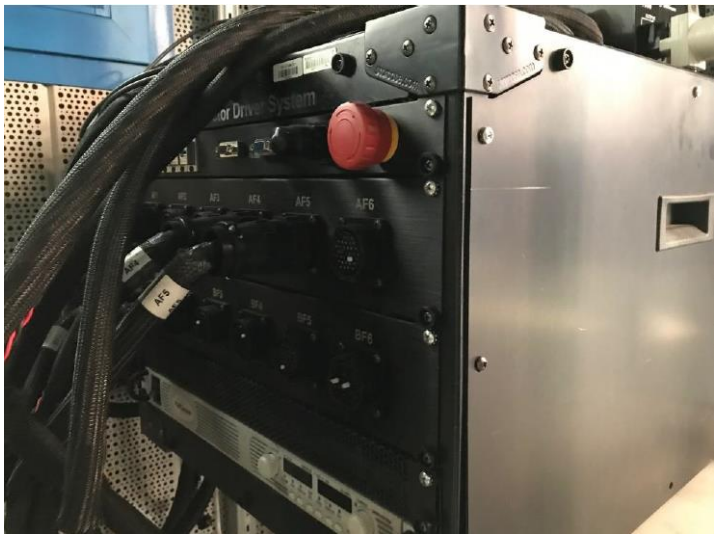

Figure 60 NI Drivven control system cabinet

Drivven system is driven by a specific software provided by NI, called SCM. With this instrument it can be possible to program custom algorithm for injection strategy In other words, it is a rapid prototyping software for injection control. In this study, an injection timing is calibrated and the energizing time of the injectors is controlled according to engine loads.

4.3 Experimental setup

The activity is focused in the study of two operating points both at 1500 rpm. The operation point chosen for the activity are reported below:

Engine load	Engine speed [rpm]
150 Nm BMEP =6,75 bar	1500
300 Nm BMEP = 13.5 bar	1500

Table 12 engine operation points

At each engine load, the activity starts from ND (Normal diesel) mode, the RCCI mode is built up replacing Diesel oil mass flow rate with gasoline flow rate, maintaining the same engine load, using two closed loop PI controllers: one for targeting engine torque, the second for engine speed. The first controller actuate pedal position, the second the eddy current brake torque by the current flow into the solenoid of the dynamometer. In order to make the system stable, it is necessary to set on of the two controller slower than the other , because if the two control speeds are the same a torque oscillation can occur.

Acting to the throttle pedal position, in order to take torque constant when adding gasoline, generates some side effects because changing operation point in the ECU controller may lead to change several parameters such as injection timing strategy, boost pressure etc. .

Therefore, in order to assess equivalent conditions switching from ND to RCCI, the EGR valve is kept closed and the boost pressure is kept constant.

The rate of substitution gradually increases, point by point. In Table 13, all the experimental points investigated are reported.

In order to compare different cases, itis necessary to define some indices:

$$X_{\text{Diesel fuel}}\,[\%] = \left(\frac{\dot{m}_{D,RCCI}}{\dot{m}_{D,CD}}\right) \cdot 100$$

(4.1)

The percentage of substitution is :

$$X_{\text{Diesel fuel}}\,[\%] - 100$$

(4.2)

Similar to the diesel fraction, the gasoline fraction of energy in comparison to the total amount in the ND mode:

$$X_{\text{Gasoline}}\,[\%] = \left(\frac{\dot{m}_G \cdot LHV_G}{\dot{m}_{D,CD} \cdot LHV_D}\right) \cdot 100$$

(4.3)

1500 rpm- 150 Nm		**1500 rpm 300 Nm**
Original injection law	Modified injection law	Original injection law
ND	ND	ND
-16.9% Diesel oil +25% gasoline	-27.6% Diesel oil +26.4% gasoline	-14% Diesel oil +17.2% gasoline
-24.6% Diesel oil +36.8% gasoline	-37.6% Diesel oil +38.8% gasoline	-18.5% Diesel oil +22.8% gasoline
-42.8% Diesel oil +42.7% gasoline	-62.1% Diesel oil +59.3% gasoline	-30% Diesel oil +33.5% gasoline
	-73.4% Diesel oil +71.6% gasoline	

Table 13 Experimental campaign operation points

4.4 Experimental Result

In this paragraph, the analysis of the results obtained comparing ND to RCCI mode are presented for each considered operation point. The main comparison is made with the analysis of the in cylinder pressure traces, mass fraction burned, ROHR (rate of heat release), and Brake thermal efficiency.

- 1500 rpm 150 Nm

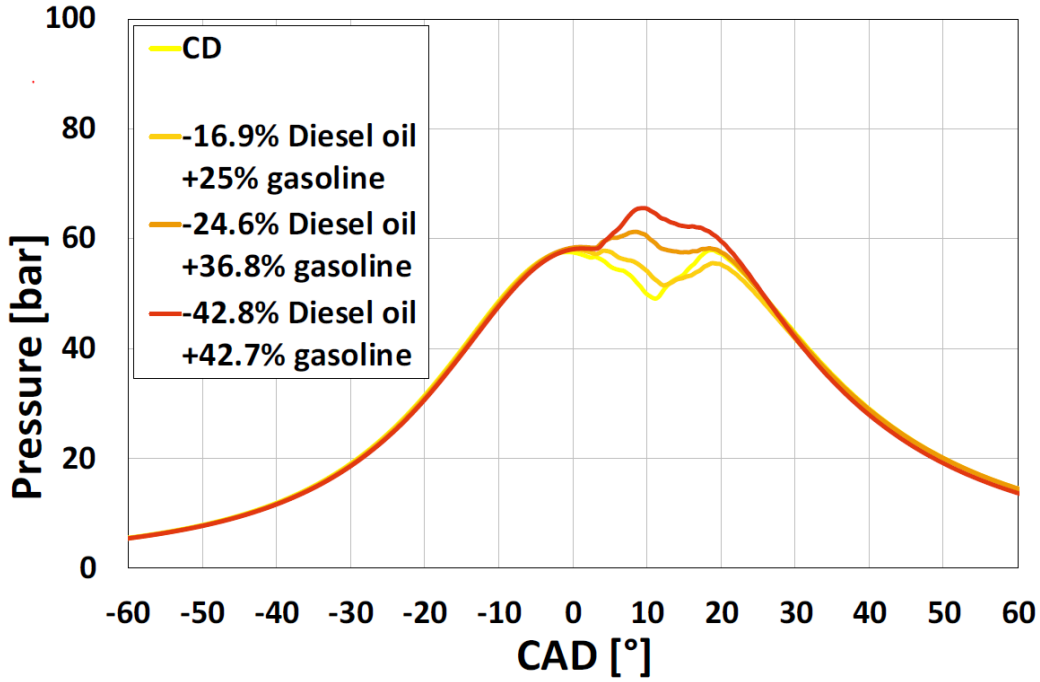

Figure 61 In-cylinder pressure traces

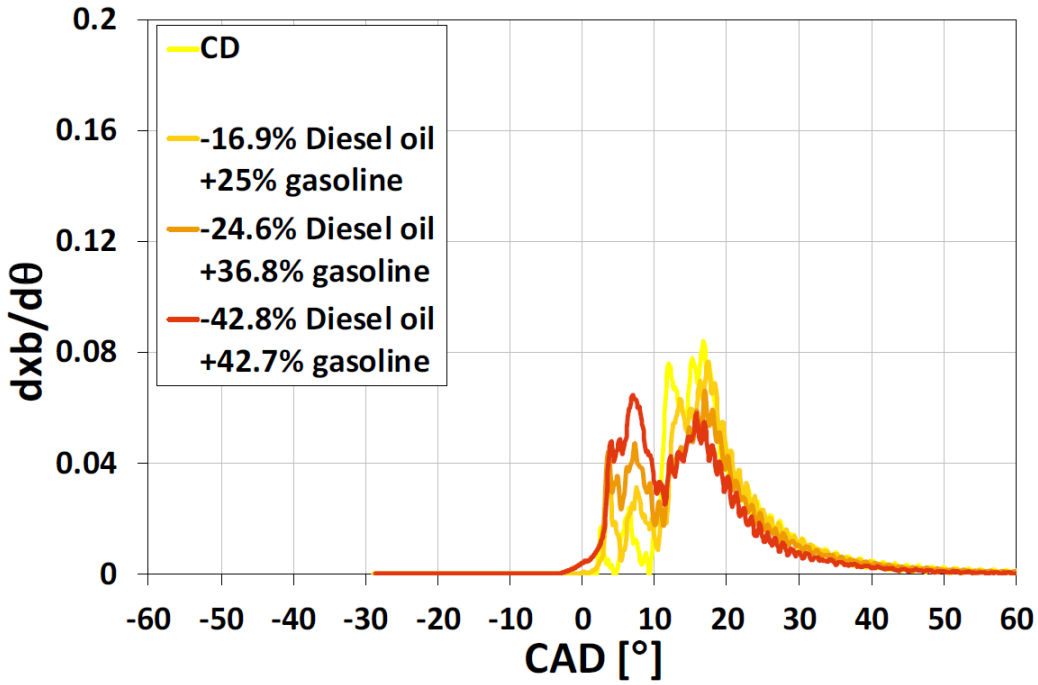

Figure 62 Rate of heat release

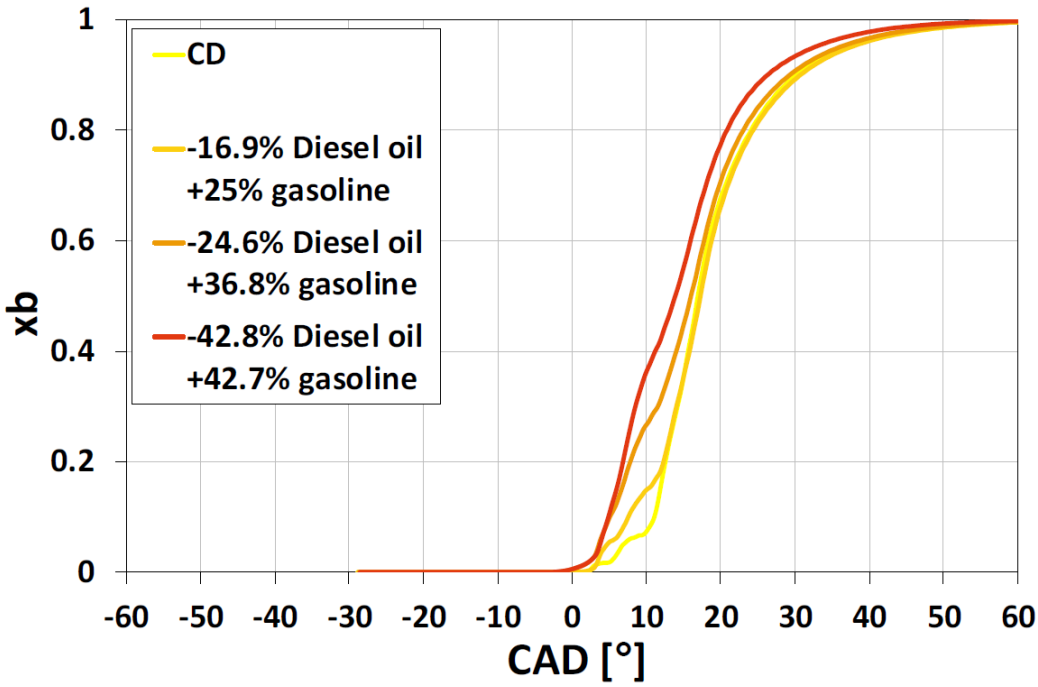

Figure 63 Mass fraction Burned

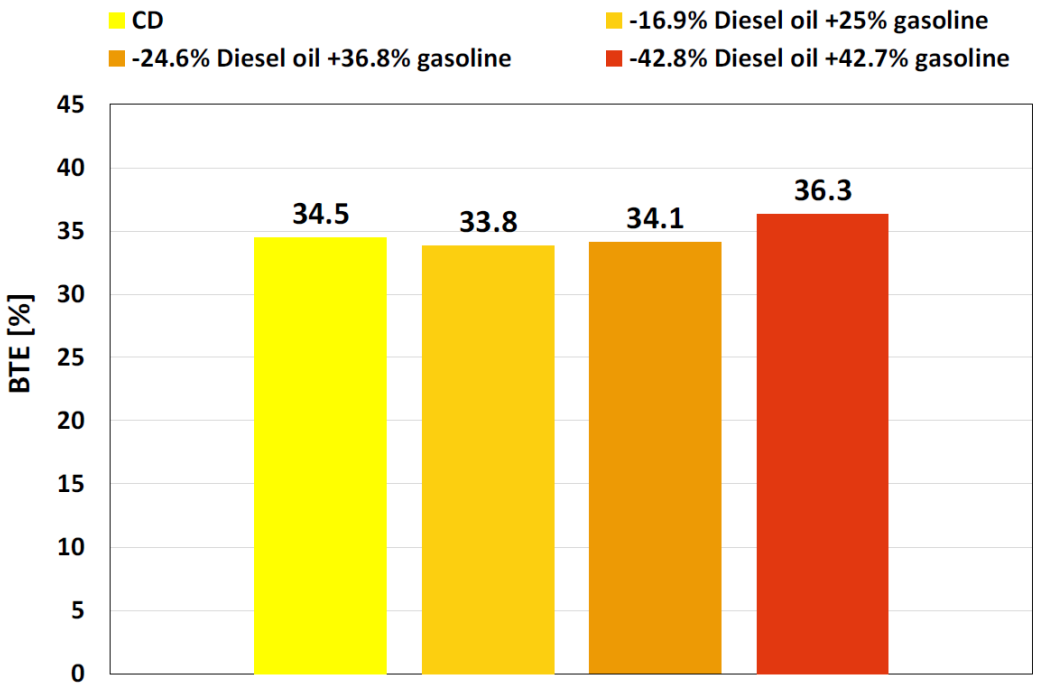

Figure 64 BTE comparison

By increasing diesel flow rate with gasoline, the peak of heat release during the main injection decreases, which is expected because decreasing gas pedal position mainly acts in the main injection energizing time (Figure 62). Regarding the same figure, it can be noticed that the heat release increases when pre-injection is injected, the premixed air-to gasoline premixed charge may burn when the pre injection ignites. The grater is the substitution in terms of gasoline, the greater is the peak of heat release observed near the TDC.

Analyzing Figure 61, the maximum peak of pressure increases as the substitution rate increases. This is due to the peak of heat release and to the burn of the premixed charge during pre-injection. Globally, the heat release is shifted toward top death center (Figure 63). As a result, in-cylinder pressure increases.

Looking at Figure 64, RCCI mode with low substitution rate of gasoline -24,6% Diesel oil +36,8 % Gasoline and -16% Diesel oil +25% Gasoline, may register a decrease in terms of

Brake thermal efficiency. This worsening is mainly due to not having optimized the calibration in terms of injection strategy.

On the other hand, at high Diesel substitutions -42,8% Diesel oil +42,7 % Gasoline even without optimization, it registers an increase of less 2% of BTE.

The main reason is the faster combustion observed in the heat release ratio. The faster the combustion is, the higher the indicated efficiency results.

After this first run, a specific campaign has been made in order to optimize injection parameters and to increase rate of substitution and BTE improvements. The obtained results are reported here below, from Figure 65 to Figure 68:

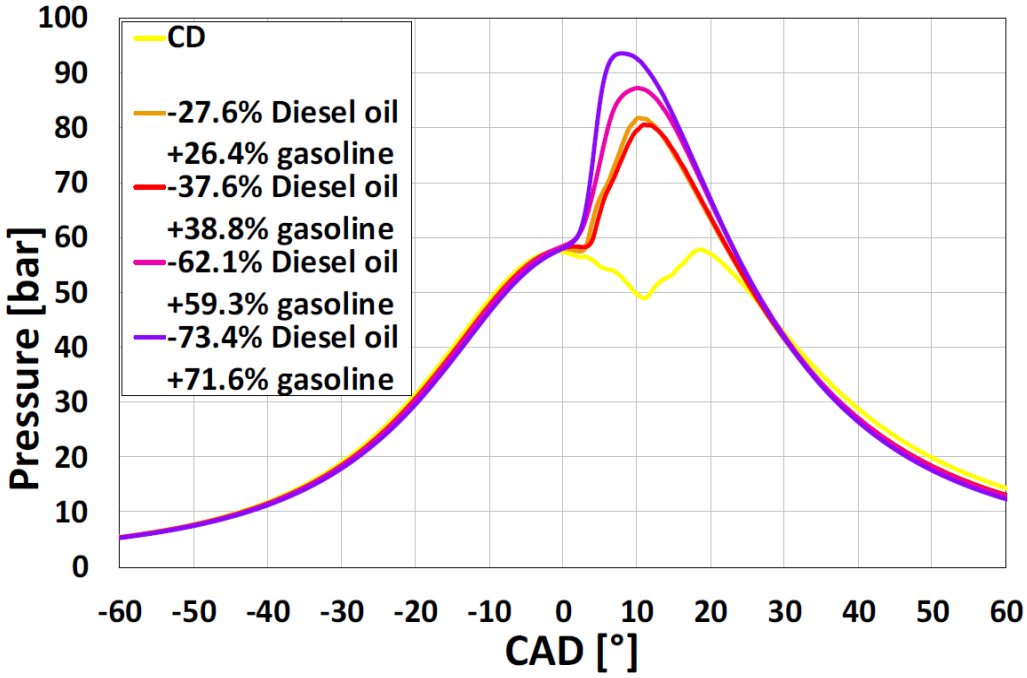

Figure 65 In-cylinder pressure traces optimized Cases

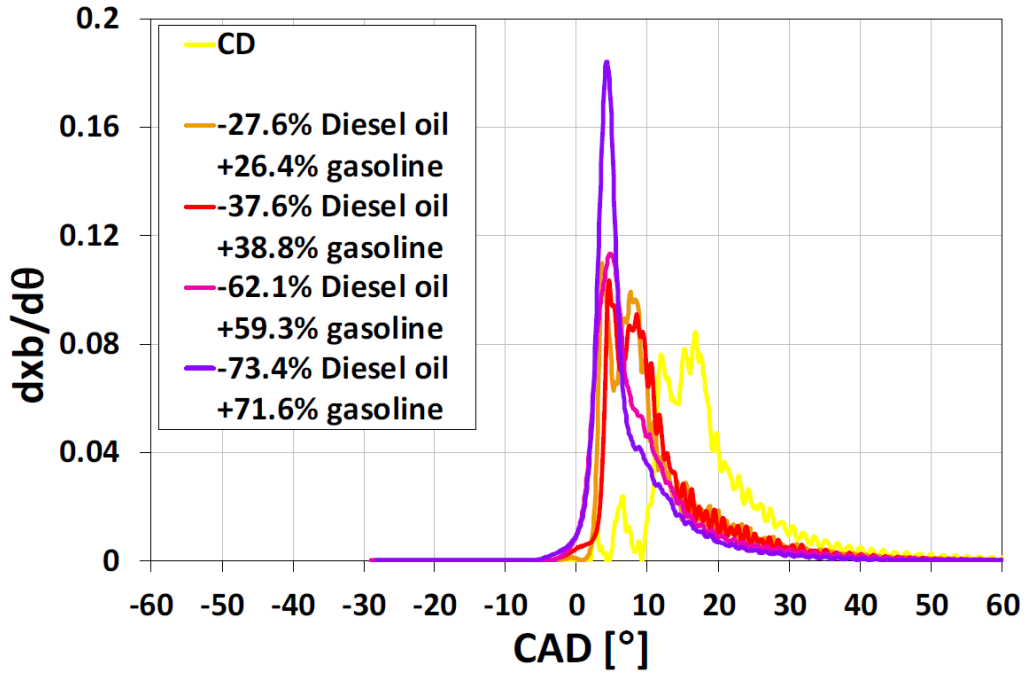

Figure 66 Rate of heat release optimized Cases

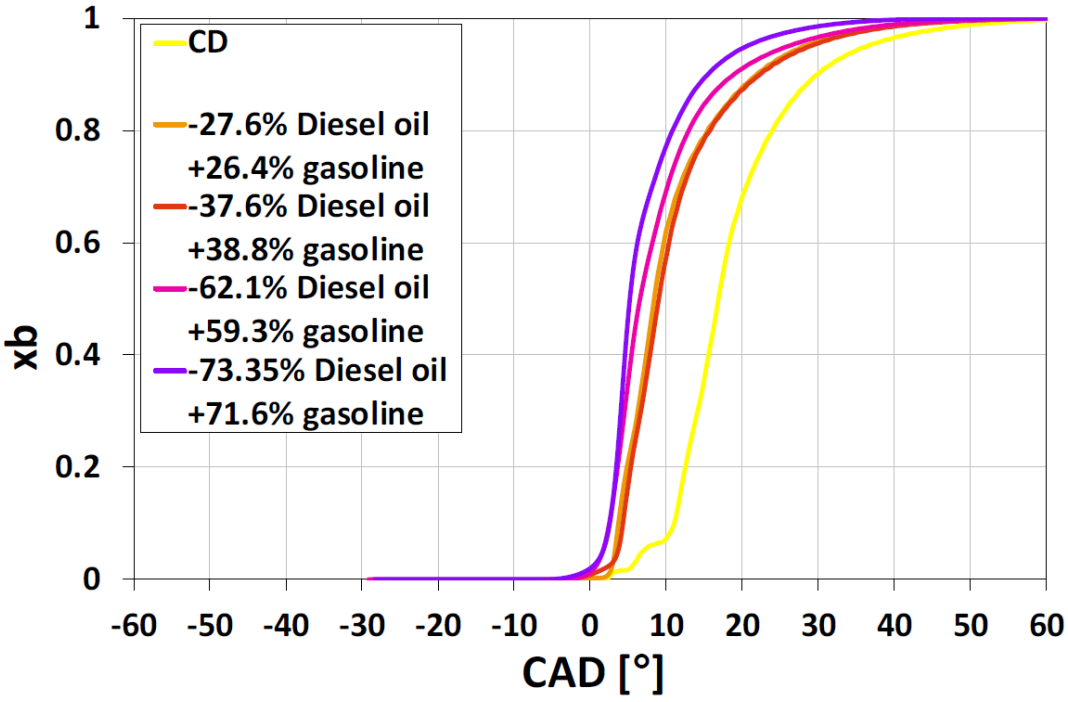

Figure 67 Mass fraction Burned optimized Cases

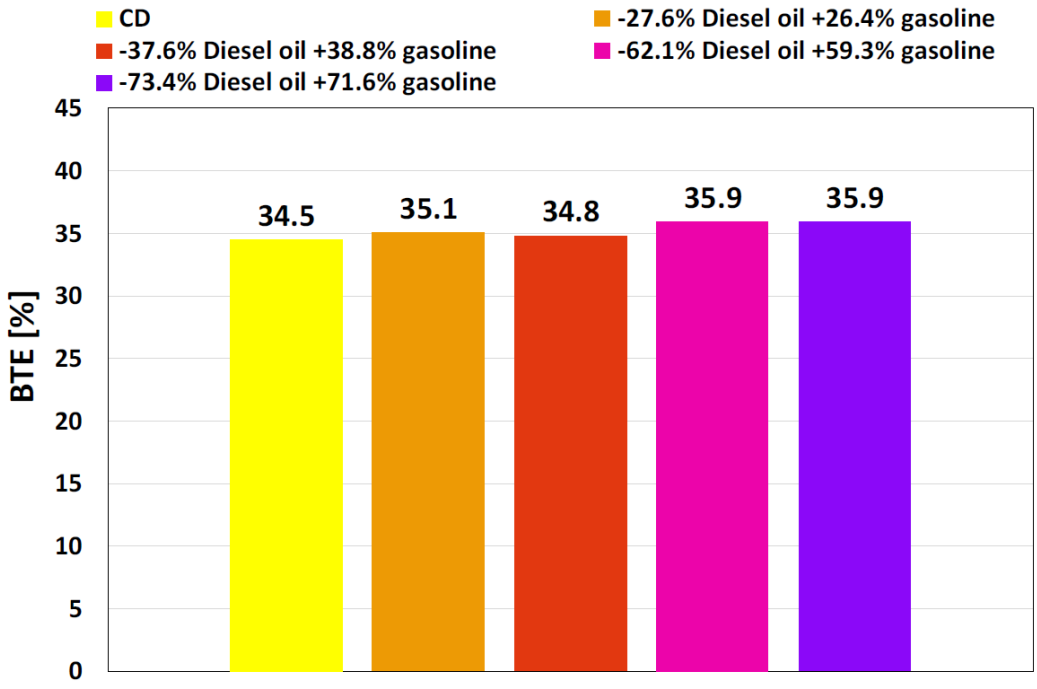

Figure 68 BTE Comparison optimized Cases

The calibration process optimize injection timing and the numbers of shots, injection amount and injection pressure. In particular, the main difference is the absence of pilot and pre injections, at the same time the advance of the main injection increases, and also the injection pressure.

It is important to underline that the higher is the substitution of diesel, the lower is the optimum injection advance, in order to get a faster and complete combustion, without obtaining an excessive increase in maximum cylinder pressure peak. As a result, of this modification in the injection strategy BTE increases up to 4% in comparison to normal diesel operation. As already seen before, this behavior becomes more evident as the substitution rate increases. This means that, at values of BMEP below 7 bars, the reduction of soot due to the substitution of Diesel fuel may be associated also to an improvement of fuel efficiency, thus of CO2 emissions.

The second operation point investigated is now considered; the results in terms of in cylinder pressure, rate of heat release, mass fraction burned and brake thermal efficiency are reported from Figure 69 to Figure 72.

The engine load for this point is 300 Nm @ 1500 rpm according to Table 1.At high loads it has been observed that the charge starts to auto-ignite before the injection of diesel fuel. This results correspond to a fast heat release Figure 70, this is due mainly to the high temperature and pressure into the charge. The chemical reaction in this environment are speeded up. The higher is the Diesel substitution rate, the richer is the air-gasoline homogenous mixture. The conversion from ND to RCCI mode in this case cause a worsening in terms of BTE Figure 72. In an attempt to avoid auto-ignition of the premixed air-gasoline mixture, the Diesel injection advance has been increased. BTE improves, but at the cost of a strong increase of peak in-cylinder pressure and combustion noise. This evidence demonstrates the importance of EGR, that plays a key role in RCCI combustion mode, and more in general in LTC, since it guarantees a much better control of ignition timing and ROHR.

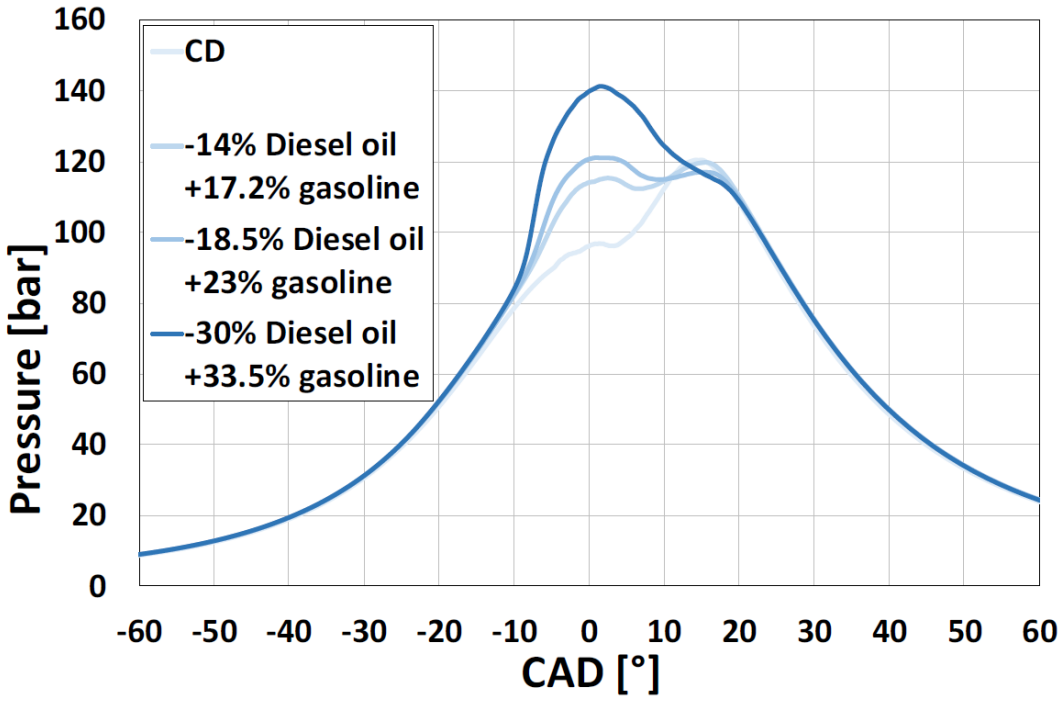

Figure 69 In cylinder pressure High loads

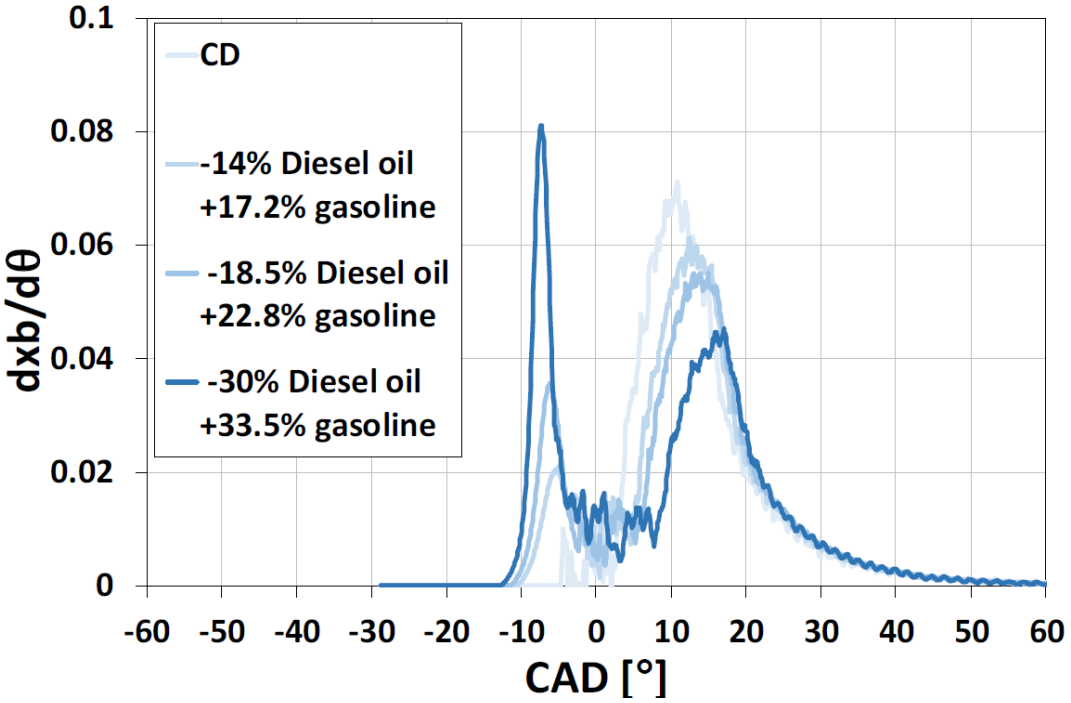

Figure 70 Rate of heat release high loads

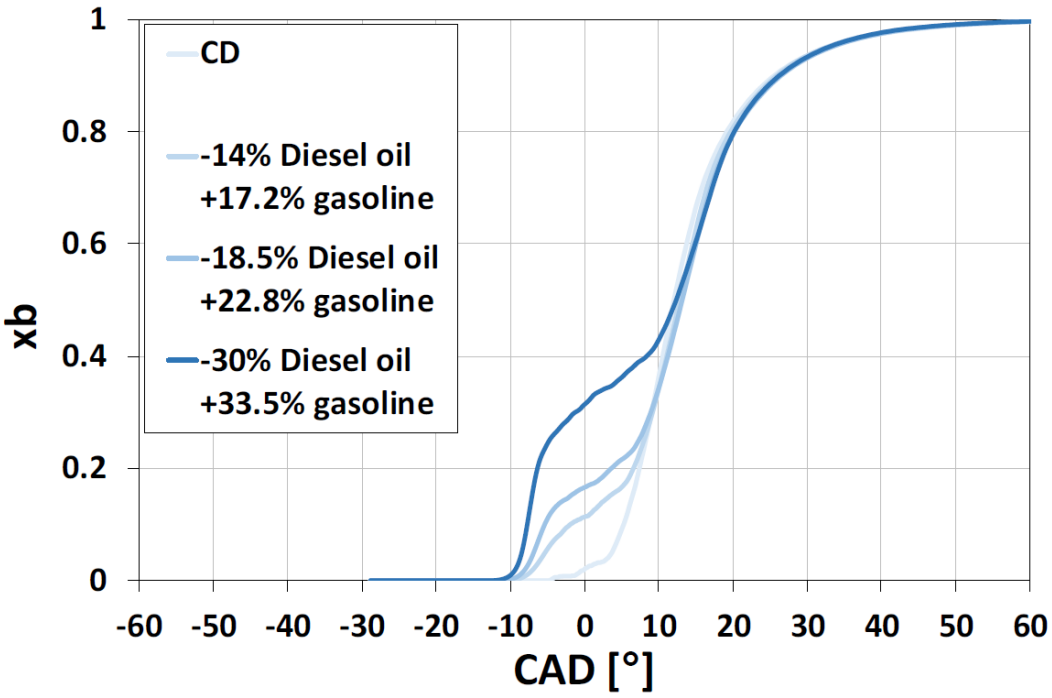

Figure 71 Mass fraction Burned high loads

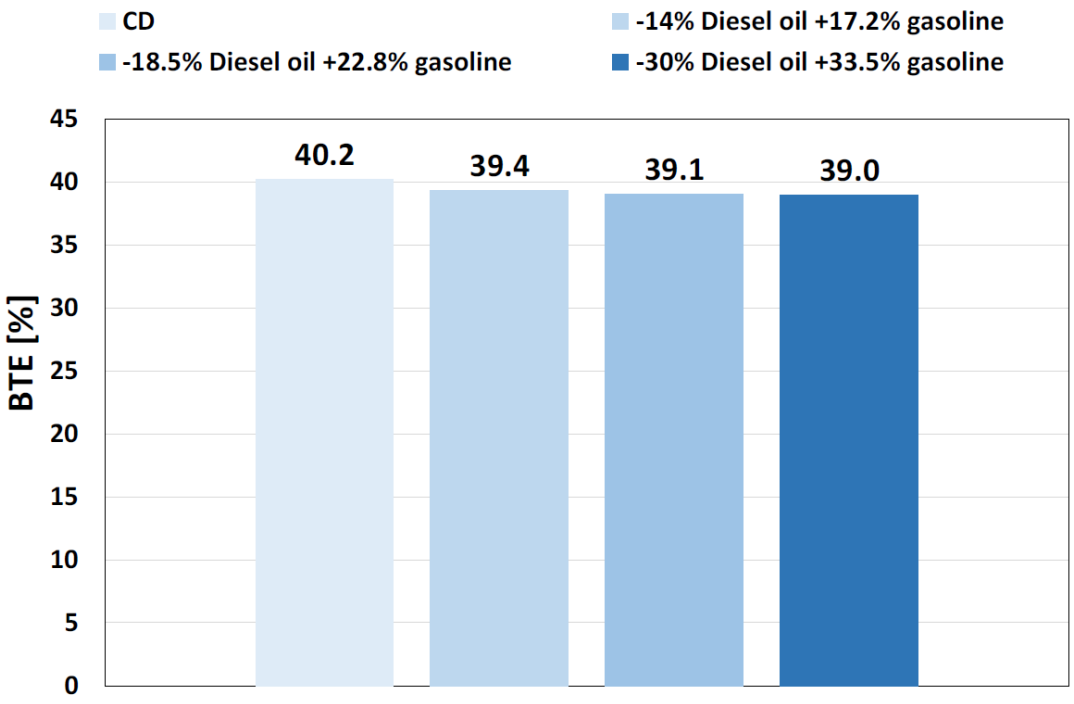

Figure 72 BTE comparison high loads

4.5 Conclusions

The focus of this research activity is to investigate RCCI combustion, where gasoline is the low reactivity fuel and diesel oil is the high reactivity fuel. In order to investigate the process, a modified light duty turbocharged euro 4 diesel engine has been chosen. The experimental campaign is focused on two operating points, at the same engine speed with two different engine load 150 Nm and 300 Nm corresponding to 6.75 and 13.5 bar of BMEP. For each point, several dual-fuel cases with different rates of substitution of diesel have been investigated, and compared to the Diesel case. Furthermore, some RCCI cases have been optimized in terms of injection strategy, in order to find some general guidelines for the RCCI combustion development.

The main result is found at medium loads, the substitution of diesel oil with gasoline without the adoption of EGR and any specific calibration results in a slightly increase of the maximum peak of in-cylinder pressure and a small decrease in terms of brake thermal efficiency. With the aim of a calibration campaign concerning mainly the injection strategy, BTE has been improved in comparison to the Diesel oil mode, without any drawbacks in terms of combustion stability and in terms of maximum peak of in-cylinder pressure.

Conversely, at high loads, 300 Nm corresponding to 13.5 bar of BMEP, combustion control becomes difficult, especially for the ignition control of the charge, which ignites before the diesel oil injection strategy starts. Every intervention made on the injection strategy results not to reduce ignition advance. This pre-ignition determines a huge increase in engine maximum pressure and consequently an increase in terms of engine noise.

Taking this last result into consideration the usage of EGR at medium high loads becomes mandatory in order to control the reactivity of the premixed charge and to avoid auto-ignition of the charge. This last observation will be set as next step for future development activities, with the main aim to investigate the role of EGR in RCCI combustion process.

5 Design of a 2-stroke SI Hybrid engine for small aircraft

5.1 Introduction

Climate changes and environment pollution leads to increase global warming in an irreversible way [50]. Electrification of powertrains has spread a lot in the latest years, mostly in automotive field. The aerospace sector is responsible of a large amount of pollutant emissions and massive emissions of Carbon dioxide. This study is focused on the development of an engine for light craft applications with a total power of 150 kW. For this power it is reasonable to expect several advantages in the adoption of a Hybrid system.[51,52]. In a single propeller aircraft, the hybrid parallel configuration seems to have several advantages in comparison to series hybrid systems[53]. If the electric motor is in series with the ICE, in case of electric failure, the engine can not be used as propeller. On the other hand, in parallel series layout the aircraft can have a redundant power supply, this characteristic can be very useful in terms of safety. Another advantage is represented by the possible reduction in terms of engine displacement, because of the energy support of the EM (electric motor); the downsizing of the engine leads to operate with a high efficiency during the flight.

Another advantage is represented by the capability to fly in electric mode for a longer time, with less noise and less pollutant emissions, or with heavier payload, than a full electric aircraft architecture[54].

Thermal ICE has to be specifically designed for this particular application, in particular two-stroke engine seems to be a possible option to be investigated. These types of engine are far from novelty in light aircraft applications; unfortunately, the specific fuel consumption and pollutant emissions are quite high in comparison to four stroke engines. Conversely, the adoption of a hybrid powertrain involves the addition of several components (e.g. inverter, electric motor, control unit, battery pack), and increase the weight and dimensions of the whole vehicle. In this way, two-stroke engine can lead to reduce ICE total mass and dimensions because less displacement is needed in order to reach power target in comparison

to four-stroke engines. On the other hand a novel design is needed in order to improve pollutant emission and engine BTE[32].

The main aim of the project is to develop a novel type of two stroke SI engine, with the capability to match lightness, BTE and pollutant emissions requirements for this specific application. The main features of the engine are showed in Table 14.

Displacement [cc]	Weight [kg]	Power [kW]	BSFC [g/kWh]
1100	60	110 @6000 rpm	< 260

Table 14 Two stroke engine design constraints

The research activity is focused in the development of the scavenging process and the design of a proper direct injection system. The process is supported by several cfd 1d and 3d simulations and CAD design of the whole engine, paying particular attention to intake port design. The main goal of the design is to keep a fuel trap efficiency higher than 95%, with the specific design of the injection system, and to avoid higher amount of internal EGR in order to reach a good combustion process and to avoid misfire occurrences.

In literature, there are already some studies concerning light hybrid aircrafts [55,56] but, at this time, there is no real application in the market of this engine field. Some other authors analyses some Hybrid Electric Aircraft (HEA) concepts focusing on their feasibility, especially in term of technological/economical readiness and complexity[57,58].

The first part of the project starts with the search for a reference engine. This reference is found in BRP-Rotax 850 e-tech 2-stroke SI engine. This engine has an excellent power-to-weight ratio (121 kW/42.2 kg) and some effective solutions for injection and scavenging system. However, as already mentioned above, a specific design for this hybrid application is mandatory, as described in [59,60].

Differently from rotax 850 e-tech, this engine is developed with a 4-stroke dry sump in order to separate lubrication system from the combustion part of the engine. This characteristic brings to adopt an external mechanical pump in order to supply air into the engine.

One of the main drawbacks of two-stroke engines, without poppet valves and loop scavenged, is the amount of fresh charge lost into the exhaust ports during the scavenging process. In order to assess high BTE, it is necessary to introduce a specific injection system that minimizes the fuel amount lost through the exhaust.

5.2 Engine design

The choice of the displacement of the engine derives from the limitations on the maximum BMEP (= 10 bar) and the maximum engine speed (6000 rpm). The mean pressure has a strong influence in thermal and mechanical load, obviously these two dependent parameters have direct influence in engine weight, dimensions and mass. Considering the power output of 110 kW, the total displacement of the engine is set at 1100 [cc] Table 14.

As already mentioned before, the crankcase lubrication system is like a conventional four-stroke dry sump. This technical specification avoids the adoption of an external supercharger. The relatively low target of maximum BMEP and the consequent relative low scavenging pressure, lead to choose a mechanical supercharger mechanically coupled to the engine by means of a belt. This solution is preferred in comparison to a conventional positive displacement supercharger, because of the compact dimensions, lower weight and higher flexibility.

The scheme chosen for the engine is the in line three cylinder for the following reasons:

- It is a good trade off in terms of unit displacement
- Instantaneous torque is quite smooth
- The exhaust system can be very light and efficient because the cylinders are joined together (cross scavenging process)
- The overall dimensions are limited

The loop-scavenged system with piston-controlled ports is selected, the main reasons are:

- Absence of poppet valves (more lightness, less components, less weight)

- Total absence of constraints in combustion chamber design (because of the absence of poppet valves). This advantage can be useful in the development of jet ignition or particular combustion concepts61,62.
- The flow field in loop scavenged engine is characterized by a high intensity of turbulences in terms of tumble vortex, that strongly support fuel mixing, and increase the combustion process in the turbulent phase
- With a high tumble vortex it is easy to implement stratified charge in comparison to other scavenging process. The implementation of these combustion process is fundamental to reduce charge enrichment at medium-high loads, mitigating the risk of knocks (knock tendency is always possible in two-stroke engines for the high gas temperature due to internal EGR).

The bore-to-stroke ratio in this kind of engine has to be close to 1; higher value tends to decrease permeability, because discharge coefficient of the ports tends to decrease, while low values drastically increase mean piston speed. Ports design has to be a compromise of two requirements. On the one hand, large scavenge and exhaust ports are necessary to increase permeability and decrease pumping losses; on the other hand, the cylinder liner may be excessively weakened by these large ports. This trade-off is solved by the application of best engineering practice which suggests a ratio between ports width and liner width of 0.8. The scavenge ports should be less than 20% of the liner width in order to avoid damages of the piston spring [63,64].

The Blu spark engine is made of 5 scavenging ports and one main exhaust port with the addition of two small ports, called boosters. The height of the ports is a key parameter in order to reach power target in terms of torque and power. This parameter is calculated and optimized by the support of several CFD 3D-1D calculations. The CFD 1D calculations provide also the amount of air needed to reach power target and, consequently, the gear ratio of the compressor.

In addition, the exhaust system can be optimized too with these calculations. For this component, several designs are compared before the final optimization:

A. Separate single pipes with convergent and divergent parts.
B. Log manifold (single exhaust pipe, fed by a set of very short ducts coming from each cylinder)
C. 3-in-1 manifold (three exhaust ducts of the same length joined to the terminal by a junction)
D. log manifold with two terminals

In comparison, the solutions have different advantages and disadvantages. The first solution leads to reach maximum power but it is very expensive and with big dimensions. The second one is compact but it introduces differences in the scavenging process in each cylinder with different amount of internal EGR. Solution C may minimize scavenging differences among the cylinders. Solution D seems to be the best compromise in terms of scavenging efficiency, performances, and packaging.

In Table 15, the main engine specifications after the first design process are reported.

Bore x Stroke [mm]	82 x 80.4
Number of cylinders	3
Compression ratio	11.6:1
Total displacement [cm3]	1243
Total Dry weight [kg]	50
Lubrication System	Forced, dry sump
Dimensions LxHxW [cm]	93x45x62
Air supply	Mechanical Supercharger (Rotrex C30-94), w/o charge cooler

Table 15 Engine main specs.

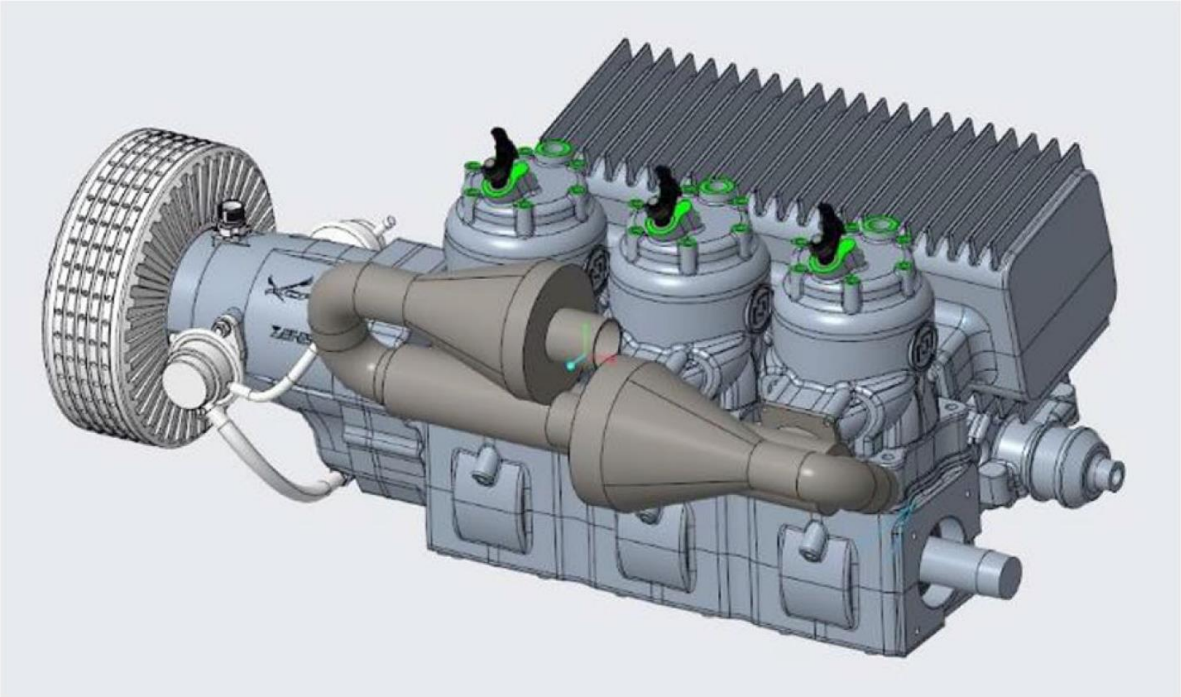

Figure 73 Blu spark engine: whole cad model

In Figure 73 the CAD design of the prototypal engine is reported. The exhaust system obviously requires a silencer (not represented).

As already described in the first paragraph, the dry sump was preferred to the wet sump because of dimensions, friction losses, more freedom for aircraft maneuvers.

The geometric detail of the scavenge ports especially for the intake ports are fundamental to improve the quality of the scavenging process, the optimization is provided by a CFD 3D simulation campaign.

The same tool has been employed to investigate injection solutions for mixture formation. The alternative investigated are:

- High pressure direct injector HPDI
- Low pressure direct injection LPDI
- Low pressure semi direct injection LPSDI

- Port injection
- A combination of semi-direct and direct injection

All these configurations obviously have pros and cons. HPDI can reach the best in terms of fuel trapping efficiency at low medium speeds, at high loads and speeds the fuel evaporation is difficult because the cycle time decreases while engine speeds increase. This evidence leads to affirm that this injection system can work well only in some load conditions. For aircraft usage, high loads do not suggest the application.[65]. LPDI is a cheaper and compact system, furthermore at high loads and high speeds the mixture of the fuel does not involve any problems, as reported in literature [66,67]. The only drawback is the heating of the tip of the injectors, facing the cylinder and exposed for a short time to the high temperatures of the combustion products. This injection system has been employed for several applications by the University of Gratz [68,69]. The overheating of the injection tip represents the main disadvantage. The PFI system seems to be the best solution in terms of reliability and calibration process. Furthermore, aircraft engine emissions are not regulated, so the increment of pollutant emissions increased by the adoption of a PFI system does not generate any homologation issue. In case of adoption of a three-way catalyst for further regulation limitations, the PFI system must be changed because the amount of unburned HC in the exhaust system will damage irreparably the CAT.

Taking these considerations into account, a composition of HPDI and LPDI seems to be the best for this application in order to be compliant with current and maybe to further legislations. The HPDI at high loads can reduce the amount of HC at exhaust outlet injecting fuel at exhaust port closing into a lean premixed charge formed by the PFI system before intake ports.

In Table 16, a qualitative comparison of the possible injection systems with a number score from 1 (poor) to 4 (excellent) are reported.

As already described above, the system chosen for the prototype is DIR+LPSDI because of global score in comparison and in relation between the easier implementation in the first engine prototype.

	HPDI	LPDI	LPSDI	PFI	DIR+ LPSDI
Fuel trapping efficiency at WOT	4	3	3	1	4
Stratifying of the charge	3	2	2	1	4
Homogenous charge formation	2	3	3	4	4
Wall impingement	2	4	3	2	4
Injector tip stress	4	1	3	4	3
Overall valuation	**3**	**2,6**	**2,8**	**2,4**	**3,8**

Table 16 Comparison of injection systems

5.3 Methods

The design process, as already motioned in the introduction section, is performed by the adoption of CFD 3D and 1D calculations and CAD design (for the scavenging system).The first step of the project has been to build a model of the reference engine ROTAX 850 e-Tech.

The first model is built by the adoption for GT-POWER CFD 1D software (provided by Gamma Technologies).

In Figure 74 the experimental validation of the CFD 1D model is reported. This model is taken as a base for the first development of the BLU SPARK engine. Figure 75 reports a comparison in terms of BSFC vs Snowmobile speed. The agreement is good and the model can be adopted as basis for further development. The results obtained by these calculation provides the boundary conditions information for the first CFD 3D calculation campaign, with the aim at discovering some initial information in scavenging process.

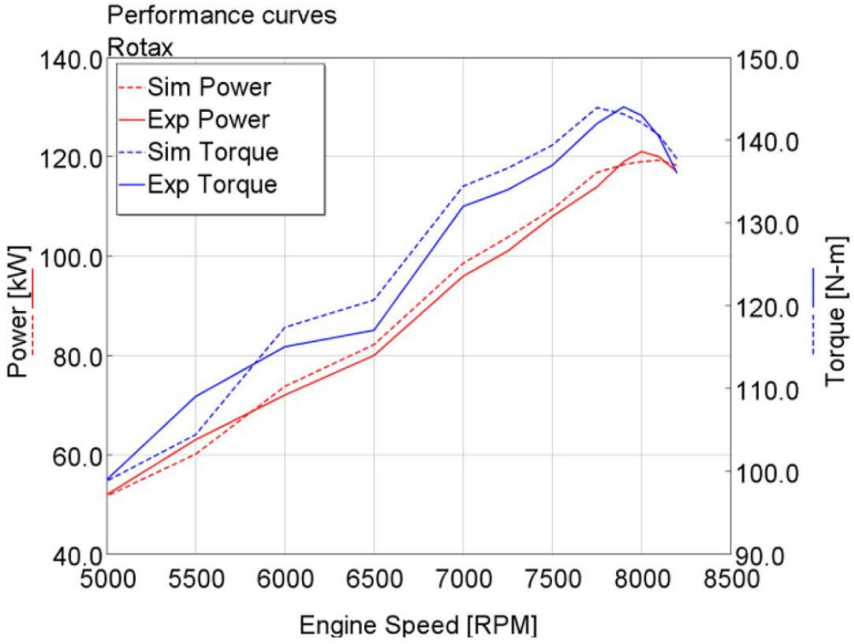

Figure 74 Numerical validation of the Rotax 850 cfd model

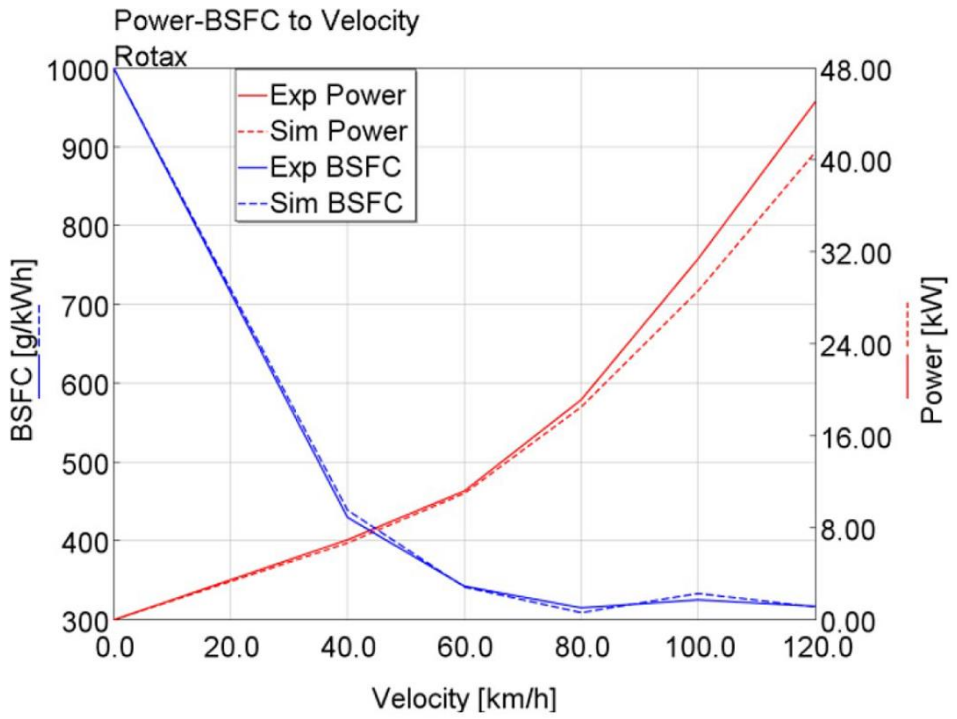

Figure 75 BSFC validation

The first run of CFD 3D simulations are a simplified calculation of the scavenging process, without any fuel injection. In particular, the fresh charge is assumed to be pure Oxygen and the exhaust gases are assumed to be pure Nitrogen. In this way, adding initial boundary conditions coming from CFD 1D calculation, it is possible to calculate the scavenging process with high accuracy. In this way, an iterative approach is followed: if the mass charge trapped at the exhaust port closing is not equal to the initial in cylinder mass, the pressure of the initial condition changes accordingly.

The main operation condition taken into account is the maximum power at maximum engine speed (6000 rpm). This is the most critical engine operating condition, especially for an aircraft, because the short cycle duration leads to decrease injection timing, while fuel mass flow is the maximum.

The result obtained by the campaign are used in three different ways:

1. They provides a detailed insight of the flow through the ports and within the cylinder, highlighting strengths and weaknesses of the current design; this information is employed for fixing the most evident issues and for improving the system in general
2. The simulated scavenging process is used to generate a zero dimensional model which globally describes the scavenging process in terms of efficiency
3. The mass flow rate in scavenging ports in the CFD 1D model are compared to the CFD 3D model and calibrated by adjusting flow discharge coefficient.
4. The scavenging process in terms of fresh charge mixed with the burned charge is represented in a model (Scavenging curve) used as input in CFD 1 D model.

Regarding point 2 of the list above, the a-dimensional parameters are defined as:

- Delivery ratio (DR): total amount of fresh charge passing through scavenging ports divided by a reference mass (typically $= Discplacement\ [cm^3] * air\ density[\frac{kg}{cm^3}]$) , density @20 °C and pressure 1 bar).
- Scavenging efficiency (SE): mass fraction of fresh charge trapped into cylinder @ a given crank angle
- Charging efficiency (CE): mass of fresh charge trapped into the cylinder @ a given angle divided by reference mass
- Trapping efficiency (TE): mass of fresh charge trapped into the cylinder @a given angle divided by the delivered mass

In Figure 76, Figure 77, Figure 78 these parameters are plotted in function of delivery ratio. It can be noticed that "EVO" configuration is slightly better then "base" design, it yields a higher permeability, due to the higher delivery ratio obtained with the same differential pressure. This evidence improves both trapping efficiency and scavenging efficiency. In Figure 79, the scavenging curve is reported, which is used to characterize composition of cylinder end exhaust gases in terms of residual ratio and fresh charge ratio. This output is used

as input to CFD 1D simulations to give global information about charge composition into the cylinder.

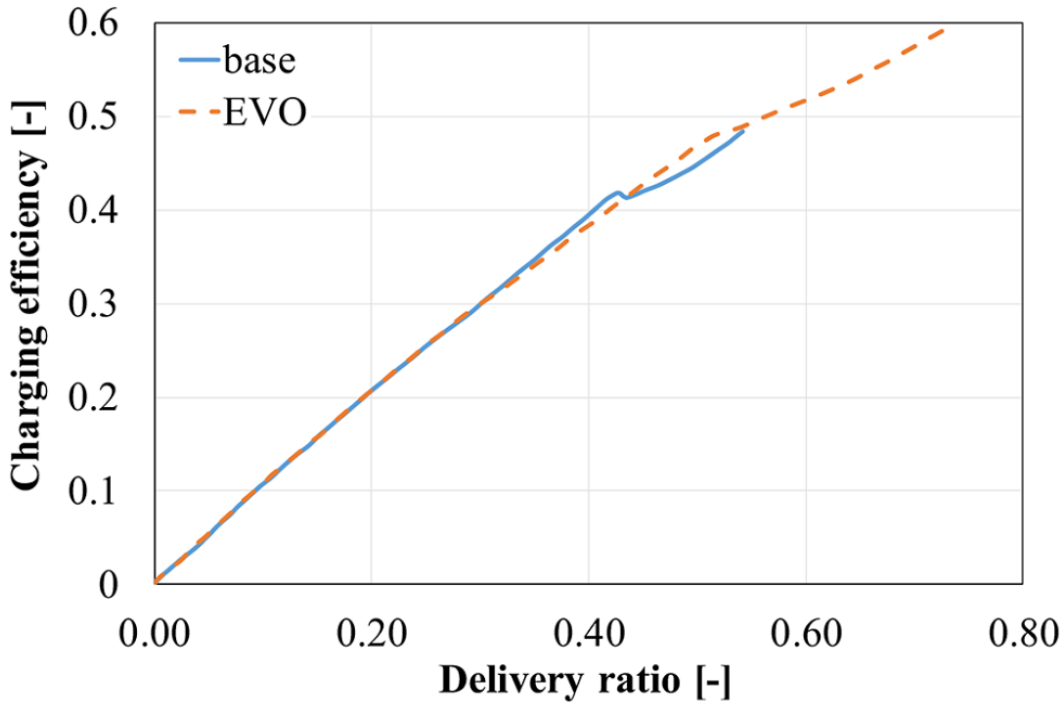

Figure 76 Charging efficiency vs Delivery ratio

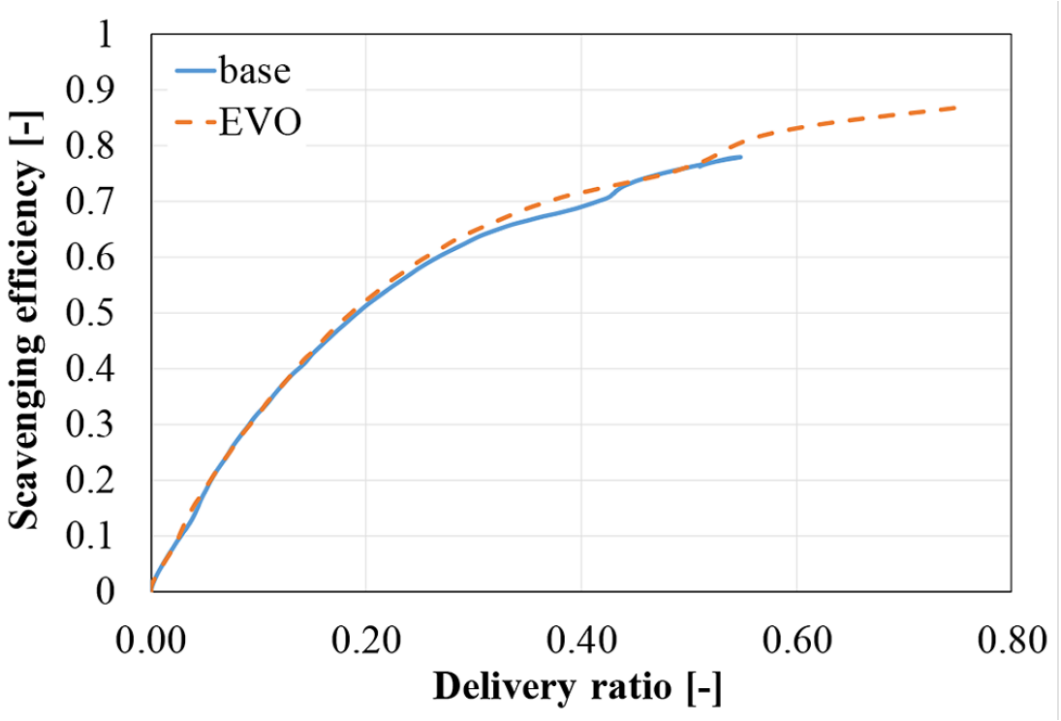

Figure 77 Scavenging efficiency vs Delivery ratio

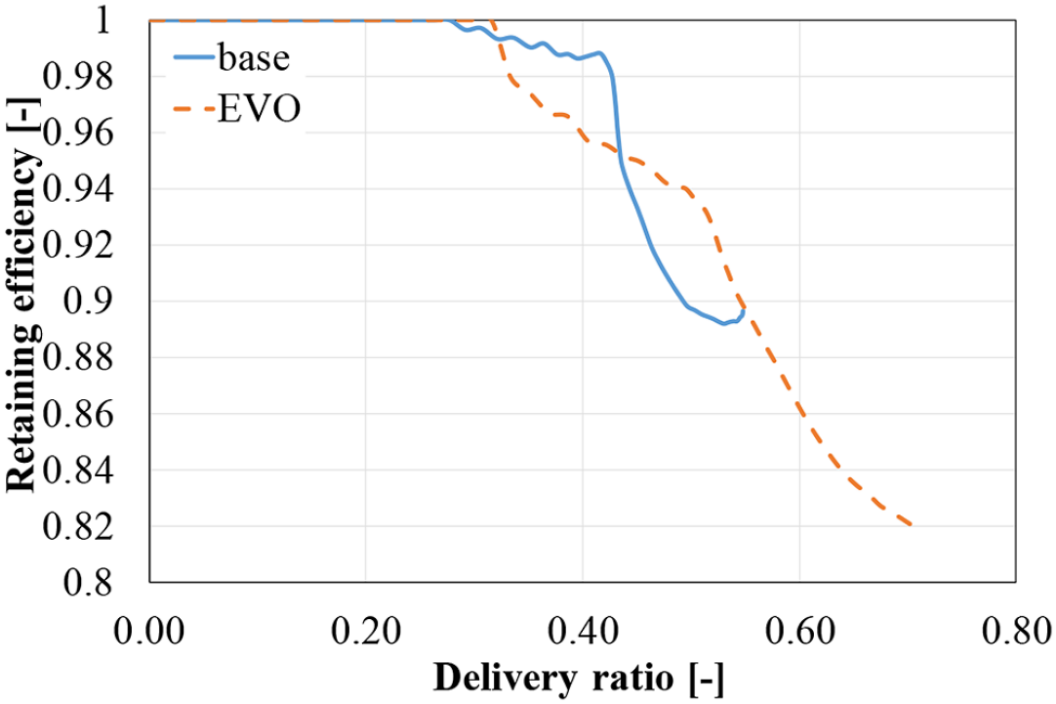

Figure 78 retaining efficiency vs Delivery ratio

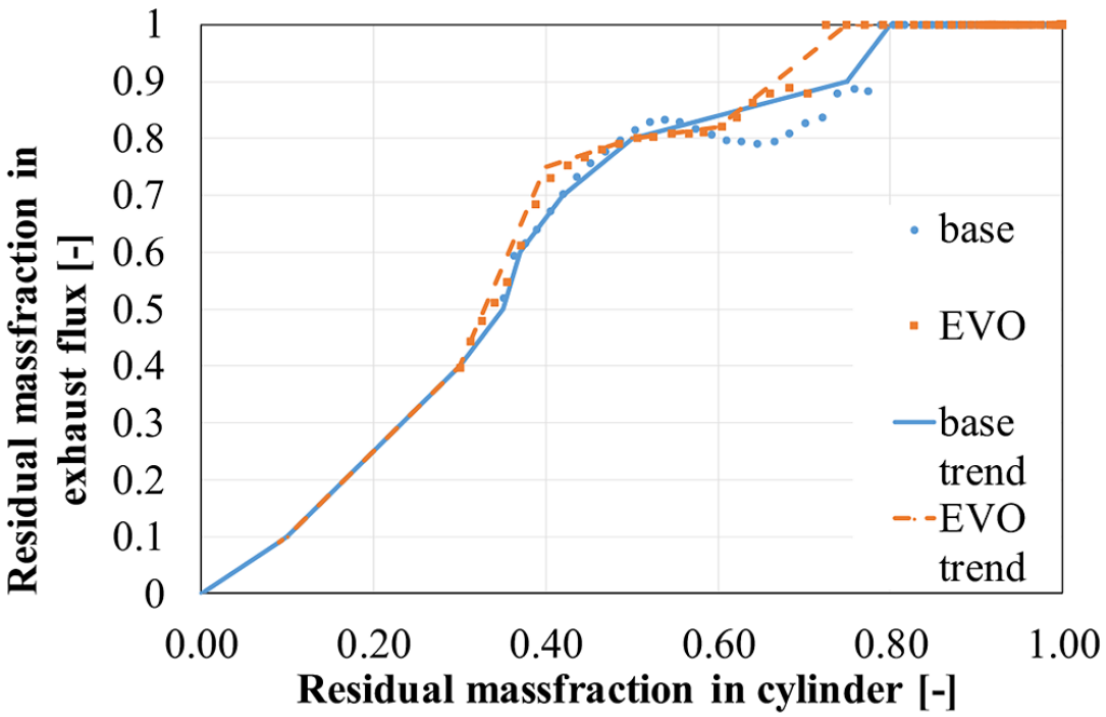

Figure 79 Scavenging curve

Figure 80 reports as example the first design of scavenging ports vs the optimized version of the ports named “EVO”. The first design starts from the reverse engineering of the Rotax engine adjusted with a different intake system in order to separate the crankcase (the intake pump is external); the second is the result of the optimization campaign. As visible, the volume of the manifold wrapped around the cylinder has been increased, in order to get a smoother path between the inlet plenum and the set of scavenge ducts.

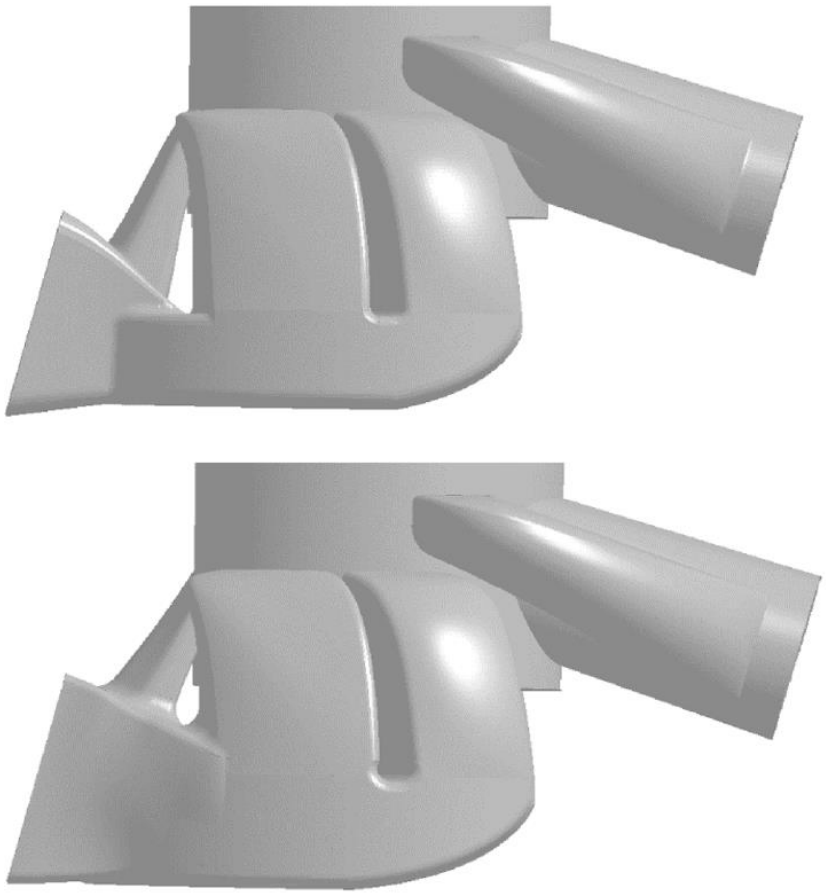

Figure 80 Scavenging ports configuration STD vs EVO_1

In Figure 81 the results of the CFD campaign are shown. They compare 3D models to 1D models in terms of air mass flow into the transfer and exhaust ports. After the calibration process provided by the iterative approach, the good agreement between the models is clear.

	Delivery ratio	**Trapping efficiency**	**Scavenging efficiency**	**Charging efficiency**	**Residual fraction**
Kiva	0.787	0.750	0.850	0.591	0.150
GT-Power	0.791	0.739	0.846	0.585	0.154
Err [%]	-0.5	1.5	0.5	1.0	-2.9

Table 17 CFD 3D vs 1D comparaison

The same results, for the seek of clarity, are also reported in Table 17. The total accuracy of the CFD 1D model is satisfactory; as far as the table maximum percentage error is concerned, it occurs in fraction of residual gas, but the value is very low (2,9%).

The model after the assessment of the accuracy has been employed for the optimization of:

- Port timing
- Compressor transmission ratio
- Exhaust system design, including silencer

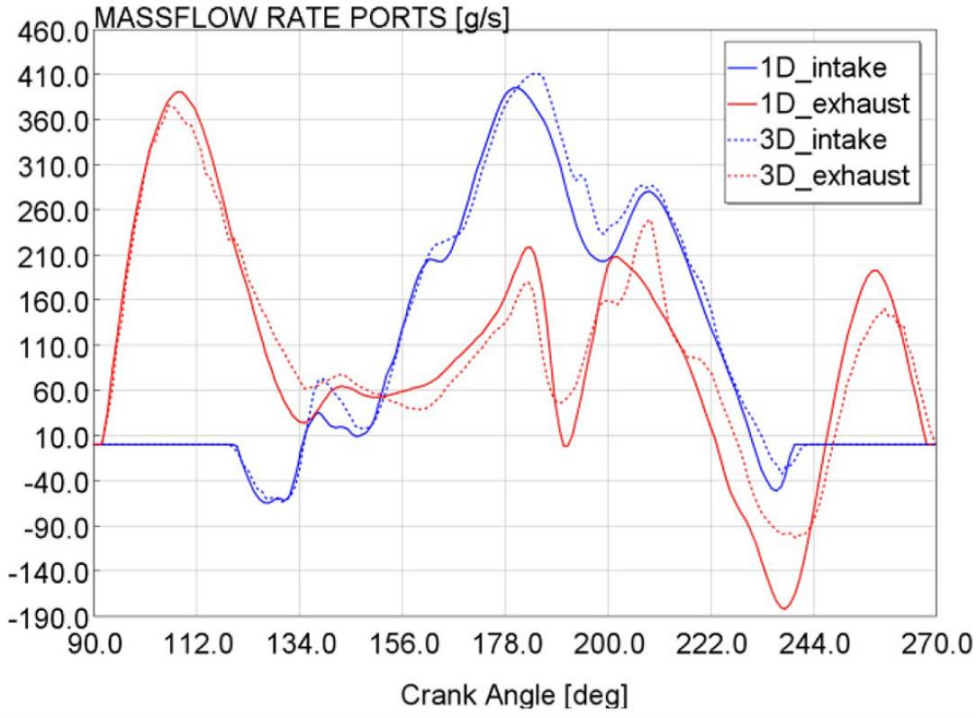

Figure 81 Mass flow rate CFD 3D vs CFD 1D

After the optimization of these parameters, the results in terms of boundary condition of the cylinder are used as input in the next CFD 3D calculation campaign, on the EVO geometry. In this campaign, the main goal is to optimize injector position and strategy, in order to obtain a good stratification of the charge. Finally, the combustion is modeled in order to evaluate performances and to calculate Weibe function for CFD 1D simulations.

5.4 Injection system

The goal of this activity is to find a configuration for the injection system in terms of positioning and main injection strategy. First of all, the main constraint is to avoid fuel flowing through the exhaust port, the maximum loss amount is set to 10%. Furthermore, the second most important parameter is the composition of the charge in terms of fraction of evaporated fuel. The ideal goal is to get a bulk of rich charge near the spark plug, in order to have an easy-to-ignite charge. Obviously the trade-off is the complete fuel evaporation before SOC.

The final layout solution is reported in Figure 82. The injector main characteristics are reported in the table below:

Number of holes	12
Hole diameter [mm]	0.29
Cone Angle	20°
Injection pressure [bar]	3-8

Table 18 Injector main characteristics

Another constraint regards fuel injection window in terms of CAD, the fuel can only be injected during the opening of scavenging ports, for about 60 CAD, in order to prevent fluid film formation and wall impingement. Regarding the last consideration, the orientation of the injectors into the scavenging ducts is fundamental. They are directed toward the cylinder head and the middle of cylinder, as far as possible from the exhaust ports and from the liner walls. The angle found to have better compromises is 20°, according to Figure 82.

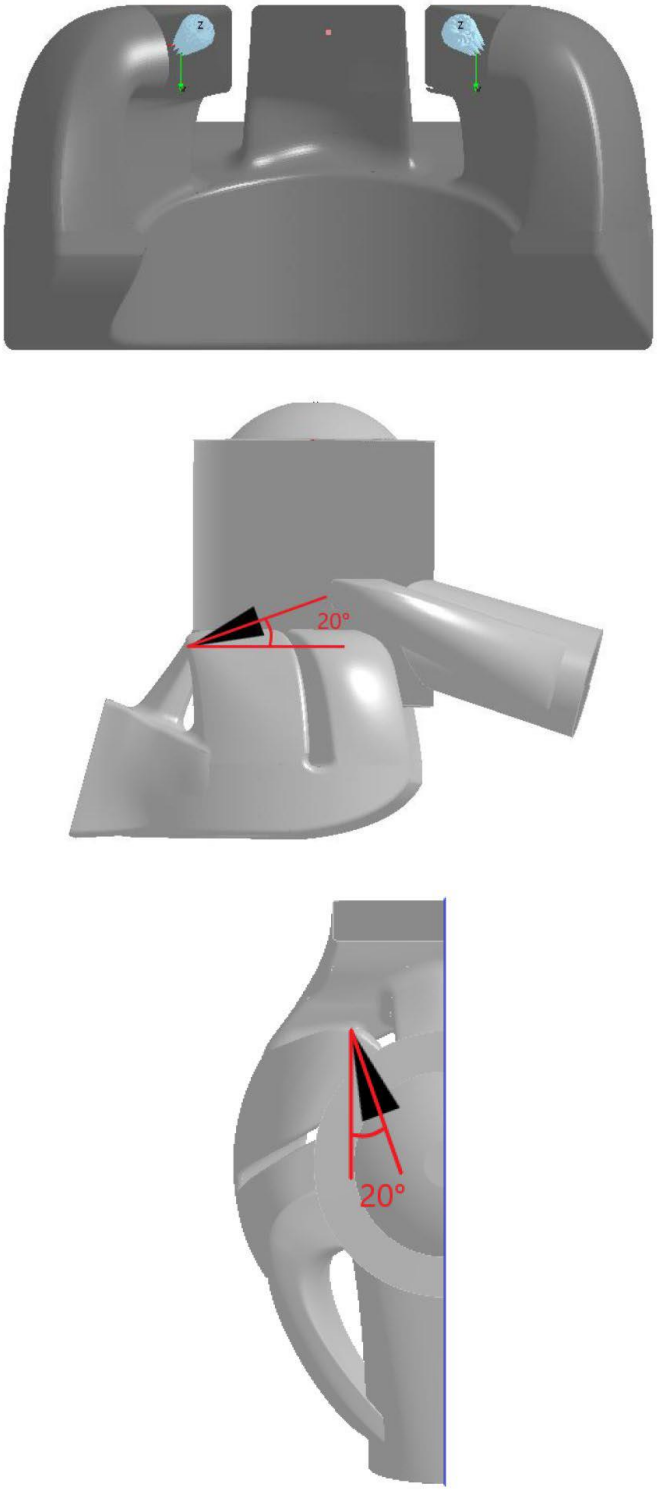

Figure 82 Injectors positioning

CFD 3D simulations has been carried out starting from 90 CAD to 330 CAD ATDC. The computational domains in terms of mesh are reported in Table 19.

	Cell size [mm]	**Refinement method**	**Activation interval**
Global Mesh	2	-	
Wall boundaries refinement	1	1 layer	Always active
Open boundaries refinement	1	1 layer	Always active
Wall boundaries port refinement	1	2 layer	Always active
Booster-intake interface refinement	0.25	16 mm radius sphere	btw 90-93 CAD ATDC
Booster-intake interface refinement	0.25	16 mm radius sphere	btw 265-270 CAD ATDC
Evaporation refinement	0.5	Gradient of fuel vapor mass fraction	btw 160-220 CAD ATDC
Velocity magnitude refinement	0.5	Gradient of velocity magnitude	btw 118-220 CAD ATDC

Table 19 Main specification of the computational grid

The computational domain is composed of three regions corresponding to exhaust, intake, and cylinder. This is mainly due to impose different gases composition at the start of simulation; as already described in the previous section the intake region is composed by pure Oxigen, the exhaust port is composed by Carbon dioxide and the cylinder is filled with Nitrogen. This

method has been used in several previous research[70,71]. The fuel injected is iso-octane (i-C_8H_{18}). The boundary conditions provided by CFD 1 D results are reported in Figure 83, injection position in Figure 82 Injectors positioning Figure 82.

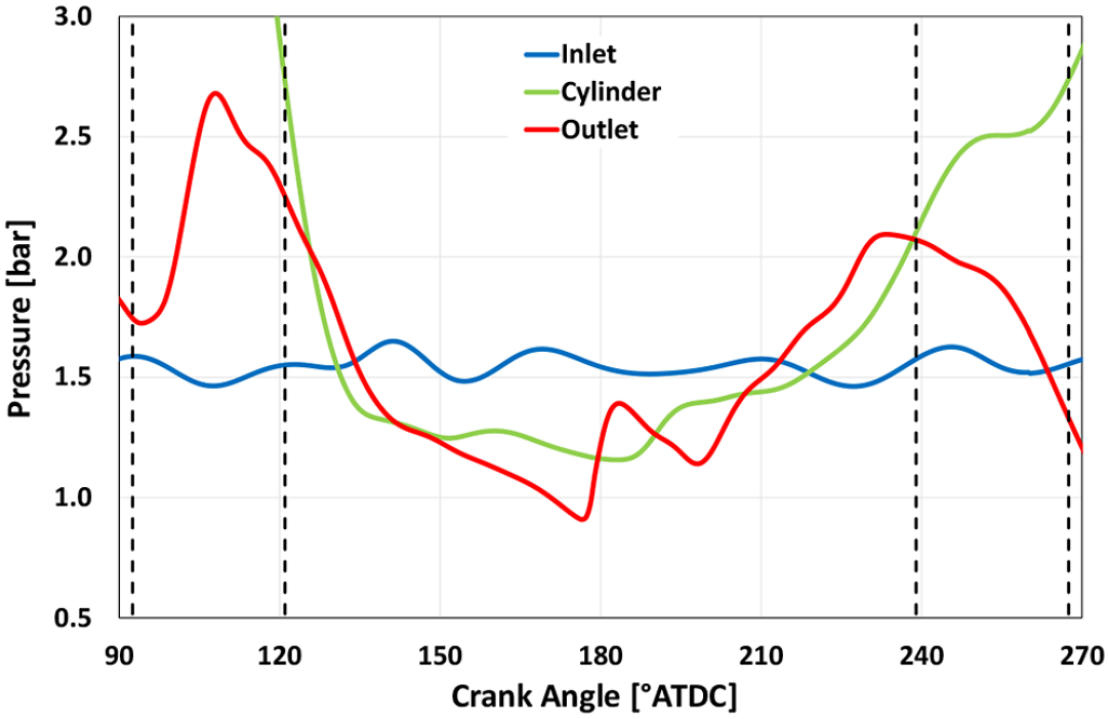

Figure 83 CFD 1D boundary conditions

The injection timing is mainly limited by the intake ports opening and directly related by the piston.

	LPSDI-49	**LPSDI-34**	**LPSDI-26**
Injected mass [mg]	27		
SOI [cad]	160	175	183
DOI [cad]	32.3	32.3	25.5
Mass flow rate	15.05	15.15	19.06
Δp $[bar]$	5	5	8
Fuel temperature [K]	330		

Table 20 Investigated injection strategy

All points analyzed are characterized by the injection advance, and the termination of the injection is set before transfer port closing e.g. LSPDI-49 means that the injection starts 49 CAD before the closure of scavenging ports. Table 20 reports the main parameters of the injection strategy. The injected fuel is obviously divided by two for each injector, the total amount is kept constant the same for temperature. The injection pressure varies in the last case mainly because of injection duration reduction. SOI is retarded of 15 CAD from the first to second case, and further 8 degree for the last case. The retard is manly due to the attempt to reduce unburned hydrocarbon through the exhaust ports.

The overall results of the calculation campaign is reviewed in Table 21.

	LPSDI-49	**LPSDI-34**	**LPSDI-26**
Trapped fuel mass into cylinder [mg/cyl/cycle]	21.71	20.95	23.76
Trapped fuel mass into intake volume [mg/cyl/cycle]	2.38	3.80	2.33
Apparent Trapping efficiency (1 cycle)	0.80	0.78	0.88
Actual Trapping efficiency (2 cycles)	0.87	0.88	0.94
Lambda (global)	1.12	1.11	1.04
Effective Lambda (Λeff)	1.04	1.01	0.97
RMS (Effective Lambda)	0.12	0.14	0.15
RMS/Λeff [%]	11.66	13.59	15.17
Lambda at spark plug	0.95	0.90	0.85

Table 21 CFD 3D result of injection strategies

It has to be noticed that a small amount of fuel is rejected into the intake manifold. In the following cycle, the fuel enters again the cylinder, and a small fraction (15%) goes out. The fuel trapping efficiency is calculated considering two consecutive cycles. Obviously, the

higher the retard is in terms of SOI, the higher fuel trapping efficiency is set. At 8 bars, the best result reached is 94%. In order to evaluate the quality of mixture at the combustion onset, it is necessary to valuate a lambda weighed on the basis of the volume of each region of the combustion chamber occupied by a homogeneous mixture. The Λeff is defined as follow:

$$\Lambda_{eff} = \frac{\sum_{i=1}^{N} \lambda_i V_i}{\sum_{i=1}^{N} V_i} \tag{5.1}$$

Where:

- $\lambda_i V_i$ are the value of the relative air to fuel ratio of each cell.
- N is the total amount of cells @ -30°

The RMS Λ_{eff} is also calculated throughout the combustion chamber, in in order to assess the non-homogeneity of the charge. The ratio of RMS to Λ_{eff} should result between 10 or 20%. on the one hand, lower values implicate a weak stratification; on the other hand, higher values may result in a poor combustion efficiency, due to the formation of unburned

HC in the ultra-lean region In Figure 84 the mixture formation in terms of lambda values in orthogonal planes in the combustion chamber is reported. The exhaust port is located at the bottom right of the images. At 327 CAD there is a rich zone near the spark plug according to stratification target of the optimization.

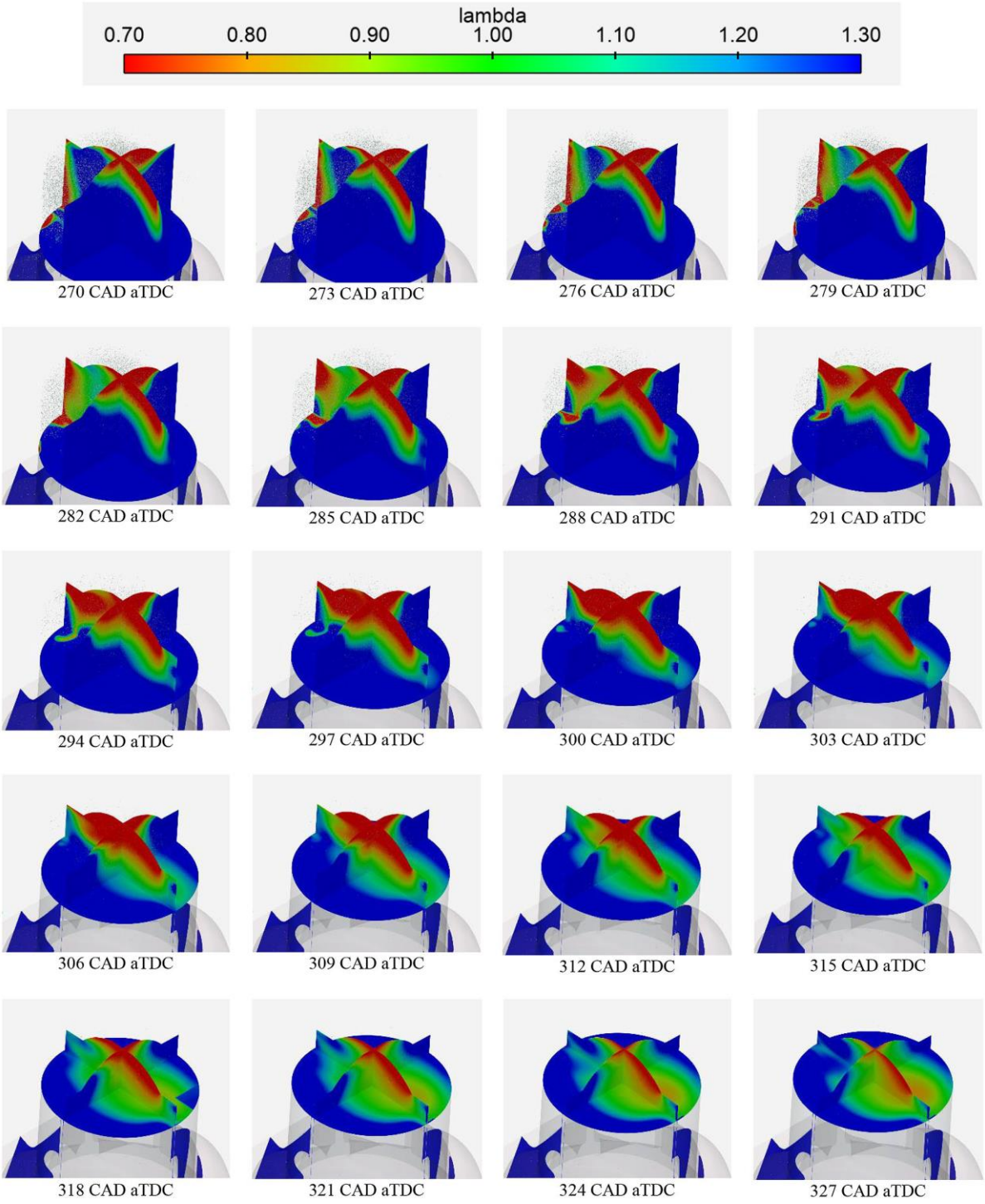

Figure 84 Mixture formation

5.5 CFD results

The design goal is to match performance target for light aircraft application (110 kW @ 6000 rpm). The main constraint regard air intake maximum temperature 70 C° and maximum in cylinder residual ratio 20%, in addition to the fuel trapping ratio of 90% reached with the injection optimization. This main goal is achieved by the intake ports optimization and the exhaust optimization. The exhaust system can provide pressure oscillation caused by pressure waves propagating into the exhaust pipes. The key is to time plugging “wave” i.e. the compression wave that arrives at exhaust ports just before closing. In this engine, featuring a log exhaust manifold, it is generated by the blowdown occurring in the cylinder firing 120 CAD after the current one. The plugging wave can improve trapping efficiency and it also helps to have better mixing of the charge and exhaust gases, avoiding the formation of higher temperature zones.

The whole process is showed in the next page in Figure 85. The O2 mass fraction is displayed in order to get information of the mixing process. The formation of a loop in the fresh charge flow can clearly be observed, especially @ 248 CAD. Furthermore, the pressure waves are clearly present in the first time of the scavenging from the cylinder to the intake and one at the end of the scavenging process, just before exhaust ports closing from the exhaust to the cylinder. The last waves may drastically increase turbulence into cylinder and also rise the trapping and charging efficiency. As already described above, the plugging wave is the result of a correct design of the exhaust system. In this case, the particular conformation allows to develop a concept called Cross Scavenging, where the pressure wave coming from one cylinder to the exhaust system is used as plugging for the second cylinder. This particular technique allows a more compact design of the exhaust system, particularly interesting in the light aero motive field.

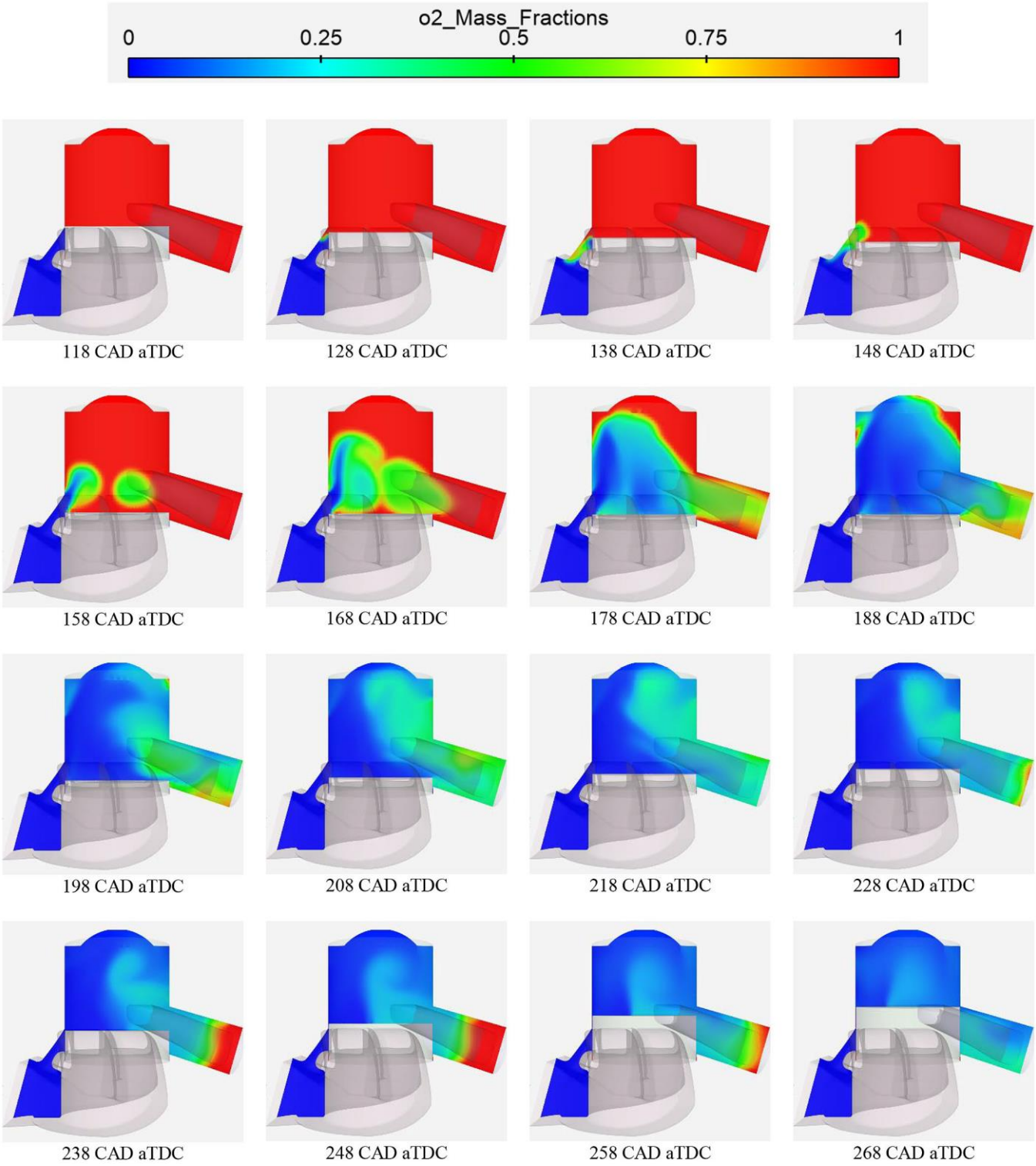

Figure 85 Scavenging process in function of CAD of "EVO" geometry @6000 rpm

In Figure 86 air mass flow through cylinder at maximum power rate is shown. As already qualitative seen in Figure 85, back flow coming from the cross scavenging from the exhaust system is clearly visible @ 240 CAD. The inlet flow starts @ 130 CAD ATDC when almost 50% of burned gases have already left the cylinder. This evidence is important for pumping losses.

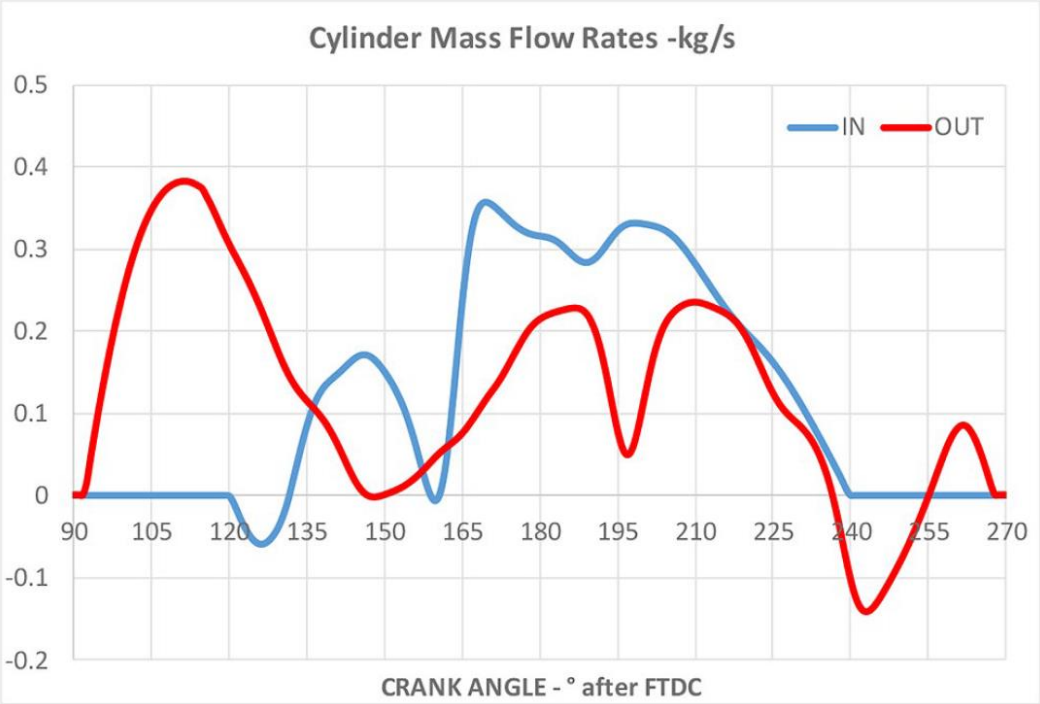

Figure 86 Air mass flow through inlet and exhaust ports

Friction losses have been modeled with Chen-Flynn model in Gt-power, using parameters derived from previous experience waiting for the first working prototype.

In Figure 87 the calculated scavenging parameters are reported. An increase of delivery ratio can be observed when engine speed increases; Consequently, charging efficiency increases, and also trapped mass. However, trapping efficiency is near 50% with the higher value at 6000 rpm (63%), where the plugging wave is tuned with engine speed. Conversely, the fraction of fresh charge is always near 90%.

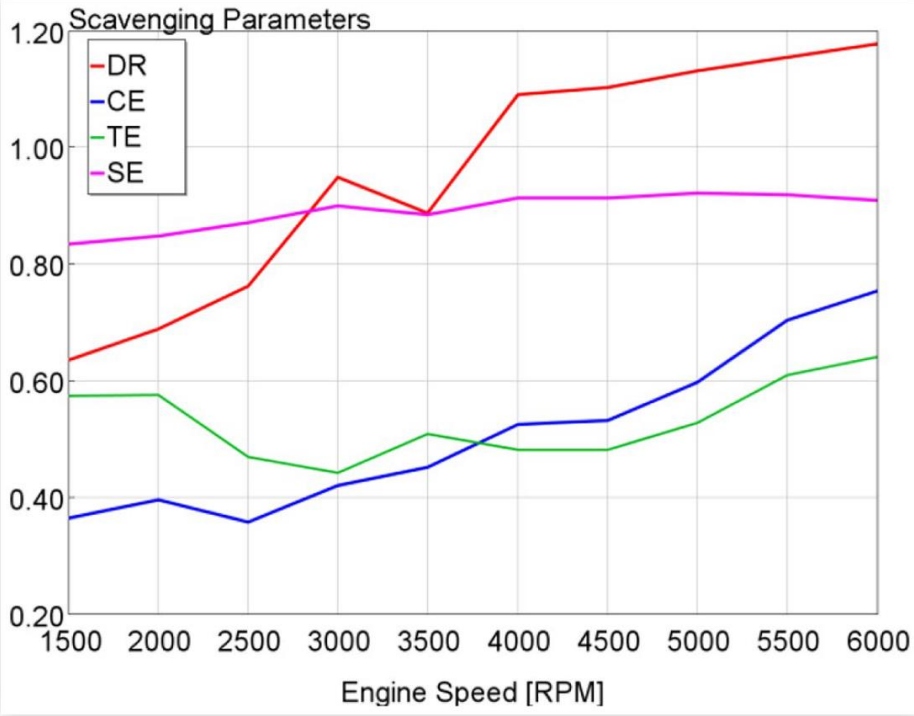

Figure 87 Scavenging parameters in function of engine speed @ WOT

Figure 88 reports the mean effective pressures in terms of BMEP IMEP and P+FMEP (pumping and friction losses). In this case, the PMEP is the work needed to run the external scavenging pump. The maximum peak in terms of BMEP is near to 9 bars and IMPEP is near to 10. These two values are slightly lower compared to a four-stroke engine with the same performances. This evidence is a good result for engine reliability.

In Figure 89 the BTE and indicated thermal efficiency (ITE) in WOT condition are reported. The mean value of BTE is near 32% and it is quite independent from engine speed. This high global efficiency can be explained analyzing Figure 90: mechanical+pumping efficiency is calculated as the ratio between BMEP and IME, adiabatic efficiency is the ratio of the effective heat available for the thermodynamic cycle to the heat released by combustion. Combustion efficiency is the ratio of the heat released by combustion to the energy associated to the mass of injected fuel. At medium engine speeds, both efficiencies are quite high, which is due to low friction and pumping losses. On the other hand, the thermodynamic efficiency decreases at high speeds, which is manly due to the early opening of the exhaust ports, when combustion process is still ongoing.

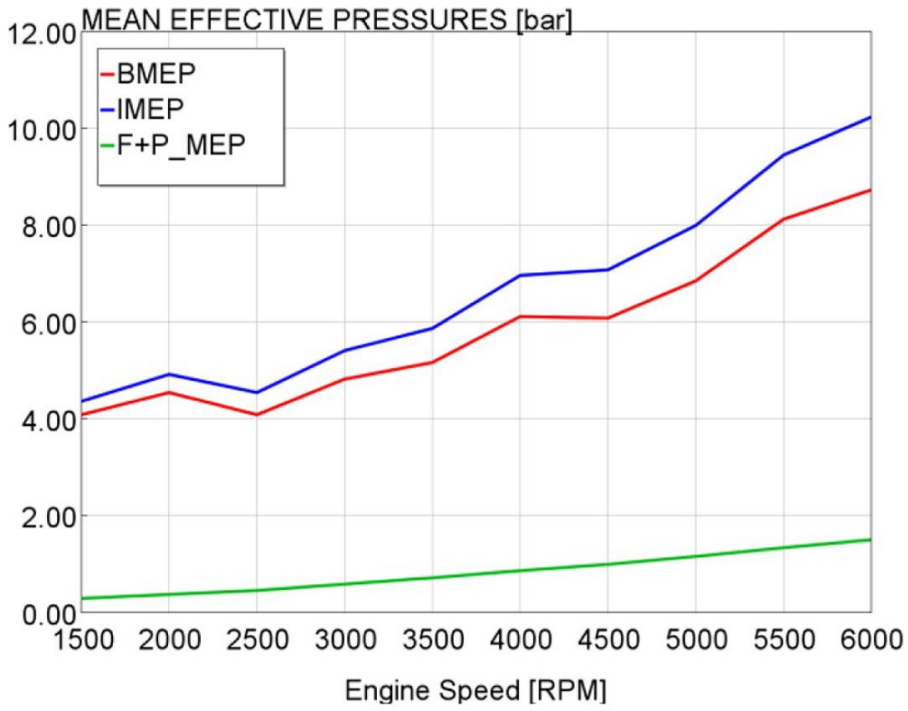

Figure 88 BMEP IMEP and F+P MEP comparison

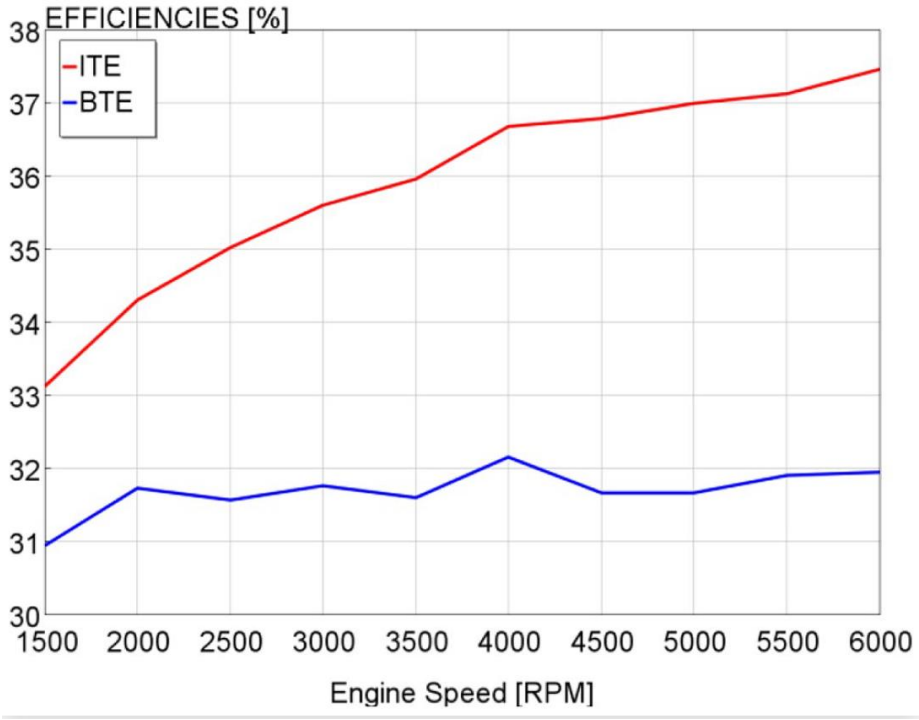

Figure 89 indicated and BTE vs engine speed

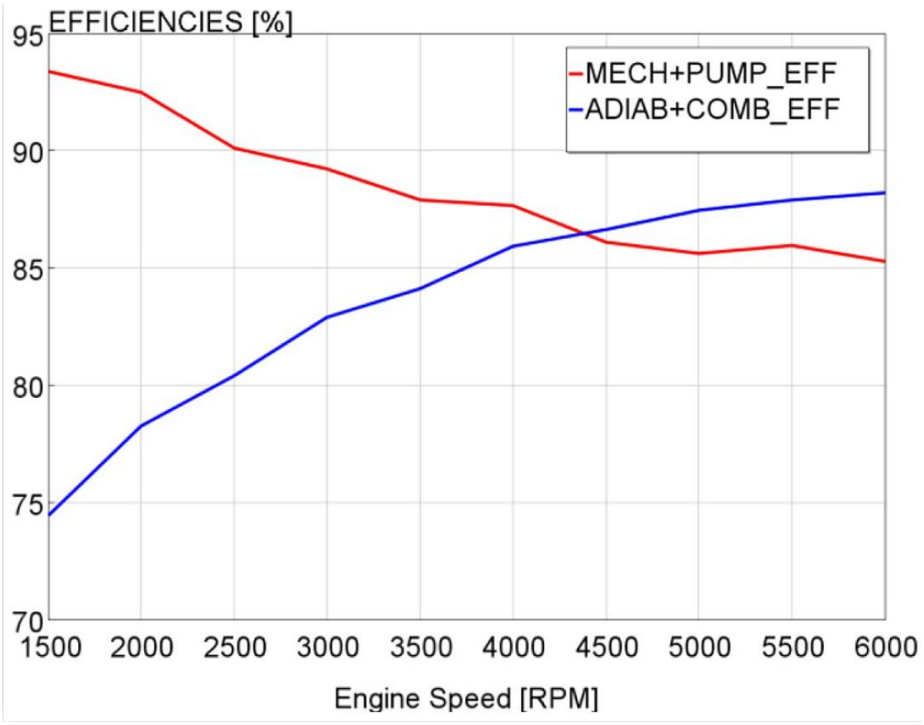

Figure 90 Mechanical+Pumping, Adiabatic+combustion efficiency @ WOT

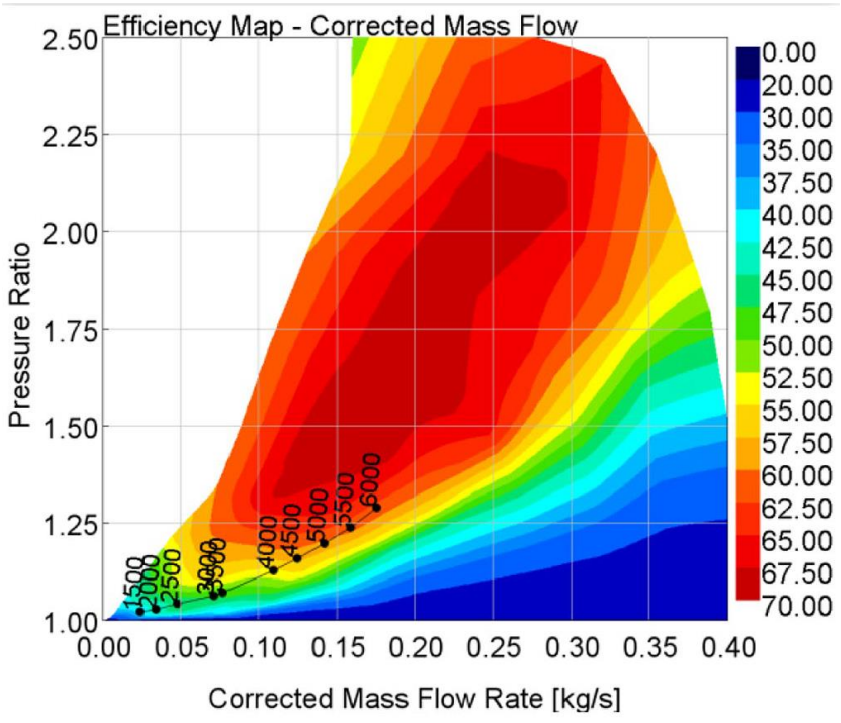

Figure 91 Compressor map with operation points @WOT

In Figure 91 the compressor efficiency map is reported, along with the operation point after the mechanical ratio optimization. The result is a mix of many compromises: first of all, a compressor with a smaller swallowing capacity could provide higher efficiencies. Nevertheless, a small compressor must revs at higher speeds, requiring different transmission ratio, this evidence decreases mechanical efficiency. The efficiency at high engine speeds is near to 50% according to the optimization made.

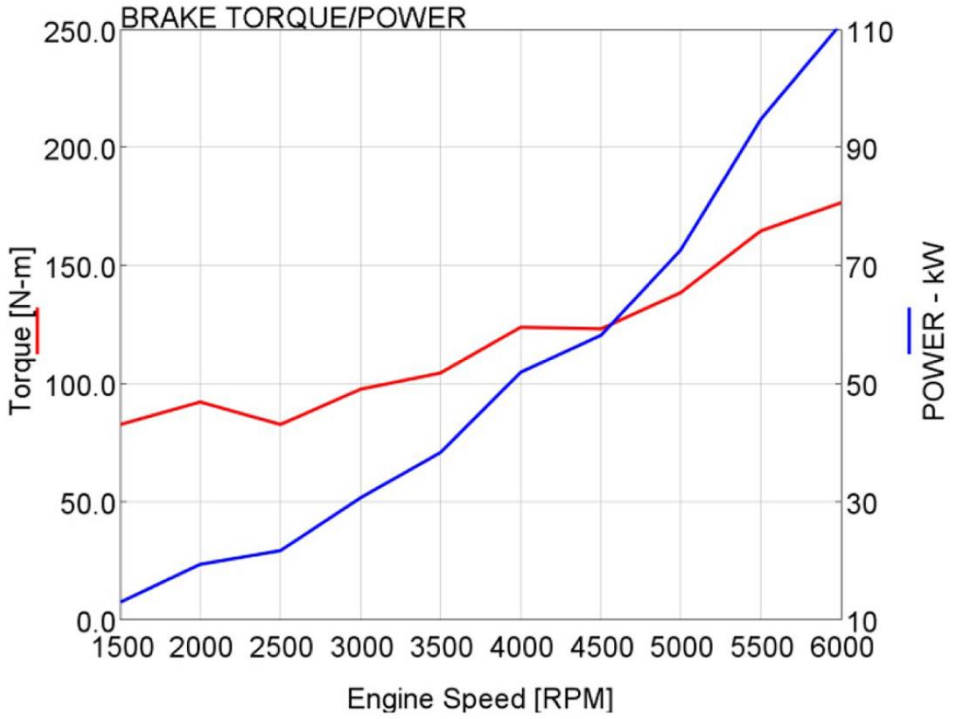

Figure 92 Brake torque and Power @WOT vs engine speed

The figure above shows torque and power at WOT condition in function of engine speed. It should be considered that the engine always runs at high speeds, even higher than 4000 rpm, because it is coupled with an EM for this specific application.

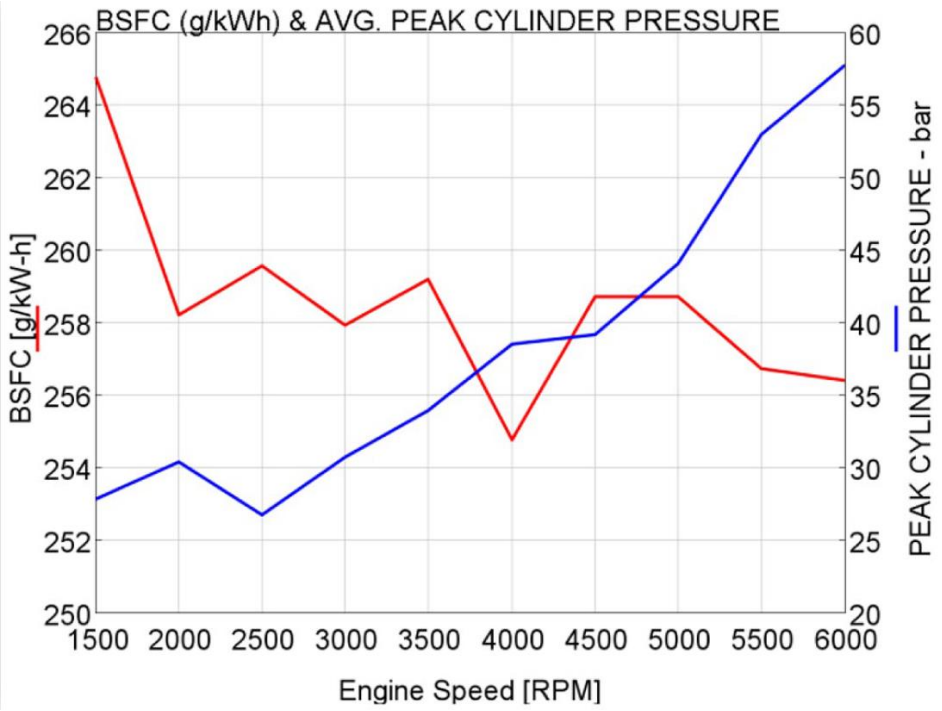

Figure 93 BSFC and Maximum in cylinder pressure peak vs engine speed

In Figure 93, BSFC is reported ; at high speeds BSFC remains at low levels, not near to values obtainable by a diesel engine but near to standard four-stroke spark-ignited engine. It is also interesting to look at the maximum in-cylinder pressure, the values are slightly low in comparison to a four-stroke spark ignited engine, this evidence is mainly due to the split of energy into 2 cycles instead of one for the four-stroke engine. Furthermore, the lower is the BMEP, the lower is the maximum peak of pressure expected.

5.6 Conclusions

The presented work reviews the design of a novel two-stroke spark-ignited light aircraft 3 cylinder loop scavenged engine. The required power output is 110 kW @ 6000 rpm. The total displacement of the engine is 1243 cm^3, it features a mechanical compressor for air supply and a semi-direct injection system for the fuel mixing optimized with a specific commercial software. The results obtained by the activity are summarized below:

- The maximum peak in terms of in cylinder pressure are quite low (< 60 bar)
- Thermal load is quite low because BMEP are lower than 9 bar
- BTE is quite good in comparison with four stroke spark-ignited engine, about 32% and quite independent from engine speed
- A further improvement of efficiency is possible because max pressure is low
- BSFC is less than 260 g/kWh at high speeds
- Scavenging efficiency is high >90%
- Low mechanical and heat losses
- Dimension of the whole engine are quite small, thanks to exhaust system

The scavenging system developed by the CFD 3D calculation campaign is optimized to reach targets in terms of trapping efficiency and scavenging efficiency, the results obtained by simulations are used as input to develop the CFD 1D model.

The injection system optimized is made of two injectors installed symmetrically to the cylinder liner. The two injectors are multi holes (6 holes for each one), angle and positioning in the intake ports ducts are optimized by the adoption of CFD 3D calculations.

At the best configuration at WOT and 6000 rpm the following results are found:

- Fuel trapping efficiency is about 94%
- Mean effective lambda 30° BTDC: 0.97, in front of a global value of Lambda of 1.04
- Relative lambda under the spark plug: 0.85

In conclusion, the presented engine can match all requirements for light aircraft applications.

6 Conclusions

The main goal of this research activity is to investigate new technologies that, applied to internal combustion engines, can reduce the environmental impact of these machines.

The attention is focused on non-conventional combustion processes, with particular interest in dual-fuel RCCI concepts. Furthermore, a novel two-stroke engine for light aircraft has been developed; this activity is linked to a European project aimed to analyze the feasibility and the performance of hybrid power units for light aircraft.

In chapter three, the results of an experimental campaign carried out on a turbocharged 4 cylinder Euro IV common rail diesel engine are reported. The engine has been modified in order to operate in dual fuel mode as a Gen-Set, and replace the conventional heavy duty diesel engines. The combustion system has been experimentally optimized, and the results provide general guidelines for the development of these specific engines. The combustion system implementation is relatively easy and cheap and consists of a few modifications, concerning the intake system and the injection system. The small displacement leads to more compact dimensions and lower weight, in comparison to conventional gen-sets; in order to keep comparable or lower BMEPs, the rotational speed is doubled (3000 rpm, instead of 1500 rpm). Reliability should not be affected; moreover, automotive engines are cheaper in comparison to heavy duty engines. In comparison to the original diesel engine, brake thermal efficiency slightly increases (+3.9%), after the optimization of the injection parameters.

In terms of pollutant emissions, the direct consequence of the increase of BTE is the decrease of carbon dioxide emissions. Furthermore, the adoption of a fuel with a lower fraction of carbon further reduces this specific emission. In the best case, the percentage reduction is close to 44%. Also soot emissions are considerably lower.

Conversely, as for HC and CO, an increase has been observed. The calibration process can reduce the engine-out emissions concentration; however, these pollutants can be easily managed by an oxidation catalyst that can work with a very high efficiency, thanks to the air excess in the exhaust flow.

NOx emissions do not have a clear trend: without specific calibration they usually decrease, but, when the engine injection system is calibrated in order to maximize BTE and reduce CO and HC emissions, they increase. However, in both cases, the specific amount remains comparable to normal diesel operation.

While the advantages are evident at high loads with high substitution rates, at low loads it is not recommended to run in dual-fuel mode, because the mixture is too lean and the combustion propagation in the premixed charge is very slow. On the other hand, low loads are of little interest for a gen-set. Should be necessary to run in these conditions, the engine can return in diesel mode, where combustion is very efficient and clean.

The second part of the activity regards a numerical analysis of the Dual Fuel combustion carried on by means of a CFD 3D model of the combustion chamber of the engine built with the adoption of a custom version of KIVA-3V code. First of all, the numerical model has been validated thought comparison with experimental data, then it has been used to investigate the influence of the injection strategy in dual fuel mode in terms of injection pressure, duration, timing and numbers of pulses for cycle. Some guidelines derive from the results obtained from the calculation campaign. For example, turning off the pre and pilot injection does not affect significantly the rate of heat release, IMEP NOx and CO_2 emissions do not change very much, while CO, HC and soot increase. Furthermore, delaying advance injection has a high impact on IMEP. Advance injection also affects the in-cylinder temperature; thus NOx emissions can increase when the injection advance increases.

In chapter four the same dual fuel engine has been investigated but with the adoption of gasoline instead of natural gas as low reactivity fuel. Several operation points have been investigated in order to assess some guidelines for the development of this combustion process. The conversion of the engine consists in the installation of a pipe designed for the injection of gasoline just after the intercooler system in order to avoid problems in gasoline evaporation and to ensure homogeneous mixture formation. Different operating point have been investigated, and, for each point a specific calibration of the injection system has been done to optimize the combustion process. One of the most interesting result regards the BTE that, as expected, show an increase in comparison to diesel oil (2% higher). When gasoline

flow rate is high the adoption of EGR in order to control the reactivity of the premixed charge is mandatory, because auto-ignition of the charge can occur and the maximum peak of pressure increases. The use of EGR can improve engine noise and decrease reliability.

At high loads, combustion becomes difficult to control, especially for auto-ignition; the heat release ratio starts before the main diesel injection. In this case, every modification made in the injection system cannot be useful to avoid this phenomenon. This result was expected because of the higher reactivity of the fuel. In comparison to Natural gas dual-fuel engine, the higher reactivity of the gasoline leads to auto ignite the charge considering the high compression ratio of the original diesel engine. In this scenario, natural gas, with its higher octane number, seems to be more flexible in the dual fuel operation mode, especially at high loads where the heat release is not too high avoiding peak of pressure and engine noise. Furthermore, maximum values in terms of BTE are observed with the adoption on NG instead of gasoline.

The last activity is focused on the development of a light aircraft two-stroke spark ignited hybrid engine. This project is focused on the application of hybrid powertrain in light aircrafts, two-stroke engine can be suitable for this application because of weight, dimensions and total displacement. Two-stroke engines are not novel in aircraft field, but in this case the design involves some new concepts, because the engine will be part of a hybrid power-unit. The activity includes the design of the scavenging ports and both 3D and 1D simulations are used to support the design process. The most interesting results of the CFD 1D simulation campaign in WOT condition at 6000 rpm are: the low maximum BMEP needed to reach power target (set at 110 kW), mainly due to two-stroke cycle, high relative value of BTE 32% with a BSFC less than 260 g/kWh, due to low friction losses and high pumping efficiency. This latter result has been obtained from the optimization of mechanical turbocharger. Furthermore, a timing optimization of the scavenging ports has been performed.

Calculation campaigns carried out in terms of CFD 3D simulations are, first of all, used for the optimization of the scavenging system improving design of inlet ports and exhaust ports. The main objective of this optimization was to limit fresh charge to flow into the exhaust system and to avoid bad mixing of the fresh charge with in-burnt gases. The calculation

campaign starts from a first design of the scavenging port to the final optimized version. The results obtained by the simulation campaign are used as input for CFD 1D model, and vice versa.

The injection system has been studied from an architectural point of view optimizing, by the adoption of the CFD 3D model, positioning, timing and pressure of the two injectors placed into the intake ports. The LPSDI (low-pressure semi direct injection) is the best configuration complying with required constraints; in particular, this system minimizes fuel flows through exhaust ports, reduces fuel consumption and avoids catalyst damage in case it is installed. Furthermore, the semi direct injection system permits the formation, if proper calibration is made, of a stratified charge inside the cylinder near the spark plug. The trapping efficiency reached is about 94%, and the relative lambda near the spark plug of 0.85 with a global mean value of 1.04.

This work aims at creating some guidelines for the analyzed combustion processes and in two-stroke engine development. As far as the combustion process is concerned, the analysis of the influence of EGR is mandatory in order to further improve performances in terms of BTE and pollutant emissions. Furthermore, implementation of specific control strategies is needed in order to assess stability at fixed loads but especially in transient conditions, which is particularly interesting for automotive applications.

Regarding the two-stroke engine developed, the next step will be the calibration of the first prototype at the test bench in order to validate and improve predictability of models.

Then the potential of a passive pre-chamber will be investigated by means of CFD 3D and 1D calculations. Moreover, an implementation of the prototypal prechamber into the engine for numerical validation and experimental development will be done. The jet ignition is particularly interesting in two-stroke engine for the flexibility in the design of combustion chamber and also for the low BMEP typically present in two stroke engines; jet ignition can lead to burn lean charge faster than a conventional spark plug, avoiding knock (frequently present in high performance two-stroke engine, due to warm EGR), improving engine performance and decreasing fuel consumption.

Moreover, also the Dual Fuel combustion can be implemented in this engine with some modifications: the design of a new combustion chamber with the adoption of a direct diesel injector. Dual fuel combustion can be attractive for two stroke because of the complete freedom in the combustion chamber design and the low value of BMEP that as already observed in this work, can lead to higher rate of low reactivity fuel instead of high reactivity fuel; being able to reach the best possible benefits of Dual fuel combustion.

References

1. Twigg MV. Progress and future challenges in controlling automotive exhaust gas emissions. *Applied Catalysis B: Environmental*. 2007;70(1):2-15. doi:10.1016/j.apcatb.2006.02.029

2. Cantore G. *Macchine*. Società Editrice Esculapio; 2020.

3. Heywood J, Heywood PJ. *Internal Combustion Engine Fundamentals*. McGraw-Hill Education; 1988.

4. Dual-Fuel Diesel Engines. Routledge & CRC Press. Accessed January 23, 2022. https://www.routledge.com/Dual-Fuel-Diesel-Engines/Karim/p/book/9780367783587

5. Srinivasan KK, Agarwal AK, Krishnan SR, Mulone V. *Natural Gas Engines: For Transportation and Power Generation*. Springer; 2019.

6. Ferrari G. *Motori a Combustione Interna*. Società Editrice Esculapio; 2019.

7. Amsden DC, Amsden AA. The KIVA story: a paradigm of technology transfer. *IEEE Transactions on Professional Communication*. 1993;36(4):190-195. doi:10.1109/47.259956

8. Amsden AA, Butler TD, O'Rourke PJ, Ramshaw JD. KIVA—A Comprehensive Model for 2-D and 3-D Engine Simulations. *SAE Transactions*. 1985;94:1-15.

9. Golovitchev VI, Montorsi L, Rinaldini CA, Rosetti A. CFD Combustion and Emission Formation Modeling for a HSDI Diesel Engine Using Detailed Chemistry. In: American Society of Mechanical Engineers Digital Collection; 2008:349-358. doi:10.1115/ICEF2006-1506

10. Amsden A, LANL. *A Block-Structured KIVA Program for Engines with Vertical or Canted Valves*. Los Alamos National Lab. (LANL), Los Alamos, NM (United States); 1999. Accessed February 3, 2022. https://www.osti.gov/biblio/1230082

11. Mattarelli E, Rinaldini CA, Savioli T. *Port Design Criteria for 2-Stroke Loop Scavenged Engines*. SAE International; 2016. doi:10.4271/2016-01-0610

12. Versteeg HK, Malalasekera W. *An Introduction to Computational Fluid Dynamics: The Finite Volume Method*. Pearson Education; 2007.

13. Spray Combustion Simulation Based on Detailed Chemistry Approach for Diesel Fuel Surrogate Model. Accessed January 23, 2022. https://www.sae.org/publications/technical-papers/content/2003-01-1848/

14. Golovitchev VI, Nordin N, Jarnicki R, Chomiak J. 3-D Diesel Spray Simulations Using a New Detailed Chemistry Turbulent Combustion Model. *SAE Transactions*. 2000;109:1391-1405.

15. ICOPE-15-1003 Experimental-analytical evaluation of sustainable syngas-biodiesel CHP systems based on oleaginous crop rotation. Accessed January 23, 2022. https://www.jstage.jst.go.jp/article/jsmeicope/2015.12/0/2015.12__ICOPE-15-_1/_article/-char/ja/

16. Golovitchev VI, Atarashiya K, Tanaka K, Yamada S. TOWARDS UNIVERSAL EDC-BASED COMBUSTION MODEL FOR COMPRESSION IGNITED ENGINE SIMULATIONS. *SAE Transactions*. 2003;112:1329-1343.

17. Rinaldini CA, Allesina G, Pedrazzi S, et al. Experimental investigation on a Common Rail Diesel engine partially fuelled by syngas. *Energy Conversion and Management*. 2017;138:526-537. doi:10.1016/j.enconman.2017.02.034

18. Mattarelli E, Rinaldini CA, Savioli T, Scrignoli F. Optimization of a High-Speed Dual-Fuel (Natural Gas-Diesel) Compression Ignition Engine for Gen-sets. *SAE Int J Engines*. 2021;14(3):369-386. doi:10.4271/03-14-03-0022

19. A review on natural gas/diesel dual fuel combustion, emissions and performance - ScienceDirect. Accessed January 14, 2022. https://www.sciencedirect.com/science/article/pii/S0378382015301715

20. An optical investigation of substitution rates on natural gas/diesel dual-fuel combustion in a diesel engine - ScienceDirect. Accessed January 14, 2022. https://www.sciencedirect.com/science/article/pii/S0306261919321439

21. Application of a Dual Fuel Diesel-CNG Configuration in a Euro 5 Automotive Diesel Engine. Accessed January 14, 2022. https://www.sae.org/publications/technical-papers/content/2017-01-0769/

22. Abdelaal MM, Hegab AH. Combustion and emission characteristics of a natural gas-fueled diesel engine with EGR. *Energy Conversion and Management*. 2012;64:301-312. doi:10.1016/j.enconman.2012.05.021

23. Lee S, Kim C, Lee S, Lee J, Kim J. Diesel injector nozzle optimization for high CNG substitution in a dual-fuel heavy-duty diesel engine. *Fuel*. 2020;262:116607. doi:10.1016/j.fuel.2019.116607

24. Liu J, Yang F, Wang H, Ouyang M, Hao S. Effects of pilot fuel quantity on the emissions characteristics of a CNG/diesel dual fuel engine with optimized pilot injection timing. *Applied Energy*. 2013;110:201-206. doi:10.1016/j.apenergy.2013.03.024

25. Zhou H, Li X, Lee CFF. Investigation on soot emissions from diesel-CNG dual-fuel. *International Journal of Hydrogen Energy*. 2019;44(18):9438-9449. doi:10.1016/j.ijhydene.2019.02.012

26. Yousefi A, Guo H, Birouk M, Liko B. On greenhouse gas emissions and thermal efficiency of natural gas/diesel dual-fuel engine at low load conditions: Coupled effect of injector rail pressure and split injection. *Applied Energy*. 2019;242(C):216-231.

27. Lounici MS, Loubar K, Tarabet L, Balistrou M, Niculescu DC, Tazerout M. Towards improvement of natural gas-diesel dual fuel mode: An experimental investigation on performance and exhaust emissions. *Energy*. 2014;64:200-211. doi:10.1016/j.energy.2013.10.091

28. A Study of the Emissions of a Dual Fuel Engine Operating with Alternative Gaseous Fuels. Accessed January 14, 2022. https://www.sae.org/publications/technical-papers/content/2008-01-1394/

29. Diesel injector nozzle optimization for high CNG substitution in a dual-fuel heavy-duty diesel engine - ScienceDirect. Accessed January 14, 2022. https://www.sciencedirect.com/science/article/pii/S0016236119319611

30. An exploration of utilizing low-pressure diesel injection for natural gas dual-fuel low-temperature combustion - ScienceDirect. Accessed January 14, 2022. https://www.sciencedirect.com/science/article/pii/S0360544218306455

31. Papagiannakis RG, Rakopoulos CD, Hountalas DT, Rakopoulos DC. Emission characteristics of high speed, dual fuel, compression ignition engine operating in a wide range of natural gas/diesel fuel proportions. *Fuel*. 2010;89(7):1397-1406. doi:10.1016/j.fuel.2009.11.001

32. Mattarelli E, Rinaldini CA, Savioli T. Dual Fuel (Natural Gas Diesel) for Light-Duty Industrial Engines: A Numerical and Experimental Investigation. In: Srinivasan KK, Agarwal AK, Krishnan SR, Mulone V, eds. *Natural Gas Engines : For Transportation and Power Generation*. Energy, Environment, and Sustainability. Springer; 2019:297-328. doi:10.1007/978-981-13-3307-1_11

33. Modified diesel engine fueled by syngas: Modeling and experimental validation. Accessed February 3, 2022. https://iris.unimore.it/handle/11380/1155087

34. Cameretti MC, Robbio RD, Tuccillo R. *Performance Improvement and Emission Control of a Dual Fuel Operated Diesel Engine*. SAE International; 2017. doi:10.4271/2017-24-0066

35. Papagiannakis RG, Hountalas DT. Experimental investigation concerning the effect of natural gas percentage on performance and emissions of a DI dual fuel diesel engine.

Applied Thermal Engineering. 2003;23(3):353-365. doi:10.1016/S1359-4311(02)00187-4

36. Mattarelli E, Rinaldini CA, Golovitchev VI. CFD-3D Analysis of a Light Duty Dual Fuel (Diesel/Natural Gas) Combustion Engine. *Energy Procedia*. 2014;45:929-937. doi:10.1016/j.egypro.2014.01.098

37. Papagiannakis RG, Hountalas DT. Combustion and exhaust emission characteristics of a dual fuel compression ignition engine operated with pilot Diesel fuel and natural gas. *Energy Conversion and Management*. 2004;45(18):2971-2987. doi:10.1016/j.enconman.2004.01.013

38. Carlucci AP, de Risi A, Laforgia D, Naccarato F. Experimental investigation and combustion analysis of a direct injection dual-fuel diesel–natural gas engine. *Energy*. 2008;33(2):256-263. doi:10.1016/j.energy.2007.06.005

39. Shu J, Fu J, Liu J, Zhang L, Zhao Z. Experimental and computational study on the effects of injection timing on thermodynamics, combustion and emission characteristics of a natural gas (NG)-diesel dual fuel engine at low speed and low load. *Energy Conversion and Management*. 2018;160:426-438. doi:10.1016/j.enconman.2018.01.047

40. A perspective on the range of gasoline compression ignition combustion strategies for high engine efficiency and low NOx and soot emissions: Effects of in-cylinder fuel stratification - Adam B Dempsey, Scott J Curran, Robert M Wagner, 2016. Accessed February 3, 2022. https://journals.sagepub.com/doi/full/10.1177/1468087415621805

41. Agarwal AK, Singh AP, Maurya RK. Evolution, challenges and path forward for low temperature combustion engines. *Progress in Energy and Combustion Science*. 2017;61:1-56. doi:10.1016/j.pecs.2017.02.001

42. Review of high efficiency and clean reactivity controlled compression ignition (RCCI) combustion in internal combustion engines - ScienceDirect. Accessed January 24, 2022. https://www.sciencedirect.com/science/article/pii/S0360128514000288

43. Fundamental phenomena affecting low temperature combustion and HCCI engines, high load limits and strategies for extending these limits - ScienceDirect. Accessed January 24, 2022. https://www.sciencedirect.com/science/article/pii/S0360128513000257

44. Dec JE. Advanced compression-ignition engines—understanding the in-cylinder processes. *Proceedings of the Combustion Institute*. 2009;32(2):2727-2742. doi:10.1016/j.proci.2008.08.008

45. Kiplimo R, Tomita E, Kawahara N, Yokobe S. Effects of spray impingement, injection parameters, and EGR on the combustion and emission characteristics of a PCCI diesel engine. *Applied Thermal Engineering*. 2012;37:165-175. doi:10.1016/j.applthermaleng.2011.11.011

46. Characterization of Partially Premixed Combustion. Accessed January 24, 2022. https://www.sae.org/publications/technical-papers/content/2006-01-3412/

47. Dual-Fuel PCI Combustion Controlled by In-Cylinder Stratification of Ignitability. Accessed January 24, 2022. https://www.sae.org/publications/technical-papers/content/2006-01-0028/

48. Experiments and Modeling of Dual-Fuel HCCI and PCCI Combustion Using In-Cylinder Fuel Blending on JSTOR. Accessed January 24, 2022. https://www.jstor.org/stable/26275404?seq=1#metadata_info_tab_contents

49. Experimental investigation on a diesel engine operated in RCCI combustion mode: AIP Conference Proceedings: Vol 2191, No 1. Accessed January 24, 2022. https://aip.scitation.org/doi/abs/10.1063/1.5138829

50. The Effects of Climate Change on GDP by Country and the Global Economic Gains From Complying With the Paris Climate Accord - Kompas - 2018 - Earth's Future - Wiley Online Library. Accessed January 28, 2022. https://agupubs.onlinelibrary.wiley.com/doi/full/10.1029/2018EF000922

51. Estimation of CO2 reduction by parallel hard-type power hybridization for gasoline and diesel vehicles - ScienceDirect. Accessed January 28, 2022. https://www.sciencedirect.com/science/article/pii/S0048969717306927

52. Doucette RT, McCulloch MD. Modeling the prospects of plug-in hybrid electric vehicles to reduce CO2 emissions. *Applied Energy*. 2011;88(7):2315-2323. doi:10.1016/j.apenergy.2011.01.045

53. Emadi A, Lee YJ, Rajashekara K. Power Electronics and Motor Drives in Electric, Hybrid Electric, and Plug-In Hybrid Electric Vehicles. *IEEE Transactions on Industrial Electronics*. 2008;55(6):2237-2245. doi:10.1109/TIE.2008.922768

54. Comparison of technical features between a More Electric Aircraft and a Hybrid Electric Vehicle | IEEE Conference Publication | IEEE Xplore. Accessed January 28, 2022. https://ieeexplore.ieee.org/abstract/document/4677663

55. Bowman CL, Felder JL, Marien TyV. Turbo- and Hybrid-Electrified Aircraft Propulsion Concepts for Commercial Transport. In: *2018 AIAA/IEEE Electric Aircraft Technologies Symposium (EATS)*. ; 2018:1-8.

56. Fletcher S, Flynn MC, Jones CE, Norman PJ. Hybrid electric aircraft : state of the art and key electrical system challenges. *The Transportation Electrification eNewsletter*. 2016;2016(Sept). Accessed January 28, 2022. http://tec.ieee.org/newsletter/september-2016/hybrid-electric-aircraft-state-of-the-art-and-key-electrical-system-challenges

57. Hoelzen J, Liu Y, Bensmann B, et al. Conceptual Design of Operation Strategies for Hybrid Electric Aircraft. *Energies*. 2018;11(1):217. doi:10.3390/en11010217

58. Brelje BJ, Martins JRRA. Electric, hybrid, and turboelectric fixed-wing aircraft: A review of concepts, models, and design approaches. *Progress in Aerospace Sciences*. 2019;104:1-19. doi:10.1016/j.paerosci.2018.06.004

59. Mattarelli E, Rinaldini CA, Wilksch M. 2-Stroke High Speed Diesel Engines for Light Aircraft. *SAE International Journal of Engines*. 2011;4(2):2338-2360.

60. Rinaldini CA, Mattarelli E, Golovitchev V. CFD Analyses on 2-Stroke High Speed Diesel Engines. *SAE International Journal of Engines*. 2011;4(2):2240-2256.

61. Ciampolini M, Bigalli S, Balduzzi F, Bianchini A, Romani L, Ferrara G. CFD Analysis of the Fuel–Air Mixture Formation Process in Passive Prechambers for Use in a High-Pressure Direct Injection (HPDI) Two-Stroke Engine. *Energies*. 2020;13(11):2846. doi:10.3390/en13112846

62. Bosi L, Ciampolini M, Romani L, Balduzzi F, Ferrara G. *Experimental Analysis on the Effects of Passive Prechambers on a Small 2-Stroke Low-Pressure Direct Injection (LPDI) Engine*. SAE International; 2020. doi:10.4271/2020-32-2305

63. Blair GP. *Design and Simulation of Two Stroke Engines*. SAE International; 1996. doi:10.4271/R-161

64. Heywood JB, Sher E. *The Two-Stroke Cycle Engine: Its Development, Operation, and Design*. Routledge; 2017. doi:10.1201/9780203734858

65. Mattarelli E, Rinaldini C. Two-Stroke Gasoline Engines for Small-Medium Passenger Cars. *SAE Technical Papers*. 2015;2015. doi:10.4271/2015-01-1284

66. Balduzzi F, Vichi G, Romani L, et al. Development of a Low Pressure Direct Injection System for a Small 2S Engine. Part I - CFD Analysis of the Injection Process. *SAE International Journal of Engines*. 2015;8(4):1885-1897.

67. Development of a Low Pressure Direct Injection System for a Small 2S Engine. Part II - Experimental Analysis of the Engine Performance and Pollutant Emissions. Accessed January 28, 2022. https://www.sae.org/publications/technical-papers/content/2015-01-1730/

68. Krimplstätter S, Winkler F, Oswald R, Kirchberger R. *Air Cooled 50cm^3 Scooter Euro 4 Application of the Two-Stroke LPDI Technology*. SAE International; 2014. doi:10.4271/2014-32-0008

69. High Efficient 125- 250 cm ^{3} LPDI Two-Stroke Engines, a Cheap and Robust Alternative to Four-Stroke Solutions? Accessed February 1, 2022. https://www.sae.org/publications/technical-papers/content/2010-32-0019/

70. Savioli T. CFD Analysis of 2-Stroke Engines. *Energy Procedia*. 2015;81:723-731. doi:10.1016/j.egypro.2015.12.078

71. Mattarelli E, Rinaldini CA, Savioli T. *Port Design Criteria for 2-Stroke Loop Scavenged Engines*. SAE International; 2016. doi:10.4271/2016-01-0610